tecnología
Glosas de innovacion aplicadas a la pyme

Edición Especial
Mayo 2021
Special Issue_May 2021
ISSN: 2254 – 4143

"TECHNOLOGY AS AN ENABLER IN BUSINESS, MANAGEMENT, ENVIRONMENTAL, AND SOCIAL SCIENCE"

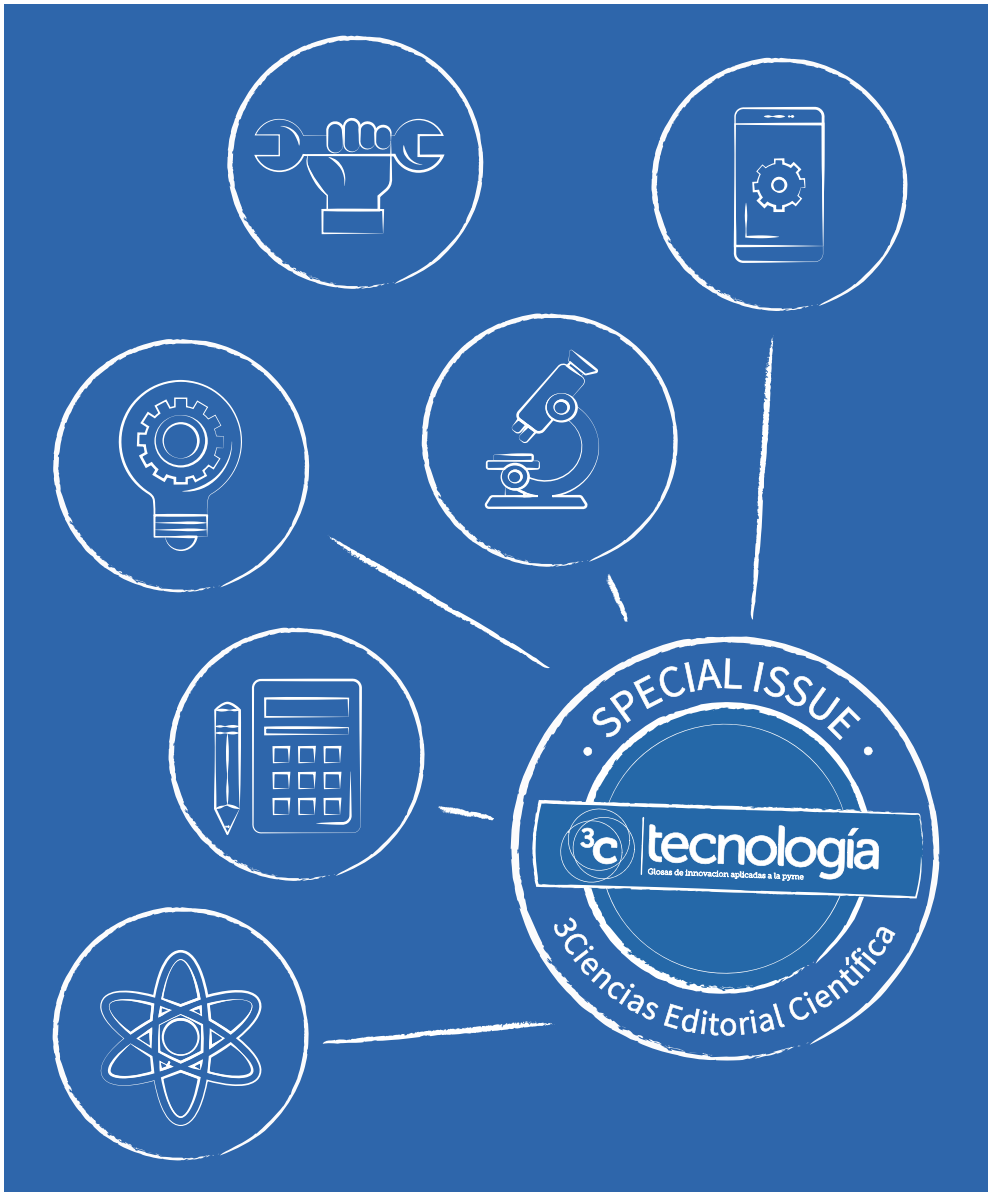

3C Tecnología. Glosas de innovación aplicadas a la pyme.

Edición Especial 37-2. Mayo 2021. *Special Issue 37-2. May 2021.*

Tirada nacional e internacional. *National and internacional circulation.*

Artículos revisados por el método de evaluación de pares de doble ciego.
Articles reviewed by the double blind peer evaluation method.

"Technology as an enabler in Business, Management, Environmental, and Social Science".

Editores invitados: *Guest Editors:*
James Swart
Central University of Technology, (South Africa).
E-mail: aswart@cut.ac.za ORCID: https://orcid.org/0000-0001-5906-2896
Bishwajeet Pandey
Gyancity Research Consultancy, Motihari, (India).
E-mail: dr.pandey@ieee.org ORCID: https://orcid.org/0000-0001-5593-8985

ISSN: 2254 – 4143
N.º de Depósito Legal: A 268 – 2012
DOI: https://doi.org/10.17993/3ctecno.2021.specialissue7

Edita:
Área de Innovación y Desarrollo, S.L.
C/Alzamora 17, Alcoy, Alicante (España)
Tel: 965030572
info@3ciencias.com _ www.3ciencias.com

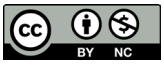

https://doi.org/10.17993/3ctecno.2021.specialissue7

https://doi.org/10.17993/3ctecno.2021.specialissue7

CONSEJO EDITORIAL EDITORIAL BOARD

https://doi.org/10.17993/3ctecno.2021.specialissue7

POLÍTICA EDITORIAL

OBJETIVO EDITORIAL

La Editorial científica 3Ciencias pretende transmitir a la sociedad ideas y proyectos innovadores, plasmados, o bien en artículos originales sometidos a revisión por expertos, o bien en los libros publicados con la más alta calidad científica y técnica.

COBERTURA TEMÁTICA

3C Tecnología es una revista de carácter científico-social en la que se difunden trabajos originales que abarcan la Arquitectura y los diferentes campos de la Ingeniería, como puede ser Ingeniería Mecánica, Industrial, Informática, Eléctrica, Agronómica, Naval, Física, Química, Civil, Electrónica, Forestal, Aeronáutica y de las Telecomunicaciones.

NUESTRO PÚBLICO

- Personal investigador.
- Doctorandos.
- Profesores de universidad.
- Oficinas de transferencia de resultados de investigación (OTRI).
- Empresas que desarrollan labor investigadora y quieran publicar alguno de sus estudios.

https://doi.org/10.17993/3ctecno.2021.specialissue7

AIMS AND SCOPE

PUBLISHING GOAL

3Ciencias wants to transmit to society innovative projects and ideas. This goal is reached thought the publication of original articles which are subdue to peer review or thorough the publication of scientific books.

TEMATIC COVERAGE

3C Tecnología is a scientific-social journal in which original works that cover Architecture and the different fields of Engineering are disseminated, such as Mechanical, Industrial, Computer, Electrical, Agronomic, Naval, Physics, Chemistry, Civil, Electronics, Forestry, Aeronautics and Telecommunications.

OUR TARGET

- Research staff.
- PhD students.
- Professors.
- Research Results Transfer Office.
- Companies that develop research and want to publish some of their works.

https://doi.org/10.17993/3ctecno.2021.specialissue7

NORMAS DE PUBLICACIÓN

3C Tecnología es una revista arbitrada que utiliza el sistema de revisión por pares de doble ciego (*double-blind peer review*), donde expertos externos en la materia sobre la que trata un trabajo lo evalúan, siempre manteniendo el anonimato, tanto de los autores como de los revisores. La revista sigue las normas de publicación de la APA (American Psychological Association) para su indización en las principales bases de datos internacionales.

Cada número de la revista se edita en versión electrónica (e-ISSN: 2254 – 4143), identificándose cada trabajo con su respectivo código DOI (Digital Object Identifier System).

PRESENTACIÓN TRABAJOS

Los artículos se presentarán en tipo de letra Baskerville, cuerpo 11, justificados y sin tabuladores. Han de tener formato Word. La extensión será de no más de 6.000 palabras de texto, incluidas referencias.

Los trabajos deben ser enviados exclusivamente por plataforma de gestión de manuscritos OJS:

https://ojs.3ciencias.com/

Toda la información, así como las plantillas a las que deben ceñirse los trabajos se encuentran en:

https://www.3ciencias.com/revista/informacion-para-autores/

https://www.3ciencias.com/normas-de-publicacion/plantillas/

https://doi.org/10.17993/3ctecno.2021.specialissue7

SUBMISSION GUIDELINES

3C Tecnología is an arbitrated journal that uses the double-blind peer review system, where external experts in the field on which a paper deals evaluate it, always maintaining the anonymity of both the authors and of the reviewers. The journal follows the standards of publication of the APA (American Psychological Association) for indexing in the main international databases.

Each issue of the journal is published in electronic version (e-ISSN: 2254 – 4143), each work being identified with its respective DOI (Digital Object Identifier System) code.

PRESENTATION WORK

The papers will be presented in Baskerville typeface, body 11, justified and without tabs. They must have Word format. The extension will be no more than 6.000 words of text, including references. Papers must be submitted exclusively by OJS manuscript management platform:

https://ojs.3ciencias.com/

All the information, as well as the templates to which the works must adhere, can be found at:

https://www.3ciencias.com/en/journals/information-for-authors/

https://www.3ciencias.com/en/regulations/templates/

https://doi.org/10.17993/3ctecno.2021.specialissue7

ESTRUCTURA

Los trabajos originales tenderán a respetar la siguiente estructura: introducción, métodos, resultados, discusión/conclusiones, notas, agradecimientos y referencias bibliográficas.
Es obligatoria la inclusión de referencias, mientras que notas y agradecimientos son opcionales. Se valorará la correcta citación conforme a la 7.ª edición de las normas APA.

RESPONSABILIDADES ÉTICAS

No se acepta material previamente publicado (deben ser trabajos inéditos). En la lista de autores firmantes deben figurar única y exclusivamente aquellas personas que hayan contribuido intelectualmente (autoría), con un máximo de 4 autores por trabajo. No se aceptan artículos que no cusmplan estrictamente las normas.

INFORMACIÓN ESTADÍSTICA SOBRE TASAS DE ACEPTACIÓN E INTERNACIONALIZACIÓN

- Número de trabajos aceptados publicados: 10.
- Nivel de aceptación de manuscritos en este número: 71,4%.
- Nivel de rechazo de manuscritos: 28,6%.
- Internacionalización de autores: 5 países (Perú, Turquía, Arabia Saudita, Pakistán y India).

Normas de publicación: https://www.3ciencias.com/normas-de-publicacion/instrucciones/

https://doi.org/10.17993/3ctecno.2021.specialissue7

STRUCTURE

The original works will tend to respect the following structure: introduction, methods, results, discussion/conclusions, notes, acknowledgments and bibliographical references. The inclusion of references is mandatory, while notes and acknowledgments are optional. The correct citation will be assessed according to the 7th edition of the APA standards.

ETHICAL RESPONSIBILITIES

Previously published material is not accepted (they must be unpublished works). The list of signatory authors should include only and exclusively those who have contributed intellectually (authorship), with a maximum of 4 authors per work. Articles that do not strictly comply with the standards are not accepted.

STATISTICAL INFORMATION ON ACCEPTANCE AND INTERNATIONALIZATION FEES

- Number of accepted papers published: 10.
- Level of acceptance of manuscripts in this number: 71,4%.
- Level of rejection of manuscripts: 28,6%.
- Internationalization of authors: 5 countries (Peru, Turkey, Saudi Arabia, Pakistan and India).

Guidelines for authors: https://www.3ciencias.com/en/regulations/instructions/

https://doi.org/10.17993/3ctecno.2021.specialissue7

INDEXACIONES INDEXATIONS

https://doi.org/10.17993/3ctecno.2021.specialissue7

INDEXACIONES INDEXATIONS

https://doi.org/10.17993/3ctecno.2021.specialissue7

/SUMARIO/
/SUMMARY/

https://doi.org/10.17993/3ctecno.2021.specialissue7

https://doi.org/10.17993/3ctecno.2021.specialissue7

/PRÓLOGO/
/PROLOGUE/

https://doi.org/10.17993/3ctecno.2021.specialissue7

PROLOGUE

James Swart
Central University of Technology, (South Africa).
E-mail: aswart@cut.ac.za
ORCID: https://orcid.org/0000-0001-5906-2896

Bishwajeet Pandey
Gyancity Research Consultancy, Motihari, (India).
E-mail: dr.pandey@ieee.org
ORCID: https://orcid.org/0000-0001-5593-8985

Technology is an enabler in all spheres of life today. In Education, it has been said that "technology will not replace teachers, but teachers who use technology will probably replace teachers who do not use it". This extends to Industry, Business and Commerce. Using technology to its full potential enables that "competitive edge" that so many organisations are vying for today. It enables efficiency of various processes, such as automation, data analytics, business intelligence and customer service. Indeed, technology is being used to the full by businessmen, managers, environmentalists, scientists and many more to achieve the mission and vision of organisations around the globe. In this regard, we have shortlisted only ten papers out of more than one hundred submissions that were presented at the "International Conference on Business, Management, Environmental, and Social Science 2021 (BMESS®-2021)" and the "7th International Conference on Recent Trends in Computer Science and Electronics" in this special issue of Web of Science/Emerging Source Citation Index Journal, 3C Tecnología. A brief synopsis of these papers follow.

In the first paper, Abosaq (2021) discusses how the Blockchain enabled Internet of Things (IoTs) has gained prominence among global researchers, academicians, planners, managers and industrialists. Both Blockchain and IoTs have the potential to achieve the 17 Sustainable Development Goals of the UN by the year 2030. Blockchain enabled IoTs has become an integrated and distributed Systems of Systems (SoS) networked technology that has been used in cloud infrastructures and in 5G/6G wireless systems. However, challenges to its use still exist which are noted in this paper, as well as further potential applications of it. A key

https://doi.org/10.17993/3ctecno.2021.specialissue7.17-21

challenge is noted regarding the lack of security in blockchain technology and resource constrained architecture of the industrialized IoTs to tackle crypto-materialized protocols.

In the second paper, Memon *et al.* (2021a) proposes a variable duty-cycle control scheme to increase the efficiency of buck converter operating in discontinuous conduction mode (DCM). In other words, they propose a control scheme to achieve a high power factor for DCM buck converters by only modulating the duty-cycle of a buck switch. The simulation results of this technology indicate that the proposed control scheme increases the efficiency and reduces the losses of a DCM buck convertor.

In the third paper, Çakır and Ulukan (2021) sort existing web (or video) platforms according to criteria determined by experts and select the best one among different alternatives for class education with the help of interval-valued fuzzy parameterized intuitionistic fuzzy soft sets. In this work, seven experts determined six criteria and their interval-valued fuzzy weights depending on educational needs. Ten video conferencing tools for educational institutions were evaluated in this regard that may also be classified under educational technologies. The results are intended to guide future research.

In the fourth paper, Memon *et al.* (2021b) concludes that our life is simpler, easier and comfortable due to power electronics. However, low power factors remain a challenge along with harmonic content that leads to higher power loss, voltage distortions and electromagnetic interference. A modified variable-on-time control scheme for an Integrated Buck-Boost Converter (IBBC) is therefore proposed in order to make the input current waveform as a sinusoidal as possible. The research methodology involves comparing a buck converter within a traditional control scheme to that with the proposed control scheme. Simulation results of this technology indicate an almost sinusoidal current waveform for the verification of the theoretical analysis.

In the fifth paper, Flores and Silva (2021) review seven models that may be used to predict divorce that has increased globally over the past two decades. They reference "The Four Horsemen of the Apocalypse" that can lead to divorce, along with the most leading cause being infidelity. The study draws on 56 questions as predictors of divorce and makes use of 4 automatic machine learning models and 3 hybrid models based on voting criteria that forms part of computer based technology. 35 experiments are presented in total for these

https://doi.org/10.17993/3ctecno.2021.specialissue7.17-21

seven models where the best results were obtained for the perceptron model. A limitation of the study relates to the context, the amount of data and the country in which the data were collected.

In the sixth paper, Panjagal and Ramaiah (2021) focus on odor pollution that can be caused by a number of factors, including the growth of urbanization with improper sanitation facilities or from unscientific dumping on vacant lands. It can lead to a number of health concerns that can negatively impact ones quality of life. They propose an intelligent mechanism for detecting, measuring and alerting individuals to the possible health effects of odor pollution. It involves the design of a solar-powered handheld electronic device (called an E-Nose) where real-time measurements are uploaded to an IoT cloud for remote monitoring and alerts. The results of these measurements were collaborated by a health survey that was completed by 80 individuals living in the area of the research site. Threshold limit values for Ammonia, Hydrogen Sulphide and Sulphur Dioxide were implemented for this technology from which alerts could be generated.

In the seventh paper, Tas *et al.* (2021) discuss an important step in the business supply chain, being supplier selection. They propose a new combined fuzzy methodology (using the SWARA and MARCOS methods that are made possible through computer based technology) to select suitable green suppliers that take into account the environment. A case study using a textile company is used where six suppliers are evaluated against 12 green criteria. The highest weight criteria were found for suppliers who have a well projected green image, a clear-cut environmental management system and options for green transportation.

In the eighth paper, Pedraza *et al.* (2021) propose the design of an ecological green area to improve the quality of life within a given district of Lima, Peru. The district was selected based on a topographic survey along with an evaluation of the climate, soil science, flora and fauna. An online survey was further used to obtain perceptions of the residents regarding the importance of green areas in their district. Results indicate that this district has only 1.69 m^2 of green area per inhabitant, which is much less than the recommended WHO standard of around 10 m^2. The proposed design, derived from computer based technology, is deemed viable and can be used to respond to the urgent need to raise the environmental quality of similar districts around the world.

https://doi.org/10.17993/3ctecno.2021.specialissue7.17-21

In the ninth paper, Memon *et al.* (2021c) presents a power factor improvement technique for a buck-convertor by only modulating the on-time of a buck switch without the need of an extra converter. Buck converters exhibit many advantages such as maintaining high efficiency for a wide range of input voltages, cost reduction, low output voltage, protection against inrush current and lifetime improvement. The technique makes use of a variable-on-time control scheme for critical current mode (CRM) buck converters. A theoretical analysis is given in the paper with simulation results to confirm the advantages of this technology.

In the tenth paper, Geldres *et al.* (2021) analyses the deficiencies of older buildings of educational institutions within a given district of Peru by using computer based technology. The methodology is based on percentage variations of the institutions by levels, where a sample of 79 educational institutions was considered, based on critical components such as their basic infrastructure, essential services, and advanced infrastructure. Percentage variations found between 2017 and 2020 reveal that maintenance does not mitigate or strengthen the educational infrastructure, but are palliatives that are worsening over time.

https://doi.org/10.17993/3ctecno.2021.specialissue7.17-21

https://doi.org/10.17993/3ctecno.2021.specialissue7.17-21

/01/

https://doi.org/10.17993/3ctecno.2021.specialissue7

BLOCKCHAIN ENABLED IOTS TOWARDS ACHIEVING THE SUSTAINABLE DEVELOPMENT GOALS

Nasser Hassan Abosaq
Assistant Professor, Computer Science and Engineering Department.
Yanbu University College, Yanbu Industrial City, (Kingdom of Saudi Arabia).
E-mail: abosaqn@rcyci.edu.sa
ORCID: https://orcid.org/0000-00031354-3170

Recepción: 14/12/2020 **Aceptación:** 03/03/2021 **Publicación:** 07/05/2021

Citación sugerida:
Abosaq, N. H. (2021). Blockchain enabled IoTs towards achieving the Sustainable Development Goals. *3C Tecnología. Glosas de innovación aplicadas a la pyme, Edición Especial,* (mayo 2021), 23-33. https://doi.org/10.17993/3ctecno.2021.specialissue7.23-33

ABSTRACT

The Blockchain enabled Internet of Things (IoTs) has emerged as an impactful research domain in recent years because of its focused global interest owing to the United Nations' commitment to achieve 17 Sustainable Development Goals by the year 2030. The Blockchain enabled IoTs has also received considerable attention from industry and academia due to its vast ranged potential applications in many explored fields. The Blockchain enabled IoTs technology has crossed the boundaries of cryptocurrency infrastructure and has become an integrated and distributed Systems of Systems (SoS) networked technology. It is because of a paradigm shift from centralized to the devolved and from static to dynamic networks of networks that this technology has received a wide enthusiasm and attention from researchers. This research is focused on challenges and opportunities of Blockchain enabled IoTs on cloud infrastructure, 5G/6G wireless systems and its computing issues for achieving United Nations' sustainable development goals by 2030 worldwide. As a use case scenario, we highlight the latest advancements in blockchain enabled IoTs, its various potential applications, future research directions and its infrastructure available in the research readings. Investigation into the important factors considered as technical challenges to the socio-economic development with respect to achieving sustainable development goals are also reviewed. Numerous case studies on Blockchain enabled IoTs in various application areas of the interest falling in SDGs domain have been performed the interpretive case study approach is selected to gather the data and its results, and a protocol is defined to design the structure.

KEYWORDS

Blockchain, IoT, 5G, 6G, Wireless technology, Sustainable development goals.

https://doi.org/10.17993/3ctecno.2021.specialissue7.23-33

1. INTRODUCTION

The Millennium Development Goals (MDGs) set forth by United Nations in 2016 were succeeded by the 17 Sustainable Development Goals (SDGs) targeted to be achieved by the year 2030 (United Nations, n.d. b). The SDGs are the targets for global wellness by easing the human lives through zero hunger, equitable quality education, sound environment, productive employment, economic growth through industrialization, green energy, global partnership, research and innovation on underwater resources, technology and many more. Emergence of 5G/6G universal telecommunication systems, 3D printing, blockchain, unmanned vehicles, drones as means of smart transportation and innovations in Artificial Intelligence (AI), Cloud computing, big data and data analytics are all set to aid in the UN's efforts for achieving SDGs by the year 2030. The world has entered a new era of technological development through fourth industrial revolution (4IR) of digital divide with many devastating challenges like COVID 19, environmental degradation, global warming, growing urbanization and natural disasters; all severely need multi-stakeholder partnerships among North-South, South-South and triangular regional and international digital connectivity. For coping with all these challenging global circumstances, nations are striving for innovative ideas and the Blockchain enabled IoTs is one of the promising technologies for designing robust digital networking responsible for connecting the humans, machines, and devices.

Internet of Things (IoTs) has integrated physical industrial operations with cyberspace technology in all its applications ranging from manufacturing to logistics to supply chain management. This has decentralized and diversified many industrial processes and systems and thus has created numerous process flow issues of interoperability of systems and devices, scalability, security, and privacy, trusted reliance and the most important one is the complex networking topologies due to Distributed Denial of Service (DDoS). The emergence of blockchain technology as a distributed system and its marriage with IoTs as a Service-oriented-Architecture have posed a sigh of relief for smooth industrial workflow of complex processes towards the successful business plans (Dorri *et al.*, 2016). Because of the inherited property of being a comparatively secure and trusted system due to chained blocks data structures, immutability, and irrevocability, blockchain technology has received a sense of trustworthiness and confidentiality to execute guaranteed operations by all its

https://doi.org/10.17993/3ctecno.2021.specialissue7.23-33

potential end users. Hence adopting the blockchain technology for secure IoT applications has gained wide acceptance both in industry and researching academia (Ahmad & Salah, 2018).

This research is focused on challenges and opportunities of Blockchain enabled IoTs on many industrial applications, cloud infrastructure and 5G/6G wireless systems for achieving United Nations' sustainable development goals by 2030 worldwide. As a use case scenario, we highlight the latest advancements in blockchain enabled IoTs, its various potential applications and future research directions. Investigation into the important factors considered as technical challenges to the socio-economic development with respect to achieving sustainable development goals are also reviewed.

2. CHALLENGES AND OPPORTUNITIES OF BLOCKCHAIN ENABLED IOTS

In Blockchain enabled IoTs security is realized as one of the main concerns by the researchers whereas the industrialized IoTs lack sufficient computing resources to tackle crypto-materialized protocols. There is an acute lack of common platform to deal with resource constrained low memory IoTs' ability to handle big data analytics challenge. Consequently, modifications in DDoS, smart contracts (Christidis & Devetsikiotis, 2016), Service oriented layered Architecture, edge-IoT system, modification in authentication procedures to secure from external threats, multi-layered decentralization both in IoTs and Blockchain and many other enabling approaches have been proposed to overcome the challenges of blockchain-IoT nexus (Ahmad & Salah, 2018).

However, the opportunities in this era outscore the present challenges. While perceiving the potential of technology in the context of achieving UN's sustainable development goals by 2030, the enormous opportunities in blockchain enabled IoTs further drag us towards researching on multi-stakeholder economic growth, Machine-to-Machine networking, smart cities' automated transportation systems, innovative startups, biomedical and healthcare applications' sensors, cybersecurity, and supply chain management of all types and, last but not the least. the information and communication technologies.

https://doi.org/10.17993/3ctecno.2021.specialissue7.23-33

2.1. ARCHITECTURAL REQUIREMENT OF BLOCKCHAIN-IOT

Blockchain enabled IoT can be realized as an information system with a set of parameters to form a physical solution of any targeted prerequisites based upon axiomatic design theory. Such an axiomatic design system is an interdependent and interconnected mechanism of three entities, i.e., the customer's domain requirements (CRs), the functional requirements (FRs) and the physical solutions (PSs) as shown in Graphic 1 (Cochran *et al.*, 2016). The axiomatic design theory is based upon mutual agreements that what customers desire to receive (FRs) is mapped to how those are produced (PSs). Hence there is a strong level of satisfaction between the involved parties as far as physical solutions are concerned.

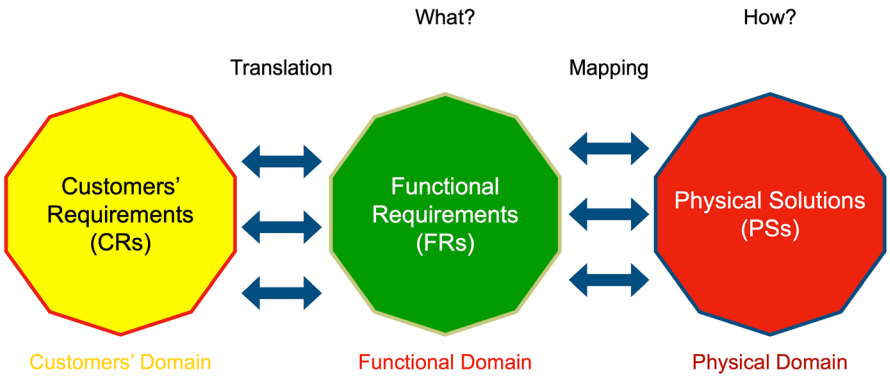

Graphic 1. ADT for complex system design.
Source: (Cochran *et al.*, 2016).

The IoT exhibits a non-static, dynamically oriented open environment where continuously changing services are involved requiring multi-vendor Quality of Service (QoS) responses to manage big data and its transmission load. Secondly the blockchain technology encompasses its inherent potential to deal with security threats due to Service oriented architecture of IoT as shown in Graphic 2. Other security threats like at Physical Layer (Interference, Insecure configuration, Spoofing and Physical Security), Network Layer Security (Like Resource Depletion, Identity and Authentication and Protocols) and Service Layer Security (like Insecure software, Single point of failure, Integrity and Privacy) can be well managed through deployment of blockchain infrastructure incorporating centralized and decentralized layers (Viriyasitavat *et al.*, 2019).

https://doi.org/10.17993/3ctecno.2021.specialissue7.23-33

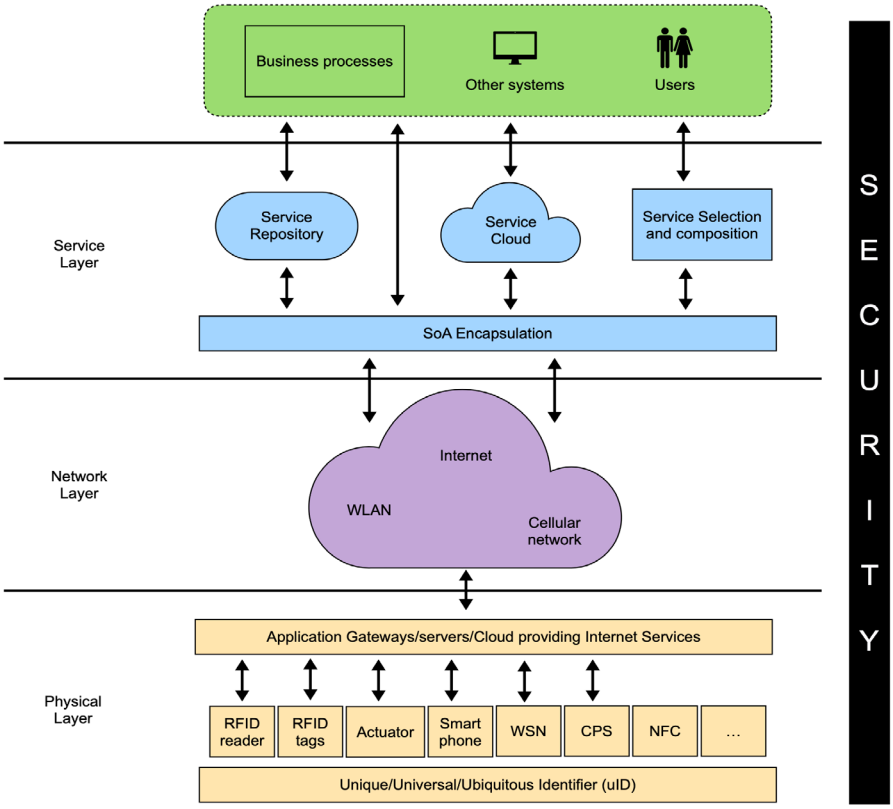

Graphic 2. SoA-based IoT Architecture.
Source: (Viriyasitavat *et al.*, 2019).

Additionally, access control protocols to safeguard IP spoofing in a distributed environment through smart contracts (Christidis & Devetsikiotis, 2016) is also essential which can be managed via blockchain ledger. This has embarked upon a novel idea of inventing Public Biometric Infrastructure in the blockchain enabled IoT.

2.2. POTENTIAL APPLICATIONS AND FUTURE RESEARCH DIRECTIONS

Alexandru Stanciu is working on a novel standard called by him as Hyperledger Fabric for blockchain enabled IoTs under the platform of IEC 61499 standard (Viriyasitavat *et al.*, 2019). This standard is inventing the development of standards for inputs, outputs, and necessary protocol operations for blockchain enabled IoTs. We are of the opinion that many of the UNs 17 SDGs can only be leveraged if technology is considered as priority option of the developing countries. The potential applications include widespread integration of contactless digital human computer interconnection with no mankind intervention. It is

https://doi.org/10.17993/3ctecno.2021.specialissue7.23-33

predicted that internet usage will be 28.5 billion devices by the year end 2022 means that per capita network connected devices will stand at 3.6 by 2022.

Certainly, such a huge mobilization of network growth will emerge in generation of trillions of bytes of data in many human prioritized applications like healthcare, smart cities, environmental issues, GIS & Remote sensing, agricultural and food security, intelligent transportation, green energy, and socio-economic technological growth. This all requires, among many other things, a systematic integration of blockchain to the industrial IoT for achieving the UNs SDGs by 2030.

3. METHODOLOGY

For validating the idea of nexus between blockchain and IoT, the many use case scenarios have been developed in the author's departments. This has facilitated tangible results to yield. For example, one use case scenario is e-networked business model consisting of student association, university administration and external and internal buyers to purchase any facilities owned by the university through advertisement mechanism. The transfer of access rights has been invoked between the involved parties or stakeholders.

The public and private blockchain benefits and disadvantages have been identified using different scenario conditions. A robust architecture is suggested comprising of different users, devices, networking resources, self-executable crypto contracts, storage repositories, auditable processes etc. An algorithm based on python file is created to act as a servicing program responsible for load balancing and leader election that provides link between the two blockchains. Our experimental setup is caried out on HP Notebook with 12 GB memory having core i7 processor. Etherum software 1.8.27 and python 3.7 programming language is used with Web3 library V 4.8.3.

Public and private nodes were designated. High-level language Solidity 0.5 is used for writing smart contracts (Christidis & Devetsikiotis, 2016). Various decentralized and non-distributed options have also been studied to analyze scalability. The scenarios developed are for Access Generation (Pal *et al.*, 2019), Electricity Cost as shown in Graphic 3 and 4 respectively, hostel accommodation cost, sweet water provision cost.

https://doi.org/10.17993/3ctecno.2021.specialissue7.23-33

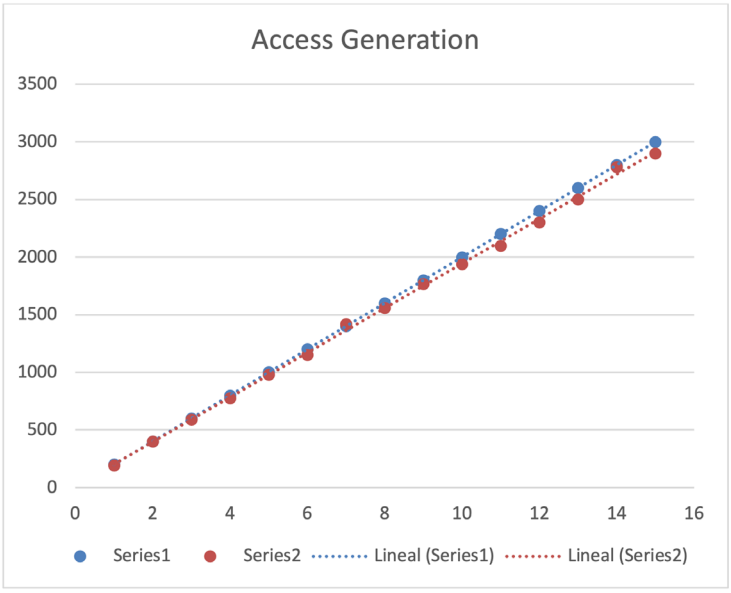

Graphic 3. Access Generation.
Source: own elaboration.

In furtherance to this experimental work, the author has executed many case studies on applications concerning blockchain enabled IoTs falling in SDGs domain.

4. RESULTS

For gathering fruitful results, the interpretive case study approach is used to gather the data. A protocol was defined to design the structure. Several interviews and brainstorm sessions were done in the author's university/ departments. 15 social domains were selected where blockchain enabled IoT data is gathered, transformed, and backed up using, ICT, AI, and Machine Learning Tools. To verify the delegation chain, two design options as serries 1 and series 2 were analyzed as shown in access generation graph using Breadth First Search algorithm to ensure the contract trail. The results show that waiting time is high enough. To reduce this waiting time, algorithm is improved in Electricity Cost as the cost has linear relationship with delegation depth as shown in Graphic 4. By introducing the novel algorithm, the blockchain efficacy has improved.

https://doi.org/10.17993/3ctecno.2021.specialissue7.23-33

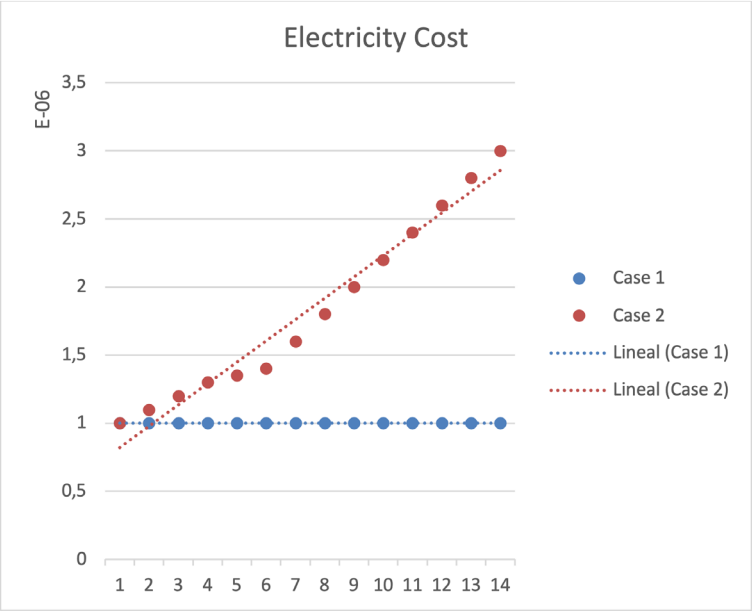

Graphic 4. Electricity Cost.
Source: own elaboration.

5. CONCLUSIONS

In this research, the author has considered the UN's 17 sustainable development goals as the motivation to use blockchain enabled IoTs as a candidate technology for achieving the goals by 2030. Having noticed the lack of security in block chain technology and resource constrained architecture of the industrialized IoTs to tackle crypto-materialized protocols, the emergence of private blockchain annexed with IoTs can contribute as a full-fledged secure system. This research shows that blockchain enabled IoTs can prove to be a promising technology towards achieving the stainability.

5. ACKNOWLEDGMENT

The author acknowledges the cooperation of Computer Science and Engineering Department and the management of Yanbu University College, Yanbu Industrial City, Kingdom of Saudi Arabia for supporting this research.

https://doi.org/10.17993/3ctecno.2021.specialissue7.23-33

REFERENCES

Ahmad, M., & Salah, K. (2018). IoT security: Review, blockchain solutions, and open challenges. *Future Generation Computer Systems, 82,* 395-411. https://doi.org/10.1016/j.future.2017.11.022

Christidis, K., & Devetsikiotis, M. (2016). Blockchains and Smart Contracts for the Internet of Things. *IEEE Access, 4,* 2292-2303. https://ieeexplore.ieee.org/document/7467408

Cochran, D. S., Jafri, M. U., Chu, A. K., & Bi, Z. (2016). Incorporating design improvement with effective evaluation using the Manufacturing System Design Decomposition (MSDD). *Journal of Industrial Information Integration, 2,* 65-74. https://doi.org/10.1016/j.jii.2016.04.005

Dorri, A., Kanhere, S. S., & Jurdak, R. (2016). Blockchain in internet of things: challenges and solutions. *arXiv preprint arXiv:1608.05187*. https://arxiv.org/abs/1608.05187

Pal, S., Rabehaja, T., Hill, A., Hitchens, M., & Varadharajan, V. (2019). On the integration of blockchain to the internet of things for enabling access right delegation. *IEEE Internet of Things Journal, 7*(4), 2630-2639. https://doi.org/10.1109/JIOT.2019.2952141

United Nations. (n.d.a). *Transforming our world: the 2030 Agenda for Sustainable Development.* Department of Economic and Social Affairs. Sustainable Development. https://sustainabledevelopment.un.org/post2015/transformingourworld

United Nations. (n.d.b). *The 17 goals. Department of Economic and Social Affairs.* Sustainable Development. https://sdgs.un.org/goals

Viriyasitavat, W., Da Xu, L., Bi, Z., & Hoonsopon, D. (2019). Blockchain Technology for Applications in Internet of Things —Mapping From System Design Perspective. *IEEE Internet of Things Journal, 6*(5), 8155-8168. https://ieeexplore.ieee.org/document/8752029

 https://doi.org/10.17993/3ctecno.2021.specialissue7.23-33

https://doi.org/10.17993/3ctecno.2021.specialissue7.23-33

/02/

https://doi.org/10.17993/3ctecno.2021.specialissue7

DISCONTINUOUS CONDUCTION MODE BUCK CONVERTER WITH HIGH EFFICIENCY

Abdul Hakeem Memon
IICT, Mehran UET, Jamshoro, Sindh, (Pakistan).
E-mail: hakeem.memon@faculty.muet.edu.pk
ORCID: https://orcid.org/0000-0001-8545-3823

Rizwan Ali
IICT, Mehran UET, Jamshoro, Sindh, (Pakistan).
E-mail: rizwanalimemon26@gmail.com
ORCID: https://orcid.org/0000-0002-3022-6356

Zubair Ahmed Memon
IICT, Mehran UET, Jamshoro, Sindh, (Pakistan).
E-mail: zubair.memon@faculty.muet.edu.pk
ORCID: https://orcid.org/0000-0001-5967-3152

Recepción: 30/11/2020 **Aceptación:** 09/02/2021 **Publicación:** 07/05/2021

Citación sugerida:
Memon, A. H., Ali, R., y Memon, Z. A. (2021). Discontinuous Conduction Mode Buck Converter with High Efficiency. *3C Tecnología. Glosas de innovación aplicadas a la pyme, Edición Especial,* (mayo 2021), 35-51. https://doi.org/10.17993/3ctecno.2021.specialissue7.35-51

ABSTRACT

Electronic devices require AC to DC converter (rectifier) to convert AC voltage from the grid to DC voltage for the electronics and its result is low power factor (PF) and harmonic current injection into the system. Nowadays, power factor correction (PFC) converters are being widely used which can achieve high power factor (PF) and reduce the harmonics caused during AC to DC conversion and buck PFC converter is one of mostly used converter. On the other hand, if this converter works with constant duty-cycle (CDC) control scheme, the overall losses are more and efficiency is less. In order to increase the efficiency of buck converter operating in discontinuous conduction mode (DCM), a variable duty-cycle (VDC) control scheme is proposed. The method of fitting VDC control scheme is given for making implementation of circuit simpler. The performance of buck converter is compared with CDC and VDC control scheme in terms of efficiency. For verifying the validity of proposed technique, the simulation results are carried out. The object of the research paper is to propose the control scheme to achieve high PF for DCM buck converter by only modulating the duty-cycle of buck switch.

KEYWORDS

Variable Duty-Cycle (VDC), Constant Duty-Cycle (CDC), Discontinuous Conduction Mode (DCM), Electromagnetic Interference (EMI), Duty-Cycle, Buck Converter.

https://doi.org/10.17993/3ctecno.2021.specialissue7.35-51

1. INTRODUCTION

Electronic devices require AC to DC converter (rectifier) to convert AC voltage from the grid to DC voltage for the electronics and its result is low power factor (PF) and harmonic current injection into the system. Nowadays, power factor correction (PFC) converters are being widely used which can achieve high power factor (PF) and reduce the harmonics caused during AC to DC conversion (Praneeth & Williamson, 2018; Williamson, Rathore & Musavi, 2015; Nussbaumer *et al.*, 2019; Anwar *et al.*, 2017; Al Gabri, Fardoun & Ismail, 2015; Badawy, Sozer & De Abreu-Garcia, 2016; Memon *et al.*, 2019a, 2019b, 2019c, 2019d, 2019e).

Power factor correction can be of two types: active PFC and passive PFC. Active PFC can be achieved by using passive elements like inductors, capacitors and inductors and passive PFC can be achieved by using electronic circuits with active switches like insulated gate bipolar junction transistor (IGBT) and metal oxide semiconductor field effect transistor (MOSFET), etc. To obtain the good value of power factor and meet the standards like IEC61000-3-2 and IEEE 519, active power factor correction (PFC) techniques are used. DC to DC converters used as power factor correction circuits with the help of active switches shape the value of supply current which not only improves the PF, but also reduce the harmonics. Among DC-DC converters, DCM buck PFC is generally utilized in many applications because of various advantages like maintaining high efficiency for the wide range of input voltage, cost reduction, low output voltage, protection against inrush current life time improvement and easy design of electromagnetic interference (EMI) filter The major drawback of the buck converter is its PF is low and efficiency is also low, especially when operated with constant duty-cycle control scheme (CDCCS).

For modifying the performance of traditional buck converter, various research has proposed various topologies and control schemes (Endo, Yamashita & Sugiura, 1992; Lee, Wang & Hui, 1997; Spiazzi & Buso, 2000; Huber, Gang & Jovanovic, 2011; Jang & Jovanović, 2011; Lamar *et al.*, 2012; Ki & Lu, 2013; Al Gabri, Fardoun & Ismail, 2015; Memon *et al.*, 2016; Memon *et al.*, 2017; Memon *et al.*, 2018a, 2018b; Memon *et al.*, 2019a, 2019b, 2019c, 2019d, 2019e; Liu *et al.*, 2020).

https://doi.org/10.17993/3ctecno.2021.specialissue7.35-51

Most of the work in the literature is done to improve the PF of the buck converter. The purpose of this paper is to introduce the control scheme which can improve the efficiency of DCM buck converter.

In this paper, a variable duty-cycle control scheme (VDCCS) is introduced for DCM buck converter to reduce peak and rms current of inductor and hence ultimately enhancing its efficiency.

This paper is divided into six sections. In section 2, the operation states of DCM buck converter are analyzed with traditional CDCCS strategy. The introduced VDCCS is discussed in section 3. Then the comparative analysis is discussed in section 4 in terms of efficiency. In section 5, the effectiveness of proposed topology is evaluated by simulation results. Finally, some conclusions are drawn in section 6.

2. RESEARCH METHODOLOGY

The research methodology is based on:

1. Mathematical analysis of the operating principle of the control schemes for DCM Buck converter with the help of MATHCAD converter.
2. Introducing the proposed control scheme to obtain high efficiency
3. Realization of control scheme through control blocks.
4. Comparative analysis of the converter for CDCC and VDCC strategy
5. Developing the simulation model of DCM Buck converter with the help of MATLAB software
6. Confirming the results.

3. CONVENTIONAL CDC CONTROL SCHEME FOR BUCK CONVERTER

Figure 1(b) shows the main circuit of a buck converter with CDC control scheme.

The input voltage before and after the bridge are given as

https://doi.org/10.17993/3ctecno.2021.specialissue7.35-51

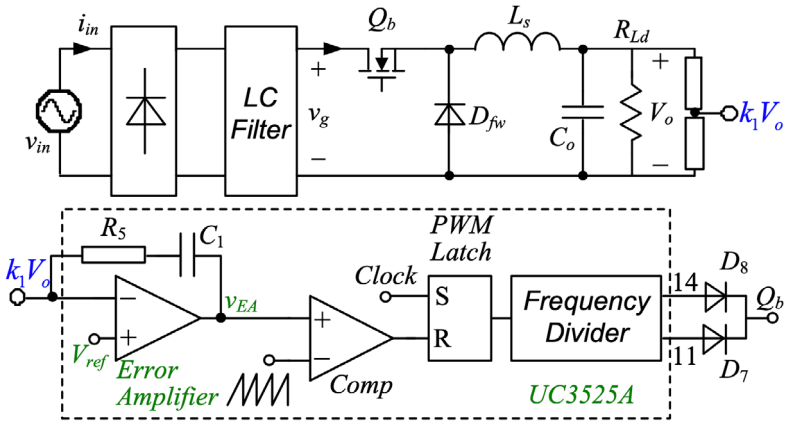

Figure 1. Buck converter with CDC control scheme.
Source: (Yao *et al.*, 2017).

$$v_{in}(\theta) = v_g = \sqrt{2}V_{rms}\sin\theta \tag{1}$$

Where V_{rms} is the rms value.

There are three switching cycles when buck converter works in discontinuous conduction mode (DCM).

When Q_b conducts, the inductor is getting charge from supply voltage in first switching cycle as depicted in Figure 2.

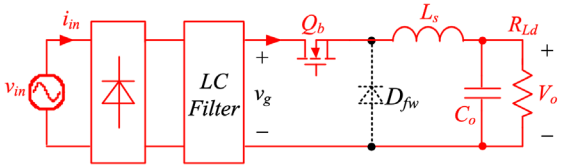

Figure 2. Buck converter during first switching cycle.
Source: (Yao *et al.*, 2017).

The peak current of inductor i_{L_pk} is given as

$$i_{L\_pk} = \frac{\sqrt{2}V_{rms}\sin\theta - V_o}{L_s} D_{on} T_s \tag{2}$$

Where D_{on} is the duty-cycle of during turn on time of switch

When Q_b is off, inductor is discharging through load and output capacitor, as shown in in Figure 3. It occurs in second switching cycle

https://doi.org/10.17993/3ctecno.2021.specialissue7.35-51

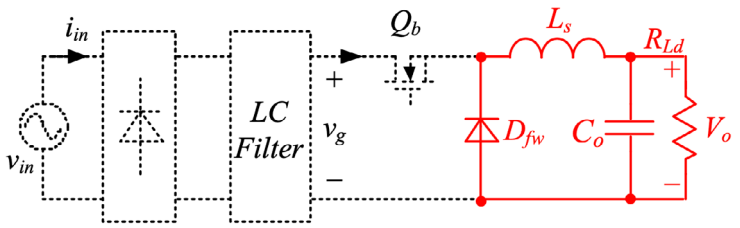

Figure 3. Buck converter during second switching cycle.
Source: (Yao *et al.*, 2017).

The peak current of inductor i_{L_pk} is

$$i_{L\_pk} = -\frac{V_o}{L_s} D_{on} T_s \tag{3}$$

By using the information of volt-second balance, following expression is obtained

$$(\sqrt{2} V_{rms} \sin\theta - V_o) D_{on} T_s = V_o D_{off} T_s \tag{4}$$

From (2) and (4), the following relation is obtained

$$D_{off} = \frac{\sqrt{2} V_{rms} \sin\theta - V_o}{V_o} D_{on} \tag{5}$$

During third switching cycle, output capacitor is discharged through load as shown in Figure 4.

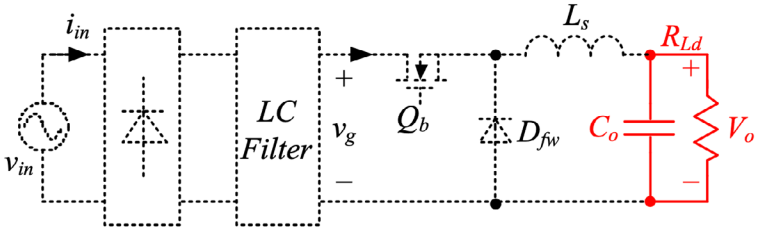

Figure 4. Buck converter during third switching cycle.
Source: (Yao *et al.*, 2017).

The value of average input current for buck converter is got as

$$i_{b\_av\_cdccs} = \frac{D_{on}^2 (\sqrt{2} V_{rms} \sin\theta - V_o)}{2 L_s f_s} \tag{6}$$

For complete half cycle, input current is expressed as

https://doi.org/10.17993/3ctecno.2021.specialissue7.35-51

$$i_{in\_b\_cdccs} = \begin{cases} \frac{D_{on}{}^2(\sqrt{2}V_{rms}\sin\theta - V_o)}{2L_s f_s} & \theta_0 < \theta < \pi - \theta_0 \\ 0 & 0 \le \theta < \theta_0 \;\&\; \pi - \theta_0 < \theta \le \pi \end{cases}$$

$$\text{Where } \theta_0 = \arcsin V_o / \text{sqrt } 2 * V_{rms} \tag{7}$$

Based on (1) and (7), the input power of the buck converter is expressed as

$$P_{in\_cdccs} = \frac{\sqrt{2}V_{rms}D_{on}^2}{2\pi L_s f_s}\int_{\theta_0}^{\pi-\theta_o}\sin\theta(\sqrt{2}V_{rms}\sin\theta - V_o)d\theta \tag{8}$$

Now D_{on} can be calculated by assuming the efficiency of buck converter as 100%

$$D_{on} = \sqrt{\frac{2\pi L_s f_s P_o}{\sqrt{2}V_{rms}\int_{\theta_0}^{\pi-\theta_o}\sin\theta(\sqrt{2}V_{rms}\sin\theta - V_o)d\theta}} \tag{9}$$

4. PROPOSED VDC CONTROL SCHEME FOR BUCK CONVERTER FOR EFFICIENCY IMPROVEMENT

4.1. VDC CONTROL SCHEME FOR EFFICIENCY IMPROVEMENT

For obtaining, high efficiency, the variation rule for duty-cycle must be

$$D_{on\_vdccs} = \sqrt{\frac{D_c V_m \sin\theta}{\sqrt{2}V_{rms}\sin\theta - V_o}} \tag{10}$$

Where Dc is a co-efficient,

By substituting the value of D_{on} in (6), we obtain

$$i_{in\_b\_vdccs} = \frac{\sqrt{2}V_{rms}\sin\theta D_c T_s}{2L_s} \tag{11}$$

The average value of input power with VDC control scheme is expressed as

$$P_{in\_b\_vdccs} = \frac{1}{\pi}\int_{\theta_0}^{\pi-\theta_0}\frac{D_c T_s\left(\sqrt{2}V_{rms}\sin\theta\right)^2}{2L_s}d\theta = P_o \tag{12}$$

The value of D_c is got from (12) as

$$D_c = \frac{4\pi L_s P_o}{\left(\sqrt{2}V_{rms}\right)^2(\pi - 2\theta_0 + \sin 2\theta_0)T_s} \tag{13}$$

By substituting the value of D_c in (11), we get

$$D_{on\_vdccs} = \sqrt{\frac{4\pi P_o L_s \sin\theta}{(\pi - 2\theta_0 + \sin 2\theta_0)\left(\sqrt{2}V_{rms}\sin\theta - V_o\right)\sqrt{2}\,\mathrm{V}_{rms}T_s}} \tag{14}$$

https://doi.org/10.17993/3ctecno.2021.specialissue7.35-51

4.2. FITTING VDC CONTROL SCHEME

For the implementation of Don_vdccs, it is essential to remove squire root term from (14). Because it is difficult to realize to it by using analogue circuits.

Defining $a=V_m/V_o$, $y=sin\theta$, eq. (14) can be simplified as

$$D_{on\_fit} = D_1\left(1-\frac{y}{2ay_0^{\,2}-y_0}\right)$$

$$\text{where } D_1 = \sqrt{\frac{D_0 a y_0}{a y_0 - 1}}\,\frac{2ay_0-1}{2(ay_0-1)}. \tag{15}$$

$y_0=0.75$

Eq. 15 can be rewritten as

$$D_{on\_fit} = D_1\frac{1.125V_m - 0.75V_o - V_o\sin\theta}{1.125V_m - 0.75V_o} \tag{16}$$

The average input current with VDCCS is given as

$$i_{b\_VDCCS} = \frac{(\sqrt{2}V_{rms}\sin\theta - V_o)}{2L_s f_s} D_{on\_fit}^{\,2} \tag{17}$$

5. EFFICIENCY COMPARISON

5.1. LOSS DUE TO BRIDGE DIODE RECTIFIER

The loss caused by bridge diode rectifier is calculated as below

$$P_{con\_bridge(cdccs)} = 2V_{FD}I_{in\_avg(cdccs)} \tag{18(a)}$$

$$P_{con\_bridge(vdccs)} = 2V_{FD}I_{in\_avg(vdccs)} \tag{18(b)}$$

KBL10 is adopted as the rectifier bridge, whose forward voltage drop VFD is 0.9 V.

The input current with CDC control scheme and VDC control scheme is given as

$$i_{b\_cdccs} = \frac{2\pi L_s f_s P_o(\sqrt{2}V_{rms}\sin\theta - V_o)}{2\sqrt{2}L_s f_s V_{rms}\int_{\theta_0}^{\pi-\theta_0}\sin\theta(\sqrt{2}V_{rms}\sin\theta - V_o)d\theta} \tag{19(a)}$$

https://doi.org/10.17993/3ctecno.2021.specialissue7.35-51

$$i_{b\_vdccs} = \frac{\left(D_1 \sqrt{\frac{D_0 a y_0}{a y_0 - 1}} \frac{2 a y_0 - 1}{2(a y_0 - 1)} \frac{1.125 V_m - 0.75 V_o - V_o \sin\theta}{1.125 V_m - 0.75 V_o} \right)^2 (\sqrt{2} V_{rms} \sin\theta - V_o)}{2 L_s f_s} \quad (19(b))$$

5.2. CONDUCTION LOSSES OF THE SWITCHES

The rms current of the on time period, i.e., the rms current of switch Q_b can be got as

$$I_{rms(Qb\_on)} = \sqrt{\frac{\int_{\theta_0}^{\pi-\theta_0} i_{L\_pk}^2 D_{on}\, d\theta}{3\pi}} \quad (20)$$

The rms current of the off time period can be determined as

$$I_{rms(Qb\_off)} = \sqrt{\frac{\int_{\theta_0}^{\pi-\theta_0} i_{L\_pk}^2 D_{off}\, d\theta}{3\pi}} \quad (21)$$

While Q_b is on and off, the current flows through the winding of the inductor, whose rms current is

$$I_{rms(cdccs)} = \sqrt{I_{rms(Qb\_on\_cdccs)}^2 + I_{rms(Qb\_off\_cdccs)}^2} \quad (22(a))$$

$$I_{rms(vdccs)} = \sqrt{I_{rms(Qb\_on\_vdccs)}^2 + I_{rms(Qb\_off\_vdccs)}^2} \quad (22(b))$$

The losses due to conduction of switches can be got as

$$P_{con\_switches(cdccs)} = I_{rms(Qb\_on\_cdccs)}^2 R_{DS(on)\_S} \quad (23(a))$$

$$P_{con\_switches(vdccs)} = I_{rms(Qb\_on\_vdccs)}^2 R_{DS(on)\_S} \quad (23(b))$$

The value of $R_{DS(On)}$ 0.19 Ω which is found from datasheet of 20N60C3.

5.3. LOSSES DUE TURN OFF SWITCHES

The loss caused by turning off the switch with CDC control scheme and VDC control scheme is calculated as

$$P_{off\_switches(cdccs)} = \frac{T_s t_f}{2\pi} \int_0^{\pi} i_{L\_pk\_cdccs} (V_m \sin\theta) d\theta \quad (24(a))$$

https://doi.org/10.17993/3ctecno.2021.specialissue7.35-51

$$P_{off\_switches(vdccs)} = \frac{T_s t_f}{2\pi} \int_0^{\pi} i_{L\_pk\_vdccs} \left(V_m \sin\theta\right) d\theta \tag{24(b)}$$

Where t_f value is 12ns for CMOS 20N60C.

5.4. THE LOSS CAUSED BY COPPER OF THE INDUCTOR

The inductor's copper loss with CDCCS and VDCCS can be found below as

$$P_{copper(cdccs)} = I^2_{rms(cdccs)Lf} R_{copper(Lf)} + I^2_{rms(cdccs)Hf} R_{copper(Hf)} \tag{25(a)}$$

$$P_{copper(vdccs)} = I^2_{rms(vdccs)Lf} R_{copper(Lf)} + I^2_{rms(vdccs)Hf} R_{copper(Hf)} \tag{25(b)}$$

Where $R_{copper(Lf)}$ is 0.16 and $R_{copper(Hf)}$ is 0.23.

The low frequency and high frequency of rms current can be found out by using below formula

$$I_{rms\_lf} = \sqrt{\frac{1}{\pi}\int_0^{\pi} i^2_{L\_ave} d\theta} = \sqrt{\frac{1}{\pi}\int_0^{\pi} \left[\frac{D_y^2 T_s v_g \left(v_g - V_o\right)}{2L_b V_o}\right]^2 d\theta} \tag{26(a)}$$

$$i_{rms\_hf} = \sqrt{\frac{1}{T_s}\int_0^{T_s} (i_L(t) - i_{L\_ave})^2 dt} \tag{26(b)}$$

$$I_{rms\_hf} = \sqrt{\frac{1}{\pi}\int_0^{\pi} i^2_{rms\_hf} d\theta} \tag{26(c)}$$

5.5. LOSS DUE TO CORE OF THE INDUCTOR

The loss caused by core of inductor with CDCCS and VDCCS is calculated as

$$P_{core(cdccs)} = \left[\int_0^{\pi} C_m f_{s(cdccs)}{}^x B_{ac(cdccs)}{}^y \left(ct_0 - ct_1 T_a - ct_2 T_a^2\right) d\theta\right] \frac{10^3 V_e}{\pi} \tag{27(a)}$$

$$B_{ac(cdccs)} = \frac{L i_{L\_pk\_cdccs}}{2NA_e} \tag{27(b)}$$

https://doi.org/10.17993/3ctecno.2021.specialissue7.35-51

$$P_{core(vdccs)} = \left[\int_0^{\pi} C_m f_{s(vdccs)}{}^{x} B_{ac(vdccs)}{}^{y} \left(ct_0 - ct_1 T_a - ct_2 T_a^2\right) d\theta\right] \frac{10^3 V_e}{\pi} \quad (27(c))$$

$$B_{ac(vdccs)} = \frac{Li_{L\_pk\_vdccs}}{2NA_e} \quad (27(d))$$

The value of core parameters can be found from [24].

5.6. THE LOSS DUE TO CONDUCTION OF THE FREEWHEELING DIODE

The conduction loss due to freewheeling diode with CDC and VDC control scheme is

$$P_{con\_freewheelingdiode(cdccs)} = \frac{V_{FD_{fw}}}{\pi} \int_0^{\pi} \frac{i_{pk(cdccs)}}{2} D_{off}\, d\theta \quad (28(a))$$

$$P_{con\_freewheelingdiode(vdccs)} = \frac{V_{FD_{fw}}}{\pi} \int_0^{\pi} \frac{i_{pk(vdccs)}}{2} D_{off}\, d\theta \quad (28(b))$$

The value of VFD is 0.67 for MUR 860 diode.

5.7. THE EFFICIENCY COMPARISON

The efficiency of DCM buck converter with CDC and VDC control scheme can be calculated as

$$\eta_{(cdccs)} = \frac{P_o}{\left[\begin{array}{l} P_o + P_{con\_bridge(cdccs)} + P_{con\_switches(cdccs)} + P_{off\_switches(cdccs)} \\ + P_{copper(cdccs)} + P_{core(cdccs)} + P_{con\_freewheelingdiode(cdccs)} \end{array}\right]} \quad (29(a))$$

$$\eta_{(vdccs)} = \frac{P_o}{\left[\begin{array}{l} P_o + P_{con\_bridge(vdccs)} + P_{con\_switches(vdccs)} + P_{off\_switches(vdccs)} \\ + P_{copper(vdccs)} + P_{core(vdccs)} + P_{con\_freewheelingdiode(vdccs)} \end{array}\right]} \quad (29(b))$$

From above equations and parameters of converter, the theoretical efficiency of converter with CDC and VDC control scheme is calculated and compared as shown in Figure 5. It can be concluded that efficiency of DCM buck converter has improved in case of VDC control scheme.

https://doi.org/10.17993/3ctecno.2021.specialissue7.35-51

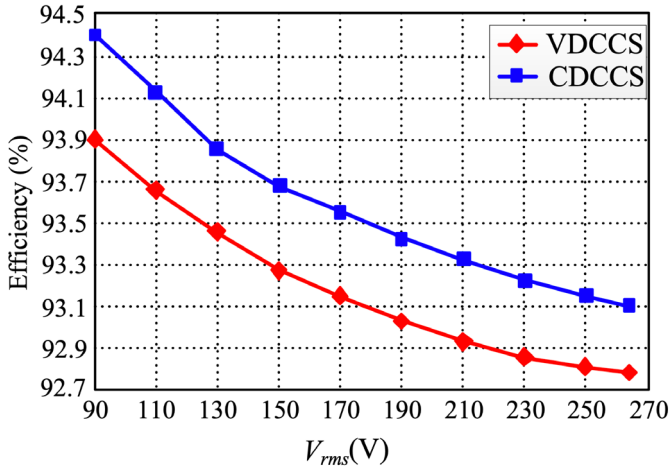

Figure 5. Efficiency at universal input voltage. Mathcad eq: (16-29).

6. SIMULATION RESULTS

For verifying the effectiveness of VDCCS strategy, simulations are carried out. The input voltage range is 90-264VAC, and the output is 80V. For ensuring the current to be in DCM, UC3525A IC is used. All the components in the circuit are selected as idea.

Figure 6 and Figure 7 show the simulation waveforms of input voltage, input current and output voltage of DCM buck converter with CDCCS and VDCCS at 220VAC inputs, respectively. It can be seen that the input current with VDCCS has less peaks as compared to input current with CDCCS is more sinusoidal as compared with CDCC.

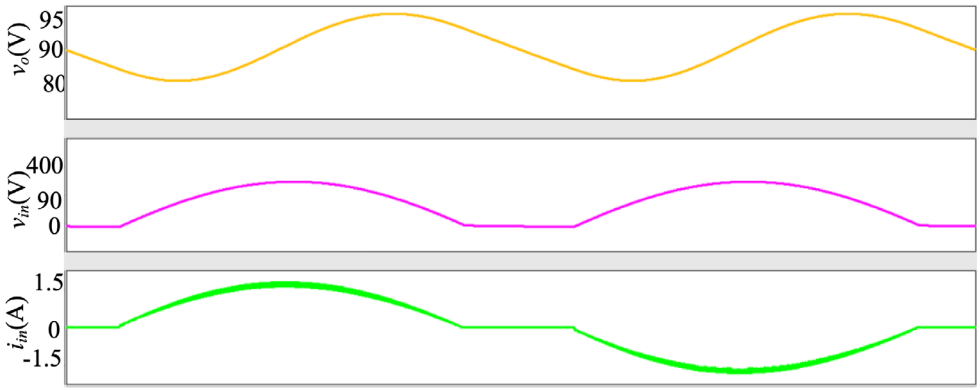

Figure 6. v_o, and v_{in}, i_{in} with CDC control scheme [Simulation waveform from Saber Software].

https://doi.org/10.17993/3ctecno.2021.specialissue7.35-51

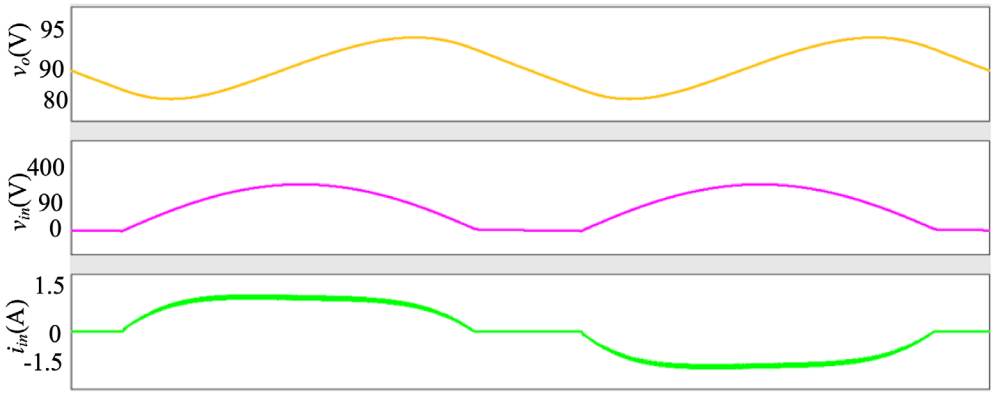

Figure 7. v_o, and v_{in}, i_{in} with VDC control scheme [Simulation waveform from Saber Software].

7. CONCLUSIONS

Electronic devices require AC to DC converter (rectifier) to convert AC voltage from the grid to DC voltage for the electronics and its result is low power factor (PF) and harmonic current injection into the system. Nowadays, power factor correction (PFC) converters are being widely used which can achieve high power factor (PF) and reduce the harmonics caused during AC to DC conversion and discontinuous conduction mode (DCM) buck PFC converter is one of mostly used converter. The DCM buck converter is generally utilized in many applications because of various advantages like maintaining high efficiency for the wide range of input voltage, cost reduction, low output voltage, protection against inrush current and life time improvement. However, its efficiency is low when operated with constant duty-cycle control scheme. For increasing the efficiency and ultimately reducing the losses of the DCM buck converter, a variable duty-cycle control scheme has been introduced. Fitting duty-cycle method is also discussed to make circuit implementation easier. For verifying the validity of proposed technique, the simulation results are carried out.

REFERENCES

Al Gabri, A. M., Fardoun, A. A., & Ismail, E. H. (2015). Bridgeless PFC-modified SEPIC rectifier with extended gain for universal input voltage applications. *IEEE Transactions on Power Electronics, 30*(8), 4272-4282. http://doi.org/10.1109/TPEL.2014.2351806

https://doi.org/10.17993/3ctecno.2021.specialissue7.35-51

Anwar, U., Erickson, R., Maksimović, D., & Afridi, K. K. (2017). A control architecture for low current distortion in bridgeless boost power factor correction rectifiers. In *2017 IEEE Applied Power Electronics Conference and Exposition (APEC)* (pp. 82-87). IEEE. http://doi.org/10.1109/APEC.2017.7930676

Badawy, M. O., Sozer, Y., & De Abreu-Garcia, J. A. (2016). A novel control for a cascaded buck–boost PFC converter operating in discontinuous capacitor voltage mode. *IEEE Transactions on Industrial Electronics, 63*(7), 4198-4210. http://doi.org/10.1109/TIE.2016.2539247

Endo, H., Yamashita, T., & Sugiura, T. (1992). A high-power-factor buck converter. In PESC'92 Record. In *23rd Annual IEEE Power Electronics Specialists Conference* (pp. 1071-1076). IEEE. http://doi.org/10.1109/TPEL.2010.2068060

Erickson, R. W., & Maksimovic, D. (2007). *Fundamentals of power electronics*. Springer Science & Business Media. https://www.springer.com/gp/book/9781475705591

Huber, L., Gang, L., & Jovanovic, M. M. (2009). Design-oriented analysis and performance evaluation of buck PFC front end. *IEEE Transactions on power electronics, 25*(1), 85-94. http://doi.org/10.1109/TPEL.2009.2024667

Jang, Y., & Jovanović, M. M. (2011). Bridgeless high-power-factor buck converter. *IEEE Transactions on Power Electronics, 26*(2), 602-611. http://doi.org/10.1109/TPEL.2010.2068060

Ki, S. K., & Lu, D. D. C. (2012). A high step-down transformerless single-stage single-switch AC/DC converter. *IEEE Transactions on Power Electronics, 28*(1), 36-45. http://doi.org/10.1109/TPEL.2012.2195505

Lamar, D. G., Fernandez, M., Arias, M., Hernando, M. M., & Sebastian, J. (2012). Tapped-inductor buck HB-LED AC–DC driver operating in boundary conduction mode for replacing incandescent bulb lamps. *IEEE Transactions on Power Electronics, 27*(10), 4329-4337. http://doi.org/10.1109/TPEL.2012.2190756

Lee, Y. S., Wang, S. J., & Hui, S. Y. R. (1997). Modeling, analysis, and application of buck converters in discontinuous-input-voltage mode operation. *IEEE Transactions on Power Electronics, 12*(2), 350-360. http://doi.org/10.1109/63.558762

Liu, X., Wan, Y., He, M., Zhou, Q., & Meng, X. (2020). Buck-Type Single-Switch Integrated PFC Converter With Low Total Harmonic Distortion. *IEEE Transactions on Industrial Electronics, 6.* http://doi.org/10.1109/TIE.2020.3007121

Memon, A. H., & Yao, K. (2018a). UPC strategy and implementation for buck–buck/boost PF correction converter. *IET Power Electronics, 11*(5), 884-894. http://doi.org/10.1049/iet-pel.2016.0919

Memon, A. H., Baloach, M. H., Sahito, A. A., Soomro, A. M., & Memon, Z. A. (2018b). Achieving High Input PF for CRM Buck-Buck/Boost PFC Converter. *IEEE Access, 6*, 79082-79093. http://doi.org/10.1109/ACCESS.2018.2879804

Memon, A. H., Memon, M. A., Memon, Z. A., & Hashmani, A. A. (2019a). Critical Conduction Mode Buck-Buck/Boost Converter with High Efficiency. *3C Tecnología. Glosas de innovación aplicadas a la pyme. Edición Especial, Noviembre 2019,* 201-219. http://dx.doi.org/10.17993/3ctecno.2019.specialissue3.201-219

Memon, A. H., Memon, Z. A., Shaikh, N. N., Sahito, A. A., & Hashmani, A. A. (2019b). Boundary conduction mode modified buck converter with low input current total harmonic distortion. *Indian Journal of Science and Technology, 12*, 17. https://doi.org/10.17485/ijst/2019/v12i17/144613

Memon, A. H., Nizamani, M. O., Memon, A. A., Memon, Z. A., & Soomro, A. M. (2019c). Achieving High Input Power Factor for DCM Buck PFC Converter by Variable Duty-Cycle Control. *3C Tecnología. Glosas de innovación aplicadas a la pyme. Edición Especial, Noviembre 2019,* 185-199. http://dx.doi.org/10.17993/3ctecno.2019.specialissue3.185-199

Memon, A. H., Noonari, F. M., Memon, Z., Farooque, A., & Uqaili, M. A. (2020a). AC/DC critical conduction mode buck-boost converter with unity power factor. *3C*

Tecnología. Glosas de innovación aplicadas a la pyme. Edición Especial, Abril 2020, 93-105. http://doi.org/10.17993/3ctecno.2020.specialissue5.93-105

Memon, A. H., Pathan, A. A., Kumar, M., & Sahito, A. J., & Memon, Z. A. (2019d). Integrated buck-flyback converter with simple structure and unity power factor. *Indian Journal of Science and Technology, 12,* 17. https://doi.org/10.17485/ijst/2019/v12i17/144612

Memon, A. H., Shaikh, N. N., Kumar, M., & Memon, Z. A. (2019e). Buck-buck/boost converter with high input power factor and non-floating output voltage. *International Journal of Computer Science and Network Security, 19(*4), 299-304. http://paper.ijcsns.org/07_book/201904/20190442.pdf

Memon, A. H., Yao, K., Chen, Q., Guo, J., & Hu, W. (2016). Variable-on-time control to achieve high input power factor for a CRM-integrated buck–flyback PFC converter. *IEEE Transactions on Power Electronics, 32*(7), 5312-5322. http://doi.org/10.1109/TPEL.2016.2608839

Memon, A. H., Samejo, J. A., Memon, Z. A., & Hashmani, A. A. (2020b). Realization Of Unity Power Factor For Ac/Dc Boundary Conduction Mode Flyback Converter With Any Specific Turn's Ratio. *Journal of Mechanics Of Continua And Mathematical Sciences,* (spl6). https://doi.org/10.26782/jmcms.spl.6/2020.01.00014

Memon, A. H., Shaikh, S. A., Memon, Z. A., Memon, A. A., & Memon, A. A. (2020c). DCM Boost Converter with High Efficiency. *Journal Of Mechanics Of Continua And Mathematical Sciences,* (spl6). https://doi.org/10.26782/jmcms.spl.6/2020.01.00006

Nussbaumer, T., Raggl, K., & Kolar, J. W. (2009). Design guidelines for interleaved single-phase boost PFC circuits. *IEEE Transactions on Industrial Electronics, 56*(7), 2559-2573. https://doi.org/10.1109/TIE.2009.2020073

Praneeth, A. V. J. S., & Williamson, S. S. (2018). A review of front end ac-dc topologies in universal battery charger for electric transportation. In *2018 IEEE Transportation Electrification Conference and Expo (ITEC)* (pp. 293-298). https://doi.org/10.1109/ITEC.2018.8450186

Spiazzi, G., & Buso, S. (2000). Power factor preregulators based on combined buck-flyback topologies. *IEEE transactions on Power Electronics, 15*(2), 197-204. https://doi.org/10.1109/63.838091

Williamson, S. S., Rathore, A. K., & Musavi, F. (2015). Industrial electronics for electric transportation: Current state-of-the-art and future challenges. *IEEE Transactions on Industrial Electronics, 62*(5), 3021-3032. https://doi.org/10.1109/TIE.2015.2409052

Yao, K., Zhou, X., Yang, F., Yang, S., Cao, C., & Mao, C. (2017). Optimum third current harmonic during nondead zone and its control implementation to improve PF for DCM buck PFC converter. *IEEE Transactions on Power Electronics, 32*(12), 9238-9248. https://doi.org/1109/TPEL.2017.2657883

https://doi.org/10.17993/3ctecno.2021.specialissue7.35-51

/03/

https://doi.org/10.17993/3ctecno.2021.specialissue7

WEB CONFERENCING SOFTWARE SELECTION WITH INTERVAL-VALUED FUZZY PARAMETERIZED INTUITIONISTIC FUZZY SOFT SETS

Esra Çakır
Department of Industrial Engineering, Galatasaray University, Istanbul, (Turkey).
E-mail: ecakir@gsu.edu.tr
ORCID: https://orcid.org/0000-0003-4134-7679

Ziya Ulukan
Department of Industrial Engineering, Galatasaray University, Istanbul, (Turkey).
E-mail: zulukan@gsu.edu.tr
ORCID: https://orcid.org/ 0000-0003-4805-2726

Recepción: 03/12/2020 **Aceptación:** 18/02/2021 **Publicación:** 07/05/2021

Citación sugerida:
Çakır, E., y Ulukan, Z. (2021). Web Conferencing Software Selection with Interval-Valued Fuzzy Parameterized Intuitionistic Fuzzy Soft Sets. *3C Tecnología. Glosas de innovación aplicadas a la pyme, Edición Especial,* (mayo 2021), 53-65. https://doi.org/10.17993/3ctecno.2021.specialissue7.53-65

ABSTRACT

Since COVID-19 has become a pandemic, education has been interrupted in many countries, and training has been temporarily resumed on online platforms. But it is difficult to determine which of the many existing web (or video) conferencing software is more suitable for class education. The aim of this study is to sort these platforms according to the criteria determined by experts and select the best one among different alternatives by using interval-valued fuzzy parameterized intuitionistic fuzzy soft sets. In the application, seven experts determined the six criteria and their interval-valued fuzzy weights depending on educational needs. The decision makers are evaluated ten video conferencing tools for educational institutions by using interval-valued fuzzy parameterized intuitionistic fuzzy soft sets. Finally, using the proper operators, the alternatives are sorted and the best video conferencing tool for class education. The results are intended to guide future research.

KEYWORDS

Fuzzy MCDM, Interval-valued fuzzy sets, Intuitionistic fuzzy soft sets, Web conferencing tool, Software selection.

https://doi.org/10.17993/3ctecno.2021.specialissue7.53-65

1. INTRODUCTION

Due to the Covid-19 epidemic, countries had to take a break from education for a while and sought new ways to continue. After curfews came in many countries, educational institutions started looking for a suitable online video conferencing platform. These software allow participants to conduct or attend meetings via the internet. They enable remote meetings based on VoIP, online video, instant messaging, file sharing, and screen sharing. Online video conferencing is fundamental to many organizations conduct business in recent years. However, it has also become a must for formal education since the announcement of the pandemic.

Web conferencing software includes presentations or webinars, conference calls, video meetings with multiple participants, running product demos and training, one-on-one meetings with remote employees and face-to-face customer support. They are also useful in enhancing communications, reducing travel costs and increasing efficiency (Grant & Cheon, 2007; Roehrs, 2013). By synchronous web conference communication, the gap between digital technologies and face-to-face teaching can be filled and this also encourages students to be attracted toward learning and in support of their self-working (Nedeva, Dineva & Atanasov, 2014).

In order to adapt these platforms, which are very advantageous in the period when they are obliged to distance education, to their systems quickly and reliably, institutions should make decisions according to some criteria. Therefore, it is necessary to use expert opinions to select them and uncertainties views must also be considered. The fuzzy set proposed by Zadeh (1965) and improved by Atanassov (1986) as intuitionistic fuzzy sets are suitable for this application. Also, interval valued fuzzy sets (Atanassov & Gargov, 1989) and intuitionistic fuzzy soft sets (Molodtsov, 1999) can sort alternatives and the robustness of their combined version has been proven (Nedeva *et al.*, 2014). Jiang *et al.* (2010) proposed the notion of the interval-valued intuitionistic fuzzy soft set theory. It is an interval-valued fuzzy extension of the intuitionistic fuzzy soft set theory or an intuitionistic fuzzy extension of the interval-valued fuzzy soft set theory. The basic properties of the interval-valued intuitionistic fuzzy soft sets are also presented in their study. Deli and Karataş (2016) defined interval-valued intuitionistic fuzzy parameterized soft sets by combining the interval-valued

https://doi.org/10.17993/3ctecno.2021.specialissue7.53-65

intuitionistic fuzzy sets and the soft sets from parametrization point of view. By using soft level sets, they construct a parameter reduction method. Tripathy and Panigrahi (2016) extend hybrid model of interval valued fuzzy set and soft set to define interval valued intuitionistic fuzzy parameterized soft set (IVIFPSS) and establish their properties. They put forth two algorithms in decision-making. Aydın and Enginoğlu (2020) proposed the concept of interval-valued intuitionistic fuzzy parameterized interval-valued intuitionistic fuzzy soft sets (d-sets) and presents several of its basic properties. By using d-sets, they suggest a new soft decision-making method and apply it to a problem concerning the eligibility of candidates for two vacant positions in an online job advertisement.

The contribution of this study to the existing literature is to sort web conferencing platforms according to the criteria determined by experts and select the best one among ten options by using interval valued fuzzy parameterized intuitionistic fuzzy soft sets.

The rest of the article is organized as follows. Section 2 examines preliminaries and ranking methodology of interval valued fuzzy parameterized intuitionistic fuzzy soft sets. Section 3 presents numerical application in the selection of web conferencing tool. Conclusion of the study are stated in Section 4, along with future research.

2. METHODOLOGY

In this section, the preliminaries and definitions of the interval valued fuzzy parameterized intuitionistic fuzzy soft sets (IVFPIFS) and aggregation operator are introduced. The steps of methodology are given at the end of the section.

2.1. PRELIMINARIES

Definition 1. (Atanassov & Gargov, 1989) Let A be a collection of objects (points) denoted by a_1. Also, let ([0,1]) be the set of all closed subintervals of the interval [0,1]. Then, an interval-valued intuitionistic fuzzy set (*IVIFS*) $\tilde{Z}$ in A is defined as

$$Z = \{\prec \gamma_Z^+ , \gamma_Z^- \succ / a_i : a_i \in A\} \quad (1)$$

where $\gamma_Z^+ = [\underline{\gamma_Z^+}(a_i), \overline{\gamma_Z^+}(a_i)]$, $\gamma_Z^- = [\underline{\gamma_Z^-}(a_i), \overline{\gamma_Z^-}(a_i)]: A \longrightarrow Int([0,1])$ are respectively called the membership function and the non-membership function of $\tilde{Z}$ with property $0 \leq \underline{\gamma_Z^+}(a_i) +$

https://doi.org/10.17993/3ctecno.2021.specialissue7.53-65

$\underline{\gamma_Z^-}(a_i) \leq 1$ and $0 \leq \overline{\gamma_Z^+}(a_i) + \overline{\gamma_Z^-}(a_i) \leq 1$. The values $\underline{\gamma_Z^+}(a_i)$ and $\overline{\gamma_Z^+}(a_i)$ denote the lower and upper degrees of membership of the element $a_i \in A$, and also the values $\underline{\gamma_Z^-}(a_i)$ and $\overline{\gamma_Z^-}(a_i)$ denote the lower and upper degrees of non-membership of the element $a_i \in A$, respectively. Note that γ_i^+ and γ_i^- notations can be use instead of $\gamma_Z^+(a_i)$ and $\gamma_Z^-(a_i)$ for $a_i \in A$.

Definition 2. (Atanassov & Gargov, 1989) Let $\gamma_1 = \prec [\underline{\gamma_1^+}, \overline{\gamma_1^+}], [\underline{\gamma_1^-}, \overline{\gamma_1^-}] \succ$ and $\gamma_2 = \prec [\underline{\gamma_2^+}, \overline{\gamma_2^+}], [\underline{\gamma_2^-}, \overline{\gamma_2^-}] \succ$ be two IVIF values. Then, the operations $\oplus$ and $\otimes$ for γ_1 and γ_2 are respectively defined as follows:

$$\gamma_1 \oplus \gamma_2 = \prec [\underline{\gamma_1^+} + \underline{\gamma_2^+} - \underline{\gamma_1^+}.\underline{\gamma_2^+}, \overline{\gamma_1^+} + \overline{\gamma_2^+} - \overline{\gamma_1^+}.\overline{\gamma_2^+}], [\underline{\gamma_1^-}.\underline{\gamma_2^-}, \overline{\gamma_1^-}.\overline{\gamma_2^-}] \succ \quad (2)$$

$$\gamma_1 \otimes \gamma_2 = \prec [\underline{\gamma_1^+}.\underline{\gamma_2^+}, \overline{\gamma_1^+}.\overline{\gamma_2^+}], [\underline{\gamma_1^-} + \underline{\gamma_2^-} - \underline{\gamma_1^-}.\underline{\gamma_2^-}, \overline{\gamma_1^-} + \overline{\gamma_2^-} - \overline{\gamma_1^-}.\overline{\gamma_2^-}] \succ \quad (3)$$

Definition 3. (Tan, 2011; Xu, 2010) Let $\gamma_i = \prec \gamma_i^+, \gamma_i^- \succ = \prec [\underline{\gamma_i^+}, \overline{\gamma_i^+}], [\underline{\gamma_i^-}, \overline{\gamma_i^-}] \succ$ be the IVIF value of $a_i \in A$,. Then, the score function and accuracy function of γ_1 are respectively defined as follows:

$$s(\gamma_i) = \frac{1}{2}(\underline{\gamma_i^+} - \underline{\gamma_i^-} + \overline{\gamma_i^+} - \overline{\gamma_i^-}) \quad (4)$$

$$a(\gamma_i) = \frac{1}{2}(\underline{\gamma_i^+} + \underline{\gamma_i^-} + \overline{\gamma_i^+} + \overline{\gamma_i^-}) \quad (5)$$

To compare two IVIF values γ_1 and γ_2, a ranking method is defined as follows:

If $s(\gamma_1) < s(\gamma_2)$ then $\gamma_1 < \gamma_2$,

If $s(\gamma_1) = s(\gamma_2)$ then

if $a(\gamma_1) < a(\gamma_2)$ then $\gamma_1 < \gamma_2$.

if $a(\gamma_1) = a(\gamma_2)$ then $\gamma_1 = \gamma_2$.

Definition 4. Let *U* be a universal set and C be the set of parameters. Also, let I be an interval-valued fuzzy set over C with the membership function ω_1:C $\rightarrow$ *Int*([0,1]). Then, an interval-valued fuzzy parameterized intuitionistic fuzzy soft set (IVFPIFS set) Ψ_X on *U* is a set of ordered pairs

https://doi.org/10.17993/3ctecno.2021.specialissue7.53-65

$$\Psi_I = \{(\omega_I(c_j)/c_j, \psi_I(c_j)): c_j \in C, \psi_I(c_j) \in IFS(U)\} \quad (6)$$

where the function ψ_I: C $\longrightarrow$ $IFS(U)$ such that $\psi_I(c_j) = \emptyset$ if $\omega_I(c_j) = [\underline{\omega_I}(c_j), \overline{\omega_I}(c_j)] = [0,0]$. Note that *IVFPIF(U)* notation denotes the set of all interval-valued fuzzy parameterized intuitionistic fuzzy soft sets on *U*.

Definition 5. Let $\Psi_I = \{(\omega_j/c_j, \{\prec \gamma_{ij}^+, \gamma_{ij}^- \succ /a_i: a_i \in U\}): c_j \in C$ be an IVFPIFS set,where $\gamma_{ij} = \prec \gamma_{ij}^+, \gamma_{ij}^- \succ \ i = 1,2,\ldots,n$ indicates an intuitionistic fuzzy value when the alternative a_1 is assessed with respect to the parameter c_j and $\omega_I(c_j) = \omega_j = [\underline{\omega_j}, \overline{\omega_j}]$ indicates an interval-valued fuzzy value of the parameter c_j. Then,

- the first IVFPIFS-aggregation operator, denoted by $\text{IVFPIFS}_{\text{aggr}}^1$, is defined by

$$\text{IVFPIFS}_{\text{aggr}}^1 : (C) \times IVFPIFSS(U) \longrightarrow IVIFS(U), \ \text{IVFPIFS}_{\text{aggr}}^1(I, \dot{\Psi}_I) = \dot{\Psi}_I \quad (7)$$

where $\dot{\Psi}_I = \{\prec [\underline{\dot{\gamma}_i^+}, \overline{\dot{\gamma}_i^+}], [\underline{\dot{\gamma}_i^-}, \overline{\dot{\gamma}_i^-}] \succ /a_i: a_i \in U\}$ which is an interval-valued intuitionistic fuzzy set on *U*. The membership degree $\dot{\gamma}_i^+ = [\underline{\dot{\gamma}_i^+}, \overline{\dot{\gamma}_i^+}]$ and the non-membership degree $\dot{\gamma}_i^- = [\underline{\dot{\gamma}_i^-}, \overline{\dot{\gamma}_i^-}]$ of $a_i \in U$ is defined as follows:

$$\dot{\gamma}_i^+ = [1 - \prod_{j=1}^m (1 - \underline{\omega_j} \cdot \gamma_{ij}^+), 1 - \prod_{j=1}^m (1 - \overline{\omega_j} \cdot \gamma_{ij}^+)] \quad (8)$$

$$\dot{\gamma}_i^- = [\prod_{j=1}^m \underline{\omega_j} \cdot \gamma_{ij}^-, \prod_{j=1}^m \overline{\omega_j} \cdot \gamma_{ij}^-] \quad (9)$$

where *m* denotes the number of parameters in C.

- the second IVFPIFS-aggregation operator, denoted by $\text{IVFPIFS}_{\text{aggr}}^1$, is defined by

$$\text{IVFPIFS}_{\text{aggr}}^2 : (C) \times IVFPIFSS(U) \longrightarrow IVIFS(U), \ \text{IVFPIFS}_{\text{aggr}}^2(I, \dot{\Psi}_I) = \ddot{\Psi}_I \quad (10)$$

where $\ddot{\Psi}_I = \{\prec [\underline{\ddot{\gamma}_i^+}, \overline{\ddot{\gamma}_i^+}], [\underline{\ddot{\gamma}_i^-}, \overline{\ddot{\gamma}_i^-}] \succ /a_i: a_i \in U\}$ which is an interval-valued intuitionistic fuzzy set on *U*. The membership degree $\ddot{\gamma}_i^+ = [\underline{\ddot{\gamma}_i^+}, \overline{\ddot{\gamma}_i^+}]$ and the non-membership degree $\ddot{\gamma}_i^- = [\underline{\ddot{\gamma}_i^-}, \overline{\ddot{\gamma}_i^-}]$ of $a_i \in U$ is defined as follows:

$$\ddot{\gamma}_i^+ = [\prod_{j=1}^m \underline{\omega_j} \cdot \gamma_{ij}^+, \prod_{j=1}^m \overline{\omega_j} \cdot \gamma_{ij}^+] \quad (11)$$

$$\ddot{\gamma}_i^- = [1 - \prod_{j=1}^m (1 - \underline{\omega_j} \cdot \gamma_{ij}^-), 1 - \prod_{j=1}^m (1 - \overline{\omega_j} \cdot \gamma_{ij}^-)] \quad (12)$$

where *m* denotes the number of parameters in C.

https://doi.org/10.17993/3ctecno.2021.specialissue7.53-65

2.2. ALGORITHM

This methodology is stated for multi criteria decision making problem. It uses interval valued fuzzy parameterized intuitionistic fuzzy soft sets to express decision makers opinion and generate interval valued intuitionistic fuzzy sets by using two different aggregation operators (Nedeva *et al.*, 2014). Score and accuracy functions help to sort the alternatives and to select best option. The steps of this methodology are as follows:

- *Step 1*: Set the problem. a_i indicates alternative *i*.
- *Step 2:* Select experts and determine criteria with weights by experts. C_j indicates criterion j and its interval-valued fuzzy weight is expressed as $\omega_j = [\underline{\omega_j}, \overline{\omega_j}]$.
- *Step 3:* Collect the fuzzy decision matrices with IVFPIFS set by experts and aggregate them by fuzzy geometric mean method of Buckley (Buckley, 1985).
- *Step 4:* Obtain the first and second aggregate interval-valued intuitionistic fuzzy set $\prec \dot{\gamma}_i^+, \dot{\gamma}_i^- \succ$ and $\prec \ddot{\gamma}_i^+, \ddot{\gamma}_i^- \succ$ of alternatives by using IVFPIFS-aggregation operators given in Def. 5.
- *Step 5:* Calculate the IVIF values $\ddot{\gamma}_i = \prec \ddot{\gamma}_i^+, \ddot{\gamma}_i^- \succ$ of alternatives by applying $\oplus$ operation given in Def. 2.
- *Step 6*: By using the score function and accuracy function on IVIF values given in Def. 3, compare the alternatives and set the highest score alternative as the best option.

3. APPLICATION

After being declared COVID-19 pandemic, educational institutions in many countries took a break for a while. In order not to fall behind in education, many institutions have evaluated opportunities for distance education. With the web (or video) conferencing software, teachers had the chance to teach their classes during the periods they set. However, these systems had to be selected and adapted to the institutions in a very short time. So, it is a problem to determine which service is better. In this application, the alternatives are evaluated, and the criteria are determined with the help of experts in Turkey. Platforms are ranked using interval valued fuzzy parameterized intuitionistic fuzzy soft sets, and the alternative with

https://doi.org/10.17993/3ctecno.2021.specialissue7.53-65

the highest score is evaluated as the best platform. According to the previous section, this application is implemented step by step as follows:

- *Step 1:* Web conferencing software used in Turkey selection is set as the problem. The ten most frequently used software during the pandemic period are determined as alternatives. The alternatives are presented as $A=\{a_1, a_2, a_3, a_4, a_5, a_6, a_7, a_8, a_9, a_{10}\}$.
- *Step 2:* Seven experts are selected, and they determined the criteria depending on educational needs and the features of tools. These criteria are given with their interval-valued fuzzy weights in Table 1.

Table 1. The criteria for web conferencing software selection with their interval-valued fuzzy weights.

Criteria code	Criteria	Interval-valued fuzzy weights "ω_i"
c_1	Performance and Compatibility	[0.6, 0.9]
c_2	File and Screen Sharing	[0.3, 0.5]
c_3	Online Meeting Quality and Recording	[0.6, 0.8]
c_4	Implementation	[0.4, 0.7]
c_5	Security	[0.7, 0.9]
c_6	Support System	[0.5, 0.8]

Source: own elaboration.

- *Step 3:* Experts decided on the degree of membership of alternatives to specified criteria with IVFPIFS set expressions and their decision matrices are aggregated by fuzzy geometric mean method of Buckley. The aggregated decision matrix is represented in Table 2.

Table 2. The aggregated IVFPIFS decision matrix.

Crt. / Alt.	c_1	c_2	c_3	c_4	c_5	c_6
	ω_1 = [0.6,0.9]	ω_2 = [0.3,0.5]	ω_3 = [0.6,0.8]	ω_4 = [0.4,0.7]	ω_5 = [0.7,0.9]	ω_6 = [0.5,0.8]
a_1	<0.72, 0.22>	<0.68, 0.21>	<0.86, 0.12>	<0.67, 0.22>	<0.67, 0.21>	<0.63, 0.36>
a_2	<0.71, 0.19>	<0.66, 0.33>	<0.83, 0.11>	<0.32, 0.51>	<0.63, 0.18>	<0.51, 0.48>
a_3	<0.63, 0.31>	<0.62, 0.15>	<0.73, 0.23>	<0.51, 0.38>	<0.65, 0.25>	<0.49, 0.51>
a_4	<0.65, 0.33>	<0.6, 0.38>	<0.82, 0.1>	<0.59, 0.24>	<0.6, 0.22>	<0.48, 0.4>
a_5	<0.68, 0.29>	<0.63, 0.27>	<0.82, 0.05>	<0.65, 0.22>	<0.63, 0.2>	<0.54, 0.37>
a_6	<0.65, 0.23>	<0.67, 0.33>	<0.78, 0.22>	<0.49, 0.36>	<0.63, 0.14>	<0.4, 0.55>

https://doi.org/10.17993/3ctecno.2021.specialissue7.53-65

a_7	<0.68, 0.17>	<0.62, 0.3>	<0.77, 0.09>	<0.62, 0.23>	<0.59, 0.31>	<0.55, 0.42>
a_8	<0.66, 0.24>	<0.63, 0.29>	<0.73, 0.14>	<0.66, 0.21>	<0.65, 0.24>	<0.55, 0.36>
a_9	<0.59, 0.4>	<0.45, 0.46>	<0.69, 0.15>	<0.52, 0.31>	<0.54, 0.28>	<0.34, 0.58>
a_{10}	<0.62, 0.26>	<0.56, 0.41>	<0.74, 0.22>	<0.48, 0.36>	<0.5, 0.31>	<0.63, 0.33>

Source: own elaboration.

- *Step 4:* The first and second aggregate interval-valued intuitionistic fuzzy set $\prec \dot{\gamma}_i^+, \dot{\gamma}_i^- \succ$ and $\prec \ddot{\gamma}_i^+, \ddot{\gamma}_i^- \succ$ of alternatives by using IVFPIFS-aggregation operators are obtained as in Table 3.

Table 3. The aggregate interval-valued intuitionistic fuzzy sets of alternatives.

Alt.	$\prec \dot{\gamma}_i^+, \dot{\gamma}_i^- \succ = \prec \left[\underline{\dot{\gamma}_i^+}, \overline{\dot{\gamma}_i^+}\right], \left[\underline{\dot{\gamma}_i^-}, \overline{\dot{\gamma}_i^-}\right] \succ$	$\prec \ddot{\gamma}_i^+, \ddot{\gamma}_i^- \succ = \prec \left[\underline{\ddot{\gamma}_i^+}, \overline{\ddot{\gamma}_i^+}\right], \left[\underline{\ddot{\gamma}_i^-}, \overline{\ddot{\gamma}_i^-}\right] \succ$
a_1	<[0.94173, 0.99242], [0.0000013, 0.0000167]>	<[0.0018, 0.021605], [0.518534, 0.683016]>
a_2	<[0.91607, 0.98383], [0.0000045, 0.0000551]>	<[0.000604, 0.007255], [0.605775, 0.79045]>
a_3	<[0.906801, 0.97983], [0.0000078, 0.000094]>	<[0.0007003, 0.008403], [0.65074, 0.81673]>
a_4	<[0.914425, 0.983378], [0.000004, 0.000048]>	<[0.000821, 0.009859], [0.59133, 0.762296]>
a_5	<[0.92635, 0.98774], [0.0000009, 0.0000115]>	<[0.001174, 0.014094], [0.52932, 0.700298]>
a_6	<[0.90677, 0.97992], [0.0000069, 0.0000839]>	<[0.000634, 0.007610], [0.62262, 0.800249]>
a_7	<[0.917029, 0.98471], [0.000002, 0.0000249]>	<[0.000987, 0.01185], [0.565806, 0.731641]>
a_8	<[0.91994, 0.98553], [0.0000026, 0.0000320]>	<[0.001082, 0.012994], [0.55262, 0.716573]>
a_9	<[0.86611, 0.961247], [0.000021, 0.0002521]>	<[0.000264, 0.003173], [0.70188, 0.863861]>
a_{10}	<[0.895486, 0.97648], [0.000013, 0.0001567]>	<[0.000587, 0.00704], [0.640429, 0.800823]>

Source: own elaboration.

- *Step 5:* The IVIF values $\dddot{\gamma}_i = \prec \dddot{\gamma}_i^+, \dddot{\gamma}_i^- \succ$ of alternatives by applying $\oplus$ operation is calculated as in Table 4.
- *Step 6:* The scores and accuracy values of IVIF values are presented in Table 5.

Table 4. The interval valued intuitionistic fuzzy values of alternatives.

Alt.	$\dddot{\gamma}_i = \prec \dddot{\gamma}_i^+, \dddot{\gamma}_i^- \succ = \prec \dot{\gamma}_i^+, \dot{\gamma}_i^- \succ \oplus \prec \ddot{\gamma}_i^+, \ddot{\gamma}_i^- \succ$
a_1	<[0.94184, 0.992584], [0.000000722, 0.0000114]>
a_2	<[0.916128, 0.983951], [0.00000278,784538, 0.0000435]>
a_3	<[0.906867, 0.9800047], [0.00000509,652078, 0.0000767]>
a_4	<[0.914496, 0.983541], [0.00000236,637966, 0.0000366]>

https://doi.org/10.17993/3ctecno.2021.specialissue7.53-65

a_5	<[0.926436, 0.987917], [0.00000051,809846133,180987]>
a_6	<[0.906831, 0.980079], [0.000004357,035645, 0.0000672]>
a_7	<[0.917111, 0.984898], [0.00000117,284747, 0.0000182]>
a_8	<[0.920028, 0.985722], [0.00000147,515918, 0.0000229]>
a_9	<[0.866147, 0.96137008], [0.0000147, 0.0002177]>
a_{10}	<[0.8955477, 0.9766463], [0.00000836,714534, 0.0001254]>

Source: own elaboration.

Table 5. The scores of alternatives.

Alternative	Score s(a_1)	Accuracy a(a_1)
a_1	-0.02538	0.967219
a_2	-0.03393	0.950064
a_3	-0.0366	0.943477
a_4	-0.03454	0.949039
a_5	-0.03074	0.957181
a_6	-0.03666	0.943491
a_7	-0.0339	0.951015
a_8	-0.03286	0.952888
a_9	-0.04771	0.913875
a_{10}	-0.04061	0.936164

Source: own elaboration.

According to the scores, the ranking of the alternatives is $a_1>a_5>a_8>a_7>a_2>a_4>a_3>a_6>a_{10}>a_9$. Since a_1 has the highest score, it is selected as the best option for education institutions based on determined criteria and expert's opinions.

4. CONCLUSIONS

Due to the COVID-19 outbreak, interest in web conferencing platforms has increased in educational institutions around the world. Since there are many different options, which software institutions choose is an important issue. The aim of this study is to compare ten video conferencing software according to the criteria determined by the experts with their imprecise opinions and to choose the best option by using interval valued fuzzy parameterized intuitionistic fuzzy soft sets. As a result of the study, alternatives are listed as

https://doi.org/10.17993/3ctecno.2021.specialissue7.53-65

$a_1 > a_5 > a_8 > a_7 > a_2 > a_4 > a_3 > a_6 > a_{10} > a_9$ and "a_1" platform is chosen as the best video conferencing tool for educational institutions according to the determined criteria.

5. ACKNOWLEDGEMENTS

This work has been supported by the Scientific Research Projects Commission of Galatasaray University under grant number # FBA-2020-1036.

REFERENCES

Atanassov, K. T. (1986) Intuitionistic fuzzy sets. *Fuzzy Sets and Systems, 20*(1), 87-96. https://doi.org/10.1016/S0165-0114(86)80034-3

Atanassov, K., & Gargov, G. (1989). Interval-valued intuitionistic fuzzy sets. *Fuzzy Sets and Systems, 31*(3), 343-349. https://doi.org/10.1016/0165-0114(89)90205-4

Aydin, T., & Enginoglu, S. (2020). Interval-valued intuitionistic fuzzy parameterized interval-valued intuitionistic fuzzy soft sets and their application in decision making. *Journal of Ambient Intelligence and Humanized Computing, 12*, 1541-1558. https://doi.org/10.1007/s12652-020-02227-0

Buckley, J. J. (1985). Fuzzy hierarchical analysis. *Fuzzy sets and Systems, 17*(3), 233-247. https://doi.org/10.1016/0165-0114(85)90090-9

Deli, I., & Karataş, S. (2016). Interval Valued Intuitionistic Fuzzy Parameterized Soft Set Theory and Its Decision Making. *Journal of Intelligent & Fuzzy Systems, 30*(4), 2073-2082.https://www.researchgate.net/publication/298735300_Interval_valued_intuitionistic_fuzzy_parameterized_soft_set_theory_and_its_decision_making

Grant, M. M., & Cheon, J. (2007). The value of using synchronous conferencing for instruction and students. *Journal of Interactive Online Learning, 6*(3), 211-226. https://citeseerx.ist.psu.edu/viewdoc/download?doi=10.1.1.530.1145&rep=rep1&type=pdf

Jiang, Y., Tang, Y. Chen, Q., Liu, H., & Tang, J. (2010). Interval-valued intuitionistic fuzzy soft sets and their properties. *Computers and Mathematics with Applications, 60*(3), 906-918. https://doi.org/10.1016/j.camwa.2010.05.036

https://doi.org/10.17993/3ctecno.2021.specialissue7.53-65

Molodtsov, D. (1999). Soft set theory-first results. *Computers & Mathematics with Applications, 37*(4-5), 19-31. https://doi.org/10.1016/S0898-1221(99)00056-5

Nedeva, V., Dineva, S., & Atanasov, S. (2014). Effective E-learning Course With Web Conferencing. In *V-th National Conference of E-Learning, Ruse, Bulgaria*. https://doi.org/10.13140/2.1.2605.6648

Roehrs, B. (2013). *Providing online classes with big bluebutton 2013-09-30a*. http://www.slideshare.net/roehrsb/providing-on-line-classes-ith-big-bluebutton-20130930a

Tan, C. (2011). A multi-criteria interval-valued intuitionistic fuzzy group decision making with Choquet integral-based TOPSIS. *Expert Systems with Applications, 38*(4), 3023-3033. https://doi.org/10.1016/j.eswa.2010.08.092

Tripathy, B. K., & Panigrahi, A. (2016). Interval-valued intuitionistic fuzzy parameterized soft set theory and its application in decision-making. In *10th International Conference on Intelligent Systems and Control (ISCO)*, 1-6. https://doi.org/10.1109/ISCO.2016.7726952

Xu, Z. (2010). Choquet integrals of weighted intuitionistic fuzzy information. Information Sciences, 180(5), 726-736. https://doi.org/10.1016/j.ins.2009.11.011

Zadeh, L. A. (1965). Fuzzy sets. *Information and Control, 8*(3), 338–353. https://doi.org/10.1016/S0019-9958(65)90241-X

https://doi.org/10.17993/3ctecno.2021.specialissue7.53-65

https://doi.org/10.17993/3ctecno.2021.specialissue7.53-65

/04/

https://doi.org/10.17993/3ctecno.2021.specialissue7

MODIFIED VARIABLE ON-TIME CONTROL SCHEME TO REALIZE HIGH POWER FACTOR FOR AC/DC INTEGRATED BUCK-BOOST CONVERTER

Abdul Hakeem Memon
Institute of Information and Communication Technologies (IICT),
Mehran UET, Jamshoro, Sindh, (Pakistan).
E-mail: hakeem.memon@faculty.muet.edu.pk
ORCID: https://orcid.org/0000-0001-8545-3823

Nazia Memon
Institute of Information and Communication Technologies (IICT),
Mehran UET, Jamshoro, Sindh, (Pakistan).
E-mail: naziamemon52@gmail.com
ORCID: https://orcid.org/0000-0003-2919-9220

Zubair Ahmed Memon
Institute of Information and Communication Technologies (IICT),
Mehran UET, Jamshoro, Sindh, (Pakistan).
E-mail: zubair.memon@faculty.muet.edu.pk
ORCID: https://orcid.org/0000-0001-5967-3152

Recepción: 09/12/2020 **Aceptación:** 10/03/2021 **Publicación:** 07/05/2021

Citación sugerida:
Memon, A. H., Memon, N., y Memon, Z. A. (2021). Modified variable on-time control scheme to realize high power factor for AC/DC integrated buck-boost converter. *3C Tecnología. Glosas de innovación aplicadas a la pyme, Edición Especial*, (mayo 2021), 67-81. https://doi.org/10.17993/3ctecno.2021.specialissue7.67-81

ABSTRACT

In today's modern era low power factor (PF) is major issue in the field of power electronics which has made our life, simpler, easier and comfortable. However, with this comfort and easiness this technology brings power quality issues because it is centered on solid-state devices. These issues introduce harmonic contained current or distorted current which has several drawbacks like high power loss, voltage distortion and EMI compatibility issues etc. The conventional boundary conduction mode (BCM) integrated buck-boost converter (BBC) operating with constant on-time control (COT) control scheme have low PF with high total harmonic distortion (THD) because of harmonic contained input current waveform. So, in order to make the input current waveform as a sinusoidal by changing the on-time of only buck switch, a modified variable-on-time (VOT) control scheme for Integrated BBC is proposed in this paper. The VOT control scheme can achieve high PF with low THD by utilizing the input and output voltage to modulate the on-time of only buck switch. The theoretical analysis is given, and the simulation results confirm the advantages of the proposed control scheme. The object of the research paper is to propose the control scheme to realize unity PF for CRM buck converter by only modulating the on-time of buck switch. The research methodology is based on: Input PF analysis of buck converter with traditional control scheme; Introduction of proposed control scheme; comparative analysis and simulation results to show the effectiveness of proposed control scheme.

KEYWORDS

Buck-Boost Converter (BBC), Constant On-Time Control (COT), Variable-On-Time (VOT), Power Factor (PF), Total Harmonic Distortion (THD), Electromagnetic Interference (EMI).

https://doi.org/10.17993/3ctecno.2021.specialissue7.67-81

1. INTRODUCTION

Power electronic technology is employed in various sorts of modern equipment's which has made our life, simpler, easier and comfortable. However, with this comfort and easiness this technology brings power quality issues because it is centered on solid-state devices. These issues introduce harmonic contained current or distorted current which has several drawbacks like high power loss, voltage distortion and EMI compatibility issues etc. Therefore, the standards are set by various industrious like IEC61000-3-2 limit and IEEE 519 (IEC Standard, 61000-3, n.d.); Langella, Testa, & Alii, 2014) to limit these harmonics. In order to meet relevant harmonic standard and reducing input current distortion, various researchers have proposed different types of power factor correction (PFC) converters (García *et al.*, 2003; Singh *et al.*, 2011; Memon *et al.*, 2016; Memon *et al.*, 2018a, 2018b; Memon *et al.*, 2019a, 2019b, 2019c, 2019d, 2019e; Memon *et al.*, 2020a, 2020b, 2020c). The DC/DC converters or choppers such as buck, boost and buck-boost etc. are normally employed for PFC application.

Each converter has its own advantages and disadvantages. The boost converter is good selection for PFC due to various advantages like high PF, less current ripples and high efficiency (Yang *et al.*, 2011), However, its efficiency is low at low input line due to use of more duty-cycle when the input is 90Vrms and the output is 400 V . The buck-boost converter can step up or step down the input voltage and its characteristics are better as compared to SEPIC, Flyback and CUK converter. However, its efficiency is low, voltage and current stress is more compared to boost and buck converter because the energy of output is charged from inductor (Chen & Maksimović, 2010; Hwang & Park, 2012).

The buck converter now days have attracted the attention of the many researchers (Mahdavi & Farzanehfard, 2010; Liu *et al.*, 2014; Wu *et al.*, 2011; Wu *et al.*, 2012; Memon *et al.*, 2016; Memon *et al.*, 2018a, 2018b; Memon *et al.*, 2019a, 2019b, 2019c, 2019d, 2019e; Liu *et al.*, 2020). It can maintain high efficiency at all input voltages. It also offers other advantages like cost reduction, low output voltage, protection against inrush current, low stress on the switch and life time improvement.

https://doi.org/10.17993/3ctecno.2021.specialissue7.67-81

The input PF of buck converter in low because of dead zone in the average input current that is present until input voltage is more than output voltage. It causes the input current to contain large harmonic disturbances.

For modifying the performance of buck converter, various researchers have proposed various techniques and control schemes. Many research attempts have been conducted to improve the performances of the conventional buck PFC converter (Mahdavi & Farzanehfard, 2010; Liu *et al.*, 2014; Wu *et al.*, 2011; Wu *et al.*, 2012; Memon *et al.*, 2016; Memon *et al.*, 2018a, 2018b; Memon *et al.*, 2019a, 2019b, 2019c, 2019d, 2019e; Liu *et al.*, 2020).

This paper is divided into six sections. In section 2, the operation states of BCM IBBC are analyzed with traditional constant on-time control scheme (COTCS). The introduced VOTCS is discussed in section 3. Then the comparative analysis is discussed in section 4 in terms of PF. In section 5, the effectiveness of proposed topology is evaluated by simulation results. Finally, some conclusions are drawn in section 6.

2. RESEARCH METHODOLOGY

The research methodology is based on:

1. Mathematical analysis of the operating principle of the traditional control scheme for BCM IBBC with the help of MATHCAD software.
2. Analysis of input PF of BCM integrated BBC.
3. Introducing the proposed control scheme to obtain high PF with low THD.
4. Comparative analysis of the converter for COT control scheme and VOT control scheme strategy in terms of input PF and THD.
5. Developing the simulation model of the converter with traditional and proposed control scheme with the help of MATLAB software.
6. Confirming the results.

https://doi.org/10.17993/3ctecno.2021.specialissue7.67-81

3. CONVENTIONAL COTCS FOR BCM IBBC

Figure 1 shows the main circuit of the IBBC. It is a buck converter in series with a boost converter with a common inductor. It works in buck mode with the boost switch opened when the instantaneous input line voltage is higher than the boundary voltage and otherwise in boost mode with buck switch closed. The boundary voltage is set a little higher than the output voltage. The converter operates in BCM and its working principle can be analyzed in two cases.

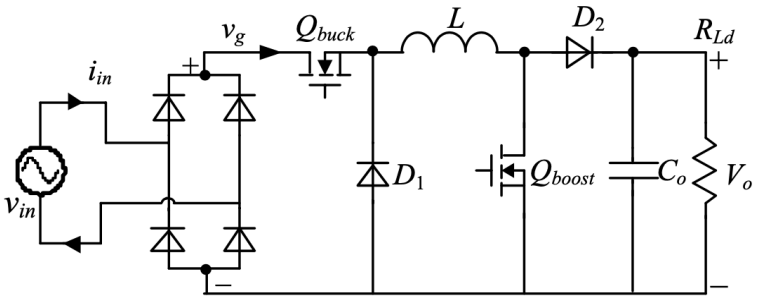

Figure 1. Schematic Diagram of IBBC.
Source: (Memon *et al.*, 2019).

The input voltage and rectified input voltage is expressed as

$$v_{in}(\theta) = \sqrt{2} V_{rms} \sin\theta \tag{1}$$

$$v_g = \sqrt{2} V_{rms} |\sin\theta| \tag{2}$$

where V_{rms} is the rms value

The IBBC is working in buck mode until input voltage is more than boundary voltage. Thus Q_{buck} is operating while Q_{boost} is off

When buck switch is on, the inductor voltage is expressed as

$$L\frac{di_L}{dt} = \sqrt{2} V_{rms} |\sin\theta| - V_o \quad (\theta_0 \le \theta \le \pi - \theta_0) \tag{3}$$

where $\theta_0 = \arcsin \dfrac{V_{boundary}}{\sqrt{2}\, V_{rms}}$

So its peak value is

https://doi.org/10.17993/3ctecno.2021.specialissue7.67-81

$$i_{L(pk1)}(\theta) = \frac{\sqrt{2}V_{rms}|\sin\theta| - V_o}{L} t_{on} \tag{4}$$

where t_{on} is the on-time of the switch.

While Q_{buck} is off, the inductor is discharged through load.

$$-L\frac{di_L}{dt} = V_o \tag{5}$$

For each switching cycle, the value of off-time is calculated from inductor's volt-second balance

$$t_{off} = \frac{L}{V_o} i_{L(pk1)}(\theta) \tag{6}$$

From (3) and (5), the following relation is obtained

$$t_{off} = \frac{\sqrt{2}V_{rms}|\sin\theta| - V_o}{V_o} t_{on} \tag{7}$$

In addition

$$t_s = t_{on} + t_{off} \tag{8}$$

Substituting (6) into (7)

$$t_s = \left(\frac{\sqrt{2}V_{rms}|\sin\theta|}{V_o}\right) t_{on} \tag{9}$$

The value of average input current for buck converter is got from

$$i_{buck(avg)}(\theta) = \frac{i_{L(pk1)}(\theta) t_{on}}{2t_s} \tag{10}$$

Substituting (3) and (8) into (9)

$$i_{buck(avg)}(\theta) = \frac{t_{on}V_o}{2L}\left(\frac{\sqrt{2}V_{rms}|\sin\theta| - V_o}{\sqrt{2}V_{rms}|\sin\theta|}\right) \tag{11}$$

The IBBC is working in boost mode until input voltage is less than boundary voltage. Thus Q_{boost} is operating while Q_{buck} is off

When boost switch is on, the inductor voltage is given as

$$i_{L(pk2)}(\theta) = \frac{\sqrt{2}V_{rms}|\sin(\theta)|}{L} t_{on} \tag{12}$$

https://doi.org/10.17993/3ctecno.2021.specialissue7.67-81

Same as (6), for each switching cycle, the value of off-time is calculated from inductor's volt-second balance

$$t_{off} = \frac{\sqrt{2}V_{rms}\left|\sin(\theta)\right|}{V_o - \sqrt{2}V_{rms}\left|\sin(\theta)\right|} t_{on} \tag{13}$$

Substituting (13) into (8), we get

$$t_s = \left(\frac{V_o}{V_o - \sqrt{2}V_{rms}\left|\sin(\theta)\right|}\right) t_{on} \tag{14}$$

The value of average input current for boost converter is determined as

$$i_{boost(avg)}(\theta) = \frac{i_{L(pk2)}(\theta)}{2} \tag{15}$$

Combining (12) and (14), we get

$$i_{boost(avg)}(\theta) = \frac{\sqrt{2}V_{rms}\left|\sin(\theta)\right|}{2L} t_{on} \tag{16}$$

Based on above analysis, the average input current of the IBBC with COTCS is as following.

$$i_{in\_COTCS}(\theta) = \begin{cases} \dfrac{\sqrt{2}V_{rms}\left|\sin\theta\right| t_{on}}{2L} & (0 \le \theta < \theta_0 \;\&\; \pi - \theta_0 < \theta \le \pi) \\ \dfrac{t_{on}V_o}{2L}\left(\dfrac{\sqrt{2}V_{rms}\left|\sin\theta\right| - V_o}{\sqrt{2}V_{rms}\left|\sin\theta\right|}\right) & (\theta_0 \le \theta \le \pi - \theta_0) \end{cases} \tag{17}$$

Based on (1) and (16), The input power of the IBBC is expressed as

$$P_{in(COTCS)} = \frac{t_{on}}{2\pi L}\left[2\int_0^{\theta_0}\left(\sqrt{2}V_{rms}\left|\sin\theta\right|\right)^2 d\theta + \int_{\theta_0}^{\pi-\theta_0} V_o\left(\sqrt{2}V_{rms}\left|\sin\theta\right| - V_o\right) d\theta\right] \tag{18}$$

Now t_{on} can be calculated by assuming the efficiency of IBBC as 100%

$$t_{on} = \frac{2\pi P_o L}{\left[2\int_0^{\theta_0}\left(\sqrt{2}V_{rms}\left|\sin\theta\right|\right)^2 d\theta + \int_{\theta_0}^{\pi-\theta_0} V_o\left(\sqrt{2}V_{rms}\left|\sin\theta\right| - V_o\right) d\theta\right]} \tag{19}$$

And input power factor can be calculated as

$$PF = \frac{P_{in}}{V_{rms} I_{rms}} \tag{20}$$

Based on (16-20) and specification, the curve of the input PF can be drawn and is given in Figure 2 from which it can be observed that the input PF is not unity for the wide range of the input voltage.

https://doi.org/10.17993/3ctecno.2021.specialissue7.67-81

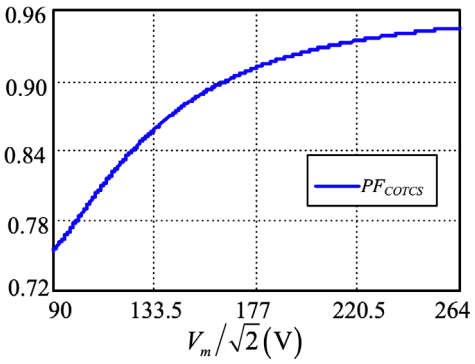

Figure 2. Input PF of COTCS [Eq: 17 to 20; Using Mathcad software].

4. PROPOSED VOTCS FOR BCM IBBC

For obtaining unity PF for the buck converter, the on-time of Q_{buck} in (11) should vary as

$$t_{on(buck)} = k_{on1} \frac{\left(\sqrt{2}V_{rms}\left|\sin\theta\right|\right)^2}{V_o\left(\sqrt{2}V_{rms}\left|\sin\theta\right| - V_o\right)} \tag{21}$$

where k_{on1} is a constant

Substituting (21) into (11), the average input current of the buck converter is

$$i_{buck(avg)}(\theta) = \frac{\sqrt{2}V_{rms}\left|\sin\theta\right|}{2L} k_{on1} \quad (\theta_0 \le \theta \le \pi - \theta_0) \tag{22}$$

From (22), it can be seen that if the on-time of the buck converter varies as (21), the input current waveform looks like pure sinusoidal and the PF is unity

From (16), it is clear that the input current of the boost converter is already sinusoidal. So there is no need of the variation of the on-time of the Q_{boost}

$$i_{boost(avg)}(\theta) = \frac{\sqrt{2}V_{rms}\left|\sin(\theta)\right|}{2L} k_{on2} \qquad (0 \le \theta < \theta_0 \;\&\; \pi - \theta_0 < \theta \le \pi) \tag{23}$$

k_{on2} is a constant.

The average input current of the IBBC with VOTCS is

https://doi.org/10.17993/3ctecno.2021.specialissue7.67-81

$$i_{in\_VOTCS}(\theta)=\begin{cases}\dfrac{k_{on2}\sqrt{2}V_{rms}|\sin\theta|}{2L} & (0\le\theta<\theta_0)\,\&\,(\pi-\theta_0<\theta\le\pi)\\ \dfrac{k_{on1}\sqrt{2}V_{rms}|\sin\theta|}{2L} & (\theta_0\le\theta\le\pi-\theta_0)\end{cases} \tag{24}$$

Because of the power balance of the input and output, the input current for the unity PF can be expressed as

$$i_{in}(\theta)=\frac{\sqrt{2}P_o|\sin\theta|}{V_{rms}} \tag{25}$$

Based on (25-26), the input current at θ_0 can be written as

$$i_{in}(\theta_0)=\frac{k_{on1}\sqrt{2}V_{rms}|\sin\theta_0|}{2L}=\frac{k_{on2}\sqrt{2}V_{rms}|\sin\theta_0|}{2L}=\frac{\sqrt{2}P_o|\sin\theta_0|}{V_{rms}} \tag{26}$$

From (26), it can be concluded that

$$k_{on1}=\frac{2P_oL}{V_{rms}^2} \tag{27}$$

$$k_{on2}=\frac{2P_oL}{V_{rms}^2} \tag{28}$$

From (27-28) it can be summarized as $k_{on1}=k_{on2}=k_{on}$ Hence, the input current of the IBBC with VOTCS is

$$i_{in\_VOTCS}(\theta)=\begin{cases}\dfrac{k_{on}\sqrt{2}V_{rms}|\sin\theta|}{2L} & (0\le\theta<\theta_0)\,\&\,(\pi-\theta_0<\theta\le\pi)\\ \dfrac{k_{on}\sqrt{2}V_{rms}|\sin\theta|}{2L} & (\theta_0\le\theta\le\pi-\theta_0)\end{cases} \tag{29}$$

Equation (29) demonstrates that input current of IBBC with VOTCS is pure sinusoidal. Thus unity PF can be realized by using proposed control scheme.

5. COMPARATIVE ANALYSIS

From (14), the input PF curve with proposed control scheme is shown in Figure 3 which also includes the PF values with traditional control scheme of Figure 2. It can be concluded that the PF of the converter with proposed control is higher as compared to COTC. The values

https://doi.org/10.17993/3ctecno.2021.specialissue7.67-81

of input PF for COTCS & VOTCS along with percentage improvement is written in Table 1. It can conclude that improvement at low line is more as compared to high line.

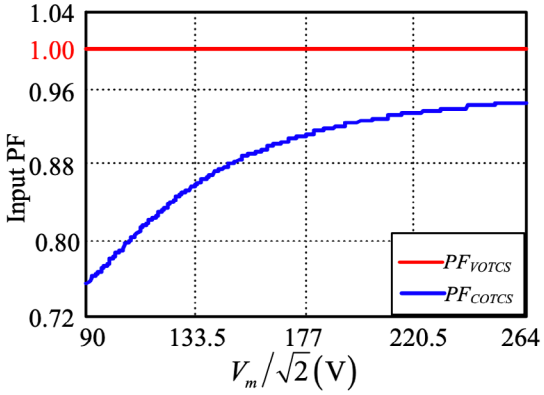

Figure 3. Input PF comparison between COTCS & VOTCS [Eq: 17 to 20 & 22 to 29; Using Mathcad software].

Table 1. Input PF comparison between COTCS & VOTCS [Eq: 17 to 20 & 22 to 29; Using Mathcad software].

S. No	Input Voltage	PF(COTCS)	PF(VOTCS)	% Improvement
1	90 V_{rms}	0.755	1	32.499
2	110 V_{rms}	0.807	1	23.887
3	130 V_{rms}	0.852	1	17.309
4	150 V_{rms}	0.884	1	13.14
5	170 V_{rms}	0.905	1	10.485
6	190 V_{rms}	0.920	1	8.737
7	210 V_{rms}	0.93	1	7.55
8	230 V_{rms}	0.937	1	6.723
9	250 V_{rms}	0.942	1	6.136
10	264 V_{rms}	0.945	1	5.827

6. SIMULATION RESULTS

In order to verify the effectiveness of VOT control scheme, simulations results are given. The range of input voltage is 90-264 V_{rms}. The output voltage is selected as 90 V. The control IC 6561 will ensure the current to be in BCM. Ideal components are used in simulation

Figure 4 illustrates the waveforms of input voltage and boundary voltage versus gate drive signal of integrated BBC. It indicates only one converter is conducting at a time depending on the boundary voltage.

https://doi.org/10.17993/3ctecno.2021.specialissue7.67-81

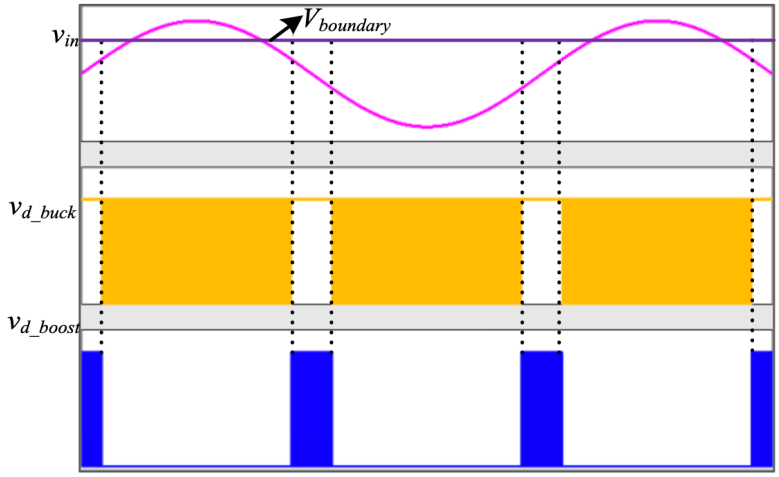

Figure 4. V_{in},V_{d_buck} and V_{d_boost} [Saber software].

Figure 5 and Figure 6 show the simulation waveforms of v_{in}, & i_{in} of integrated BBC with COT control scheme and VOT control scheme at 220VAC inputs, respectively. It can be conducted that current is almost sinusoidal in case of VOTCS as compared to COTCS. Thus, VOTCS can attain unity PF.

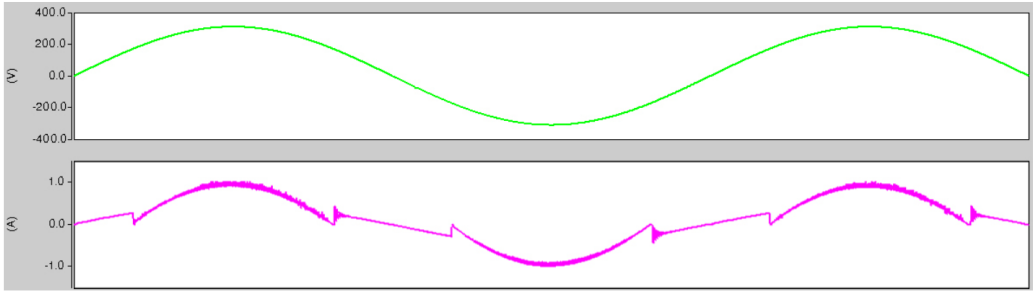

Figure 5. Input voltage and current of IBBC with COTCS [Saber software].

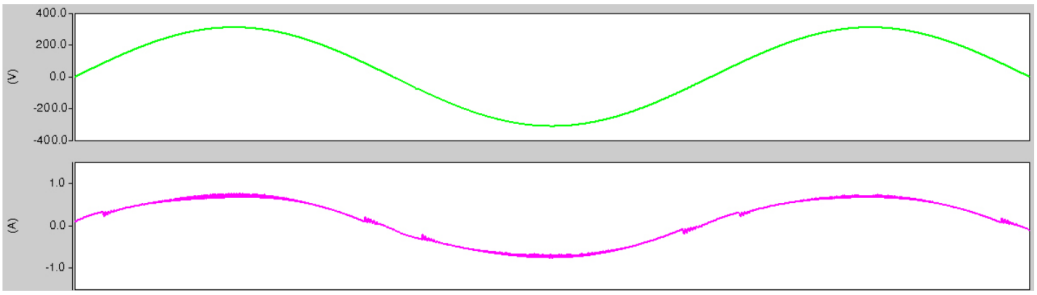

Figure 6. Input voltages and current of IBBC with VOTCS [Saber software].

https://doi.org/10.17993/3ctecno.2021.specialissue7.67-81

7. CONCLUSIONS

In this paper, integrated BBC is presented and analyzed. It is composed of buck and boost converter. With COT control scheme, the input PF of the IBBC is low. In order to attain high input PF, VOT control scheme is proposed. Simulation results are presented for the verification of the analysis.

REFERENCES

Chen, F. Z., & Maksimović, D. (2010). Digital control for improved efficiency and reduced harmonic distortion over wide load range in boost PFC rectifiers. *IEEE Transactions on Power Electronics, 25*(10), 2683-2692. https://doi.org/10.1109/TPEL.2010.2050702

IEC Standard, 61000-3. (n.d.). *Electromagnetic compatibility (EMC). Limits for Harmonic Current Emissions* (Equipment input current≤ 16A per phase).

García, O., Cobos, J. A., Prieto, R., Alou, P., & Uceda, J. (2003). Single phase power factor correction: A survey. *IEEE Transactions on Power Electronics, 18*(3), 749-755. https://doi.org/10.1109/TPEL.2003.810856

Hwang, T. S., & Park, S. Y. (2012). Seamless boost converter control under the critical boundary condition for a fuel cell power conditioning system. *IEEE Transactions on Power Electronics, 27*(8), 3616-3626. https://doi.org/10.1109/TPEL.2012.2185250

Langella, R., Testa, A., & Alii, E. (2014). IEEE recommended practice and requirements for harmonic control in electric power systems. *IEEE Std. 519-2014.* IEEE.

Liu, X., Wan, Y., He, M., Zhou, Q., & Meng, X. (2020). Buck-Type Single-Switch Integrated PFC Converter With Low Total Harmonic Distortion. *IEEE Transactions on Industrial Electronics, 6.* http://doi.org/10.1109/TIE.2020.3007121

Liu, X., Xu, J., Chen, Z., & Wang, N. (2014). Single-inductor dual-output buck–boost power factor correction converter. *IEEE transactions on Industrial electronics, 62*(2), 943-952. https://doi.org/10.1109/TIE.2014.2334659

Mahdavi, M., & Farzanehfard, H. (2010). Bridgeless SEPIC PFC rectifier with reduced components and conduction losses. *IEEE Transactions on Industrial Electronics, 58*(9), 4153-4160. https://doi.org/10.1109/TIE.2010.2095393

Memon, A. H., & Yao, K. (2018a). UPC strategy and implementation for buck–buck/boost PF correction converter. *IET Power Electronics, 11*(5), 884-894. http://doi.org/10.1049/iet-pel.2016.0919

Memon, A. H., Baloach, M. H., Sahito, A. A., Soomro, A. M., & Memon, Z. A. (2018b). Achieving High Input PF for CRM Buck-Buck/Boost PFC Converter. *IEEE Access, 6,* 79082-79093. http://doi.org/10.1109/ACCESS.2018.2879804

Memon, A. H., Memon, M. A., Memon, Z. A., & Hashmani, A. A. (2019a). Critical Conduction Mode Buck-Buck/Boost Converter with High Efficiency. *3C Tecnología. Glosas de innovación aplicadas a la pyme. Edición Especial, Noviembre 2019,* 201-219. http://dx.doi.org/10.17993/3ctecno.2019.specialissue3.201-219

Memon, A. H., Memon, Z. A., Shaikh, N. N., Sahito, A. A., & Hashmani, A. A. (2019b). Boundary conduction mode modified buck converter with low input current total harmonic distortion. *Indian Journal of Science and Technology, 12*. https://doi.org/10.17485/ijst/2019/v12i17/144613

Memon, A. H., Nizamani, M. O., Memon, A. A., Memon, Z. A., & Soomro, A. M. (2019c). Achieving High Input Power Factor for DCM Buck PFC Converter by Variable Duty-Cycle Control. *3C Tecnología. Glosas de innovación aplicadas a la pyme. Edición Especial, Noviembre 2019*, 185-199. http://dx.doi.org/10.17993/3ctecno.2019.specialissue3.185-199

Memon, A. H., Noonari, F. M., Memon, Z., Farooque, A., & Uqaili, M. A. (2020a). AC/DC critical conduction mode buck-boost converter with unity power factor. *3C Tecnología. Glosas de innovación aplicadas a la pyme. Edición Especial, Abril 2020,* 93-105. http://doi.org/10.17993/3ctecno.2020.specialissue5.93-105

Memon, A. H., Pathan, A. A., Kumar, M., & Sahito, A. J., & Memon, Z. A. (2019d). Integrated buck-flyback converter with simple structure and unity power factor.

Indian Journal of Science and Technology, 12. https://doi.org/10.17485/ijst/2019/v12i17/144612

Memon, A. H., Shaikh, N. N., Kumar, M., & Memon, Z. A. (2019e). Buck-buck/boost converter with high input power factor and non-floating output voltage. *International Journal of Computer Science and Network Security, 19*(4), 299-304. http://paper.ijcsns.org/07_book/201904/20190442.pdf

Memon, A. H., Yao, K., Chen, Q., Guo, J., & Hu, W. (2016). Variable-on-time control to achieve high input power factor for a CRM-integrated buck–flyback PFC converter. *IEEE Transactions on Power Electronics, 32*(7), 5312-5322. http://doi.org/10.1109/TPEL.2016.2608839

Memon, A. H., Samejo, J. A., Memon, Z. A., & Hashmani, A. A. (2020b). Realization Of Unity Power Factor For Ac/Dc Boundary Conduction Mode Flyback Converter With Any Specific Turn's Ratio. *Journal of Mechanics Of Continua And Mathematical Sciences,* (spl6). 10.26782/jmcms.spl.6/2020.01.00014. https://doi.org/10.26782/jmcms.spl.6/2020.01.00014

Memon, A. H., Shaikh, S. A., Memon, Z. A., Memon, A. A., & Memon, A. A. (2020c). DCM Boost Converter with High Efficiency. *Journal Of Mechanics Of Continua And Mathematical Sciences,* (spl6). https://doi.org/10.26782/jmcms.spl.6/2020.01.00006

Singh, B., Singh, B. N., Chandra, A., Al-Haddad, K., Pandey, A., & Kothari, D. P. (2003). A review of single-phase improved power quality AC-DC converters. *IEEE Transactions on industrial electronics, 50*(5), 962-981. https://www.researchgate.net/publication/3218193_A_review_of_single-phase_improved_power_quality_AC-DC_converters

Wu, X., Yang, J., Zhang, J., & Qian, Z. (2012). Variable on-time (VOT)-controlled critical conduction mode buck PFC converter for high-input AC/DC HB-LED lighting applications. *IEEE Transactions on power Electronics, 27*(11), 4530-4539. https://doi.org/10.1109/TPEL.2011.2169812

Wu, X., Yang, J., Zhang, J., & Xu, M. (2011). Design considerations of soft-switched buck PFC converter with constant on-time (COT) control. *IEEE transactions on power electronics, 26*(11), 3144-3152. https://doi.org/10.1109/TPEL.2011.2145391

Yang, F., Ruan, X., Yang, Y., & Ye, Z. (2011). Interleaved critical current mode boost PFC converter with coupled inductor. *IEEE Transactions on power electronics, 26*(9), 2404-2413. https://doi.org/10.1109/TPEL.2011.2106165

https://doi.org/10.17993/3ctecno.2021.specialissue7.67-81

/05/

https://doi.org/10.17993/3ctecno.2021.specialissue7

MACHINE LEARNING MODEL TO PREDICT THE DIVORCE OF A MARRIED COUPLE

Nahum Flores
Student, Artificial Intelligence Group, Faculty in Systems Engineering and Computer Science, National University of San Marcos. Lima, (Peru).
E-mail: nahum.flores@unmsm.edu.pe
ORCID: https://orcid.org/0000-0002-5807-4323

Sandra Silva
Student, Artificial Intelligence Group, Faculty in Systems Engineering and Computer Science, National University of San Marcos. Lima, (Peru).
E-mail: sandra.silva3@unmsm.edu.pe
ORCID: https://orcid.org/0000-0003-0253-7883

Recepción: 09/12/2020 **Aceptación:** 10/03/2021 **Publicación:** 07/05/2021

Citación sugerida:
Flores, N., y Silva, S. (2021). Machine learning model to predict the divorce of a married couple. *3C Tecnología. Glosas de innovación aplicadas a la pyme, Edición Especial,* (mayo 2021), 83-95. https://doi.org/10.17993/3ctecno.2021.specialissue7.83-95

ABSTRACT

Divorce usually impacts the closest family members, over the years the divorce rate has increased dramatically, especially in the last two decades and worsening with the pandemic, where there has been a significant increase in the divorce rate in many countries of the world. We draw on Yöntem's work where he poses 56 questions as predictors of divorce. In addition, we make use of 4 automatic learning models (perceptron, logistic regression, neural networks and randomized forest) and 3 hybrid models based on voting criteria. Each of these models was trained in 5 different scenarios, making a total of 35 experiments, the best performance obtained in terms of precision, sensitivity and specificity is 0.9853, 1.0 and 0.9667 respectively, corresponding to the perceptron model and a hybrid model; however, although the results show a high performance, the context, the amount of data and the country in which the data were collected must be considered.

KEYWORDS

Machine learning, Neural networks, Divorce predict, Voting.

https://doi.org/10.17993/3ctecno.2021.specialissue7.83-95

1. INTRODUCTION

The divorce rate worldwide has increased dramatically in recent years. This assertion is based in figures. First, is the American divorce rate. If we compare the figures for 2018 with those of 1900, it shows that there are four times more divorced women (Schweizer, 2020). In Spain, this rate doubled (2018) compared to 2000 (INE, 2018). In Mexico, such rate tripled from 2000 to 2019 (INEGI, 2019) and in Peru the number of divorces registered in 2018 (INEI, 2018) is eight times higher than those registered in 2000 (INEI, 2010).

The current pandemic context has only exacerbated this phenomenon, as the confinement has brought with its greater increase. This applies for the United States, which, in couples with at least 5 years of marriage, registered 16% more divorces in the third quarter of 2020 than in the same period of 2019 and an increase of 5% in couples with children that have less than 18 years (Legal Templates, 2020). An even more noticeable case occurs in Xi'an (China) where divorce requests have increased to such an extent that they have reached their daily limit (Díez, 2020). Naturally, this situation has consequences that can affect close members of the families involved (Sánchez, 2019).

In this regard, different studies have identified multiple factors to predict divorce. One of the most significant works was that of Gottman. He identified "The Four Horsemen of the Apocalypse" that can end a marriage: criticism, contempt, stonewalling and defensiveness (Gottman & Silver, 2014). Using just these four variables in a longitudinal study conducted with newlywed couples, Gottman estimated which couples would have an early divorce with 85% accuracy. Gottman also identified that quality sexual satisfaction, love, and passion in marriages depend directly (by 70%) on the quality of friendship they have (Gottman & Silver, 2015). On the other hand, there are studies that show infidelity as the main ground for divorce. This is not surprising: infidelity is the leading cause of divorce in the United States (Mark, Janssen, & Milhausen, 2011) as well as in more than 160 cultures (Betzig, 1989), because it has negative effects on the relationship, and can be the most feared and devastating experience in a matrimony (Pittman, 1994), thus leading it to an end (Zordan & Strey, 2011).

In the last decade, the use of Machine Learning models in psychology has become popular, leaving behind numerous methods of estimation, statistical analysis and data mining for

https://doi.org/10.17993/3ctecno.2021.specialissue7.83-95

predictions. In the first place is Amiriparian, who used audio spectrograms to diagnose bipolar disorder (Amiriparian *et al.*, 2019), obtaining an Unweighted Average Recall (UAR) of 46.2%. Second are Eastwick and Joel, who used a random forest method to predict the appereance of a relationship based on traits and preferences; out of 192 couples, it was able to predict 4% to 18% of actor variance (average tendency to romantically desire other people) and 7% to 27% of the partner variance (to be desired by other people) (Joel, Eastwick, & Finkel, 2017). Finally, Flesia's work predicted the stress levels that are caused by COVID-19 from 18 psychosocial variables, achieving a sensitivity of 76%.

For the particular case of the prediction of divorce, we checked the following background: the work of Großmann *et al.* (2019), which used a linear regression model to predict the future of a relationship based on the analysis of personality traits, the work of Yöntem *et al.* (2019) with ANN models that achieved a precision of 98.85% and the work of Narendran, Abilash & Charulatha (2020) that made use of a voting classifier with decision trees, bagging classifier and XGBoost prediction models, achieving a performance of 94.14%.

Using fresher classification methods, the present work aims to compare the high performance obtained with an analysis based on the correlation of variables, making available the proposed models and their respective trained results.

2. MATERIALS AND METHODS

2.1. DATASET

In this research we will use the same dataset as the one in Yöntem's *et al.* work (2019) which is composed of 54 questions. 6 of them can be seen in Table 1: they were answered by 170 people –84 divorced and 86 married–. As divorce predictor, each question had different probabilities of impact. Answers are on a 5-point scale (0 = Never, 1 = Rarely, 2 = Average, 3 = Often, 4 = Always).

Table 1. Questions formulated in Yöntem's work.

ID	Questions
Atr1	If one of us apologizes when our discussion deteriorates, the discussion ends.
Atr2	I know we can ignore our differences, even if things get hard sometimes.

https://doi.org/10.17993/3ctecno.2021.specialissue7.83-95

Atr3	When we need it, we can take our discussions with my spouse from the beginning and correct it.
…	…
Atr52	I wouldn't hesitate to tell my spouse about her/his inadequacy.
Atr53	When I discuss, I remind my spouse of her/his inadequacy.
Atr54	I'm not afraid to tell my spouse about her/his incompetence.

Source: adapted from (Yöntem *et al.*, 2019).

2.2. PREPROCESSING

Data normalization is one of the preprocessing approaches where the data is scaled or transformed to obtain an equal contribution from each characteristic, thus translating into a significant improvement in the performance of Machine Learning algorithms (Singh & Singh, 2019). In this work, the 54 questions contain numerical data between 0 to 4, values that were re-scaled between -1 and 1, as shown in Figure 1.

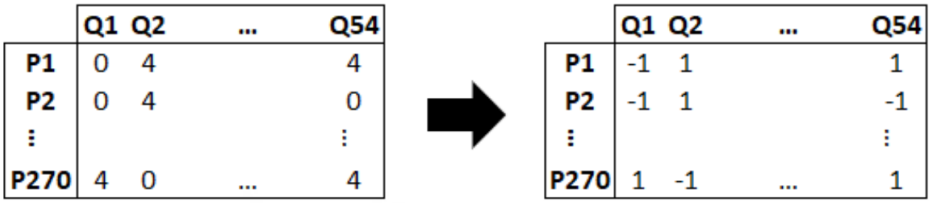

Figure 1. Normalization of the answers.
Source: own elaboration.

2.3. FEATURE SELECTION

Considering each question as a characteristic, we use Pearson's correlations for the selection. Thus, we measure the degree of relationship between the variables (Liu *et al.*, 2020). Table 2 shows the 20 variables with the highest correlation.

Table 2. Question with the highest correlation.

Id	Score	Id	Score
Atr22	0.7853	Atr42	0.6423
Atr54	0.7685	Atr48	0.6336
Atr28	0.7621	Atr53	0.6114
Atr44	0.7530	Atr47	0.5827
Atr34	0.7498	Atr52	0.5755
Atr32	0.7397	Atr45	0.5102
Atr50	0.7254	Atr43	0.4822
Atr31	0.6992	Atr7	0.4280

https://doi.org/10.17993/3ctecno.2021.specialissue7.83-95

Atr51	0.6841	Atr46	0.4003
Atr49	0.6748	Atr6	0.2871

Source: own elaboration.

2.4. CLASSIFICATION

For the classification, this work uses four models of Machine Learning. The first is the Perceptron model, with a stop criterion of 1e-4. The second model is a logistic regression with lbfgs as the optimization parameter. The third model are neural networks, composed of 7 layers, as seen in Figure 2, all with a sigmoidal activation function and 30 epochs for their training. The fourth is a Random Forest model with 100 estimators and a depth of 2. Generally, hybrid models based on voting criteria have superior performance (Kuncheva & Rodríguez, 2012; Liu, Reviriego, Lombardi, & Hernandez, 2020), for which 3 hybrid models were created from the 4 models mentioned. The classification models can be seen in Table 4.

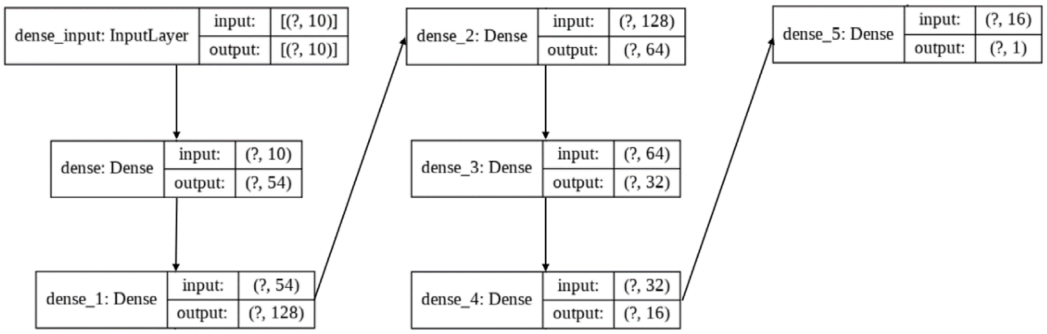

Figure 2. Architecture of a neural network model.
Source: own elaboration.

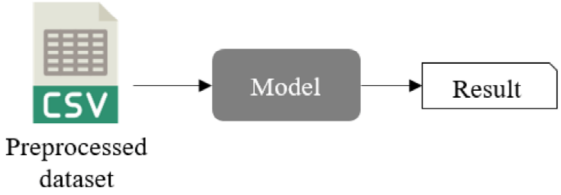

Figure 3. Training scheme for each model.
Source: own elaboration.

For the training, test and training data was randomly divided, in the proportions shown in Table 3. Each model was trained with the scheme in Figure 3.

Table 3. Proportion of training and test data.

https://doi.org/10.17993/3ctecno.2021.specialissue7.83-95

Label		Proportion (%)				
		50/50	60/40	70/30	80/20	90/10
Divorced	Training	42	50	59	67	76
	Test	42	34	25	17	8
Married	Training	43	52	60	69	77
	Test	43	34	26	17	9

Source: own elaboration.

Table 4. Models used for prediction.

ID	Models
M1	Logistic Regression
M2	Neural Networks
M3	Random Forest
M4	Perceptron, Logistic Regression and Neural Networks
H1	Perceptron, Neural Networks and Random Forest
H2	Perceptron, Logistic Regression and Random Forest
H3	Perceptron

Source: own elaboration.

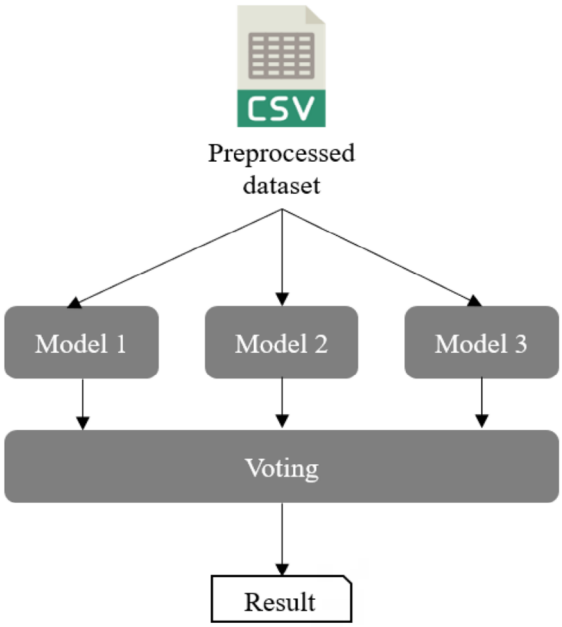

Figure 4. Voting criteria for hybrid models.
Source: own elaboration.

The proposed model was implemented using Python 3 in Google Colab (Carneiro, Medeiros, & Nepomuceno, 2018) using a 2.3 GHz Xeon CPU with 13gb RAM and a 16gb RAM Nvidia Tesla V100 graphics card.

https://doi.org/10.17993/3ctecno.2021.specialissue7.83-95

2.5. EVALUATION

To measure the performance of the classification, the proposed model used performance metrics in terms of sensitivity (Sen), specificity (Spe) and Accuracy (Acc).

A divorced person properly classified is called "true positive" (TP). A divorced person that is not properly classified is called "true negative" (TN). When a divorced person is classified as married, it is called a "false negative" (FN), and when a married person is classified as divorced, it is called a "false positive" (FP).

Sensitivity shows divorced people correctly classified, defined as (Lyusin & Ovsyannikova, 2016):

$$Sensitivity = \frac{TP}{TP+FN} \quad (1)$$

Specificity shows divorced and married people properly classified. It is calculated as follows (Glaros & Kline, 1988):

$$Specificity = \frac{TN}{TN+FP} \quad (2)$$

Accuracy indicates the ratio of correctly classified people, obtained with the formula (Pedersen, Cheng, & Rasmussen, 1989):

$$Accuracy = \frac{TP+TN}{TP+FP+TN+FN} \quad (3)$$

On the other hand, hybrid models are evaluated by the voting criterion (see Figure 4), where the label that was repeated the most is selected.

3. RESULTS

In this work, multiple experiments were generated with the four models defined in the "classification" section. These were trained with the proportions defined in Table 3. When training the model with the Yöntem work dataset, the results of Table 5 are obtained.

Table 5. Accuracy results of the training.

	Training/Test (%)				
Model	**50/50**	**60/40**	**70/30**	**80/20**	**90/10**
Perceptron	0.9529	0.9853	0.9608	0.9412	0.9412
Logistic Regression	0.9412	0.9559	0.9804	0.9706	0.9412

https://doi.org/10.17993/3ctecno.2021.specialissue7.83-95

Neural Networks	0.9647	0.9559	0.9804	0.9706	0.9412
Random Forest	0.9294	0.9412	0.9804	0.9706	0.9412
H1*	0.9647	0.9853	0.9804	0.9706	0.9412
H2*	0.9412	0.9706	0.9804	0.9706	0.9412
H3*	0.9412	0.9706	0.9804	0.9706	0.9412

Source: own elaboration.

Table 6. Sensitivity results of the training.

	Training/Test (%)				
Model	**50/50**	**60/40**	**70/30**	**80/20**	**90/10**
Perceptron	0.9783	1.0000	0.9630	0.9444	1.0000
Logistic Regression	1.0000	1.0000	1.0000	1.0000	1.0000
Neural Networks	1.0000	1.0000	1.0000	1.0000	1.0000
Random Forest	1.0000	1.0000	1.0000	1.0000	1.0000
H1*	1.0000	1.0000	1.0000	1.0000	1.0000
H2*	1.0000	1.0000	1.0000	1.0000	1.0000
H3*	1.0000	1.0000	1.0000	1.0000	1.0000

Source: own elaboration.

Table 7. Sensitivity results of the training.

	Training/Test (%)				
Model	**50/50**	**60/40**	**70/30**	**80/20**	**90/10**
Perceptron	0.9231	0.9667	0.9583	0.9375	0.9000
Logistic Regression	0.8718	0.9000	0.9583	0.9375	0.9000
Neural Networks	0.9231	0.9667	0.9583	0.9375	0.9000
Random Forest	0.8462	0.8667	0.9583	0.9375	0.9000
H1*	0.9231	0.9667	0.9583	0.9375	0.9000
H2*	0.8718	0.9333	0.9583	0.9375	0.9000
H3*	0.8718	0.9333	0.9583	0.9375	0.9000

Source: own elaboration.

4. CONCLUSIONS

In this work, 7 models were used for the prediction of divorce, trained with the dataset from Yöntem's *et al.* (2019) work and the dataset collected in this research. Each of these models was trained in 5 different scenarios, making a total of 35 experiments. Among these, the best results were obtained with the perceptron model and the first hybrid model; however, due to the amount of data, the hybrid models did not perform better.

https://doi.org/10.17993/3ctecno.2021.specialissue7.83-95

Although the results show high performance, the context, the amount of data and the country in which the data was collected must be considered. In order to feed the dataset to retrain the models, in the future we plan to collect couple's data from different countries, evaluating their performance.

Divorce is a major problem, especially in a context of confinement, where the rates of divorced couples have increased considerably, indirectly affecting the closest members of the family (such as children). Also, couples can lose a lot by going through a divorce process. This study can help them prevent these consequences. The prediction models in this study would help people decide whether to make the decision to marry or not, give them the opportunity based on compatibility to have a successful marriage.

The best performance of a model was obtained by using the 60/40 ratio of the training and test data. The results were 0.9853 precision, 1.0 sensitivity and 0.9667 specificity. We make the models and training results available in our GitHub repository (https://github.com/NahumFGz/DivorcePredict).

REFERENCES

Amiriparian, S., Awad, A., Gerczuk, M., Stappen, L., Baird, A., Ottl, S., & Schuller, B. (2019). Audio-based Recognition of Bipolar Disorder Utilising Capsule Networks. *IEEE Xplore*. https://doi.org/10.1109/ijcnn.2019.8852330

Betzig, L. (1989). Causes of Conjugal Dissolution: A Cross-cultural Study. *Current Anthropology*, 654-676.

Carneiro, T., Medeiros, R., & Nepomuceno, T. (2018). Performance Analysis of Google Colaboratory as a Tool for Accelerating Deep Learning Applications. *IEEE, 9*. https://doi.org/10.1109/ACCESS.2018.2874767

Díez, P. M. (2020, March 21). *Divorce epidemic in China due to coronavirus quarantines.* ABC. https://www.abc.es/sociedad/abci-epidemia-divorcios-china-cuarentenas-coronavirus-202003200152_noticia.html

https://doi.org/10.17993/3ctecno.2021.specialissue7.83-95

Glaros, A., & Kline, R. (1988). Understanding the accuracy of tests with cutting scores: The sensitivity, specificity, and predictive value model. *Journal of Clinical Psychology, 44*(6), 1013-1023. https://doi.org/10.1002/1097-4679(198811)44:6<1013::aid-jclp2270440627>3.0.co;2-z

Gottman, J., & Silver, N. (2014). *How to Maintain Love. Secrets from the Love Lab*. Varlık Publications.

Gottman, J., & Silver, N. (2015). *Seven Principles of Keeping Married.* Varlık Publications.

Großmann, I., Hottung, A., & Krohn-Grimberghe, A. (2019). Machine learning meets partner matching: Predicting the future relationship quality based on personality traits. *PLOS ONE, 14*(3).

INE. (2018, September 30). *Eurostat Statistics Eplained.* https://www.ine.es/prodyser/espa_cifras/2018/14/

INEGI. (2019). *INEGI. Instituto Nacional de Estadística y Geografía*. https://www.inegi.org.mx/temas/nupcialidad/

INEI. (2010). *National Institute of Statistics and Informatics.* https://www.inei.gob.pe/media/MenuRecursivo/publicaciones_digitales/Est/Lib1045/cap04.pdf

INEI. (2018). *National Institute of Statistics and Informatics.* https://www.inei.gob.pe/media/MenuRecursivo/publicaciones_digitales/Est/Lib1698/libro.pdf

Joel, S., Eastwick, P., & Finkel, E. (2017). Is Romantic Desire Predictable? Machine Learning Applied to Initial Romantic Attraction. *Psychological Science, 28*(10), 1478-1489.

Kuncheva, L., & Rodríguez, J. (2012). A weighted voting framework for classifiers ensembles. *Knowledge and Information Systems, 38*(2), 259-275. https://doi.org/10.1007/s10115-012-0586-6

Legal Templates. (2020, July 29). *US Divorce Rates Soar During COVID-19 Crisis.* https://legaltemplates.net/resources/personal-family/divorce-rates-covid-19/#divorces-increase-in-couples-with-children

https://doi.org/10.17993/3ctecno.2021.specialissue7.83-95

Liu, S., Reviriego, P., Lombardi, F., & Hernandez, J. A. (2020). Voting Margin: A Scheme for Error-Tolerant k Nearest Neighbors Classifiers for Machine Learning. *IEEE Transactions on Emerging Topics in Computing.* https://doi.org/10.1109/tetc.2019.2963268

Liu, Y., Mu, Y., Chen, K., Li, Y., & Guo, J. (2020). Daily Activity Feature Selection in Smart Homes Based on Pearson Correlation Coefficient. *Neural Processing Letters, 2*(1771-1787), 51. https://doi.org/10.1007/s11063-019-10185-8

Lyusin, D., & Ovsyannikova, V. (2016). Measuring two aspects of emotion recognition ability: Accuracy vs. sensitivity. *Learning and Individual Differences, 52,* 129-136. https://doi.org/10.1016/j.lindif.2015.04.010

Mark, K. P., Janssen, E., & Milhausen, R. R. (2011). Infidelity in Heterosexual Couples: Demographic, Interpersonal, and Personality-Related Predictors of Extradyadic Sex. *Archives of Sexual Behavior, 40*(5), 971-982. https://doi.org/10.1007/s10508-011-9771-z

Narendran, D. J., Abilash, R., & Charulatha, B. S. (2020). Exploration of Classification Algorithms for Divorce Prediction. *Proceedings of International Conference on Recent Trends in Machine Learning, IoT, Smart Cities and Applications*, 291-303. https://doi.org/10.1007/978-981-15-7234-0_25

Pedersen, P., Cheng, G., & Rasmussen, J. (1989). On Accuracy Problems for Semi-Analytical Sensitivity Analyses. *Mechanics of Structures and Machines, 17*(3), 373-384. https://doi.org/10.1080/089054508915647

Pittman, F. (1994). *Private Lies: Infidelity and the Betrayal of Intimacy.* Artes Médicas.

Sánchez, T. (2019). *Consequences of divorce on children. The need for a new way of intervening: The joint work of a lawyer and a psychologist.* https://eprints.ucm.es/54965/

Schweizer, V. (2020). Divorce: More than a Century of Change, 1900-2018. *Family Profil,* 1-2. https://www.bgsu.edu/content/dam/BGSU/college-of-arts-and-sciences/NCFMR/documents/FP/schweizer-divorce-century-change-1900-2018-fp-20-22.pdf

https://doi.org/10.17993/3ctecno.2021.specialissue7.83-95

Singh, D., & Singh, B. (2019). Investigating the impact of data normalization on classification performance. *Applied Soft Computing, 1*05524. https://doi.org/10.1016/j.asoc.2019.105524

Yöntem, M., Adem, K., İlhan, T., & Kılıçarslan, S. (2019). Divorce Prediction Using Correlation Based Feature Selection And Artificial Neural Networks. *Nevşehir Hacı Bektaş Veli University SBE Dergisi, 9*(1), 259-273. https://dergipark.org.tr/tr/pub/nevsosbilen/issue/46568/549416

Zordan, E. P., & Strey, M. N. (2011). *Marital separation: Aspects involved in this decision, reversion and future projects.* https://www.semanticscholar.org/paper/Separa%C3%A7%C3%A3o-conjugal%3A-aspectos-implicados-nessa-e-Zordan-Strey/6e25b5932d14c86e3aa3f191bb9761876e76eb9c

https://doi.org/10.17993/3ctecno.2021.specialissue7.83-95

/06/

https://doi.org/10.17993/3ctecno.2021.specialissue7

ODORSENSE: MEASURING, ASSESSMENT AND ALERTING THE HEALTH EFFECTS OF ODOR POLLUTION

Santhosh B. Panjagal
Research Scholar, VTU Belagavi. Associate Processor, KEC-Kuppam, (India).
E-mail: santupanjagal@gmail.com
ORCID: https://orcid.org/0000-0002-6263-1727

G. N. Kodanda Ramaiah
Professor & Dean, KEC-Kuppam, (India).
E-mail: gnk.ramaiah@gmail.com
ORCID: https://orcid.org/0000-0002-1692-9629

Recepción: 09/12/2020 **Aceptación:** 02/03/2021 **Publicación:** 07/05/2021

Citación sugerida:
Panjagal, S. B., y Ramaiah, G. N. K. (2021). OdorSense: Measuring, Assessment and Alerting the Health Effects of Odor Pollution. *3C Tecnología. Glosas de innovación aplicadas a la pyme, Edición Especial*, (mayo 2021), 97-113. https://doi.org/10.17993/3ctecno.2021.specialissue7.97-113

ABSTRACT

Nowadays there is an increased conflict between residents and government bodies /or industries due to unpleasant or offensive Odor smells emanating from different sources, interfacing with person's enjoyment of life as they are frequent and persistent. The main concern among all the residents is the health effects of toxic Odor gases (like, ammonia, Sulphur dioxide, nitrogen, hydrogen sulphide) released from the waste dumping sites, drainages, food & meat processing industries, etc., causing dreadful diseases to the living beings. There is urgent need of an intelligent mechanism, which allows every common people access the Odor pollution information through user friendly applications. Hence the main objective of the proposed research work was to develop an intelligent mechanism for detecting, measuring and alerting the health effects of Odor pollution. The research work follows design o an artificial olfaction system based electronic nose using low cost, low power and improved accuracy sensors for detection and real-time measurement of Odor concentrations at various sources of Odor emissions, uploading the Odor concentrations to IoT cloud for remote monitoring and alerting. User friendly interface application developed for providing real time information about the Odor levels at the desired source and alerting the health effects if the Odor concentration levels increases above the threshold levels.

KEYWORDS

Odor pollution, Odor Measurement, Odor concentration, Artificial olfaction system (E-Nose), User Interface (Mobile Application), Health survey, IoT Cloud, Risk Assessment.

https://doi.org/10.17993/3ctecno.2021.specialissue7.97-113

1. INTRODUCTION

Odor pollution is most complex problem due to its distinctly different characteristics, as they possess different physical and chemical properties, and they are present at a concentration ranges from high parts per million (ppm) to low parts per billion (ppb) (Shinde *et al.*, 2017). Till date very little attention has been paid towards Odor pollution issues in India, therefore Odor pollution and its problems has become objectionable proportion with the growing population, industrialization, and urbanization. The main cause of Odor pollution and its problems is due to urbanization with improper sanitation facilities (Nicolas *et al.*, 2006).

At the same time there are many sources which contributes to Odor pollution, they are classified as 1. Point sources (vents, stacks, and exhausts), 2. Area sources (Sewage treatment plants, wastewater treatment plants, solid waste landfill, composting, household manure settling lagoons, etc.) (Elwell, 2001; Nicolas, 2006; Pagans, 2006), 3. Building sources (Pig sheds, hog confinement chickens) (Misselbrook *et al.*, 1993) 4. Fugitive sources (soil bed or bio-filter surfaces). Hence, Odor can arise from many sources, most are manmade garbage or unscientific dumping on vacant lands (Di *et al.*, 2013; CPCB, 2007).

The Major Odor pollution are Industries Pulp & Paper, Fertilizer, Pesticides, Tanneries, Sugar & Distillery, Chemical, Dye & Dye Intermediates, Bulk Drugs & Pharmaceuticals etc., Large Livestock operations, Poultry/chicken Farms (Hayes *et al.*, 2006), Slaughterhouses, Food processing industries, Agricultural activities like decaying of vegetation, production and application of compost etc. (Yan-li Zhu, 2016; CPCB, 2007), In urban and metropolitan areas, improper maintenance of public amenities like toilets, bus/railway stations, hospitals, shopping complex etc. generate pungent Odor, which affects the peoples as well as neighborhood residents. Important issue is Odor cannot escape from Congested markets, thus causing problems to shop-keepers as well as to customers (CPCB, 2007).

Generally, the most common Odors released from various sources are putrid, pungent, or musky etc., from these Odors some toxic gases are also released like ammonia, Sulphur dioxide, hydrogen sulfide (Sarkar *et al.*, 2002) which can cause dreadful diseases to living beings, hence strong Odors released from different sources, causes irritation to eyes, nose, throat or lungs, nausea, loss of memory & sleep, coughing due burning sensation, headache,

https://doi.org/10.17993/3ctecno.2021.specialissue7.97-113

dizziness, wheezing or other breathing/respiratory problems (NIOSH, 2007, OSHA, 2011, ACGIH, 2021).

Now the Odor pollution nuisance has become most important environmental issue among all pollution problems, leading to more number complaints and conflicts between residents, industries and government (Nicolas *et al.,* 2006; Takano, 2014). Therefore, demanding more stringent policies to regulate Odor annoyance and need for continuous efforts to manage and limit the Odor exposure in the neighborhood to identifying, quantifying and monitoring the Odor emission (Wenjing *et al.,* 2015).

Generally, there are various measurement techniques to quantify the Odor concentrations, among them some techniques (human olfaction and conventional analytical) provide only perception real Odor and mixture composition, but not applicable for continuous real-time measurement in the field and also don not provide global information relating to Odor perception (Nicolas *et al.,* 2006). There is a need to develop an appropriate new system to measure and monitor Odor concentration based on devices rather than depending on biological human olfaction involving trained human panelists (Deshmukh *et al.*, 2017).

In this research study, an embedded electronic device is designed to measure the concentration of Odor pollution at selected areas. The design of artificial olfactory electronic nose (Gongora *et al.*, 2019; Erisman, 2001) incorporates most desirable industrial Odor sensors; TGS2602 Metal Oxide Semiconductor (MOS) type Sensor for detecting Hydrogen Sulfide (H2S), Ammonia (NH3), Volatile Organic Compounds (VOCs) and 110-601 Sulphur Dioxide (SO2) sensor, Solar harvesting unit for powering the portable electronic nose, Odor threshold level indicator, Communication network unit (Wi-Fi) for uploading processed data onto the IoT cloud storage and mobile application for retrieving the Odor concentration from IoT cloud, performing risk assessment based on standard threshold levels (EPA, 2021) and then providing the alert information to end users. Finally, the Data processor (Atmega328) coordinates and controls all the peripherals connected to the system, processes the sensor data and sends the sensed information to the Cloud.

https://doi.org/10.17993/3ctecno.2021.specialissue7.97-113

2. MATERIALS AND METHODS

2.1. STUDY AREA

The different odour emission sources in and around the Kuppam Town, Andhra Pradesh, India, selected for studying the Odour pollution and its Risk assessment based on standard odour threshold levels. The most commonly selected odour emission sources (areas) are; agriculture practices (fertilizer, pesticides), large livestock operations, poultry farms, fish market, drainages, Municipal Solid waste dumping yards & public amenities like toilets of cinema hall, bus / railway stations, hospitals, shopping complex, etc.

Some of the Municipal Solid waste dumping yards, drainages, fish markets in Kuppam areas as shown in the Figure 1.

Figure 1. Study areas like fish market, landfills and drainages etc. Images taken at Kuppam.

Source: own elaboration.

The selected study area in Kuppam, weather in the wet season is muggy and overcast, the dry season is partly cloudy, and it is hot year round. The temperature typically varies from 18°C to 38°C, Average rainfall varies from 4 mm to 124 mm, Extreme variation in the perceived humidity varies from 29% to 89% and the seasonal variation of the wind speed over the course of the year is 2.7 m/s to 6.1 m/s (Weather Spark, 2020).

https://doi.org/10.17993/3ctecno.2021.specialissue7.97-113

2.2. METHODOLOGY

The development of methods includes:

- Design of artificial olfactory Electronic device (E-Nose).
- Mathematical modelling.
- Measurement of Odour concentration & Sampling.
- Data processing, Storage & Remote Monitoring.
- Risk assessment & Standard Guidelines.

The odour concentration were measured using artificial olfactory Electronic device called Electronic Nose from different sources of odour emission, risk assessment was done based on the standard safety and threshold concentration levels prescribed by like Occupational Safety and Health Administration (OSHA), National Institute for Occupational Safety and Health (NIOSH) (NIOSH, 2007; OSHA, 2011).

2.2.1. DESIGN OF ARTIFICIAL OLFACTORY ELECTRONIC DEVICE (E-NOSE)

In this research study, an embedded electronic device is designed to measure the concentration of odour pollution at selected areas. The design of artificial olfactory electronic nose incorporates most desirable industrial Odour sensors; TGS2602 Metal Oxide Semiconductor (MOS) type Sensor for detecting Hydrogen Sulphide (H2S), Ammonia (NH3), Volatile Organic Compounds (VOCs) and 110-601 Sulphur Dioxide (SO2) sensor, Solar harvesting unit for powering the portable electronic nose, Odour threshold level indicator, Communication network unit (Wi-Fi) for uploading processed data onto the IoT cloud storage and mobile application for retrieving the odour concentration from IoT cloud , performing risk assessment based on standard threshold levels and then providing the alert information to end users. Finally, the Data processor (Atmega328) coordinates and controls all the peripherals connected to the system, processes the sensor data and sends the sensed information to the Cloud. The artificial olfactory Electronic device (E-Nose) design block diagram is as shown in Figure 2.

https://doi.org/10.17993/3ctecno.2021.specialissue7.97-113

Figure 2. Block diagram of Proposed Electronic Node Design.

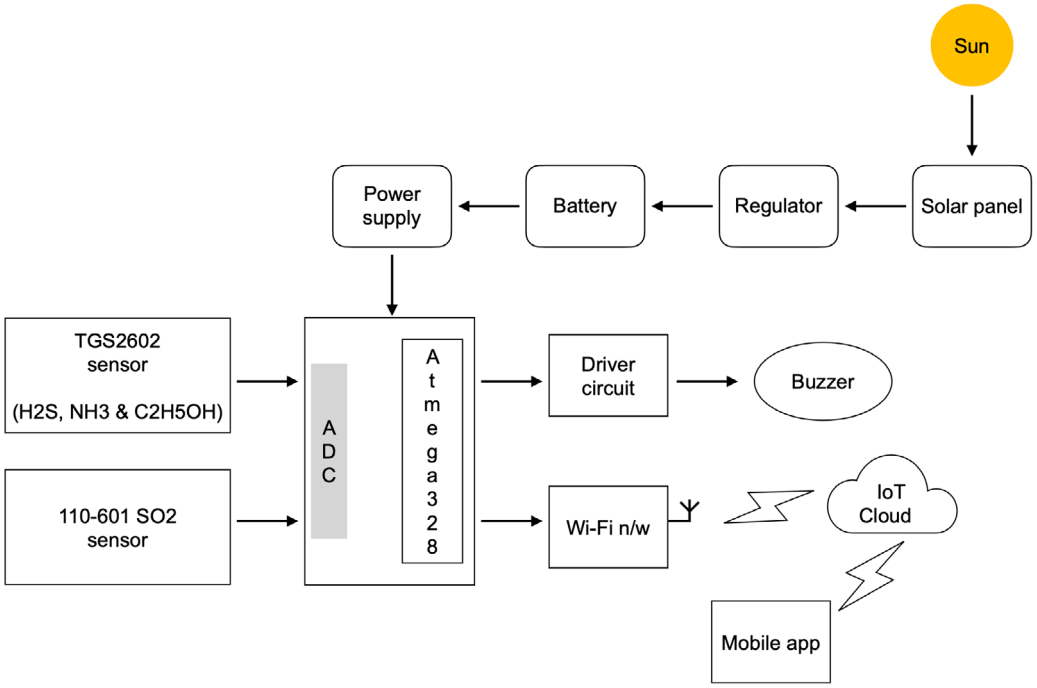

Source: own elaboration.

2.2.2. MATHEMATICAL MODELLING

The mathematical modelling involves the development the mathematical algorithms for calculating sensor coefficients (calculating sensor resistance (Ro) in fresh air, sensor resistance (Rs) in displayed gases at various concentrations) from the sensitivity curve of sensor datasheet and converting the analog output values of the odour sensors into Parts Per Millions (PPM) standard.

Sensor coefficients can be calculated in to ways either using straight line equation or using power Regression analysis.

To calculate the sensor coefficients using straight line equations sensitivity curve and the basic measuring circuit of the sensor is considered as shown in Figure 3.

https://doi.org/10.17993/3ctecno.2021.specialissue7.97-113

Figure 3. Basic measuring circuit of TGS2602 sensor.

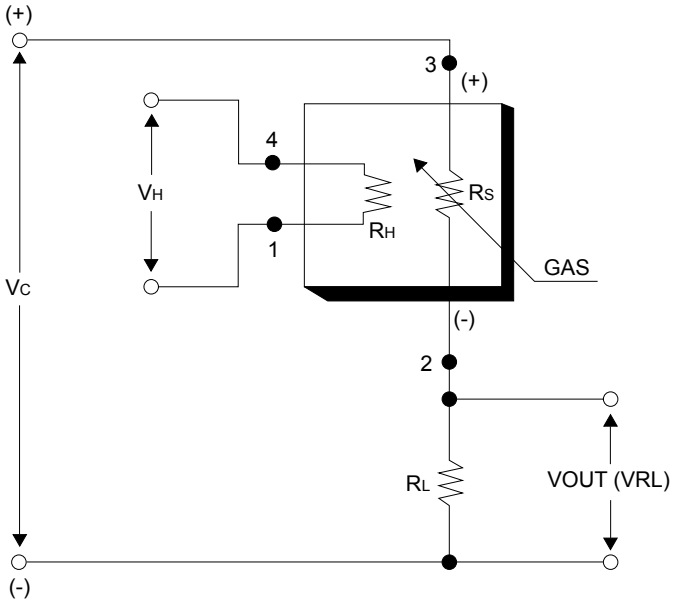

Source: TGS2602 Sensor Datasheet, FIGARO USA, INC.

The sensor resistance Rs can be determined using Ohm's Law: V = I x R

from basic measuring circuit is output current is equal to: I = VC / (Rs+RL)

Ro/RL: sensor resistance in the clean air.

Rs: sensor resistance at various concentrations of gases.

Then; Rs = [(Vc x RL) / VRL] – RL (1)

Equation 1 will help us find the values of the sensor resistance for different gases. To calculate sensor resistance Ro, the value of the RS in fresh air needs to be determined. This is done by taking the average of analog readings from the sensor and converting it to voltage.

The sensitivity curve/graph of the sensor is in log-log scale, so the straight-line equation for finding coefficients is;

y = mx + b

Where: y: Y value on Y axis

https://doi.org/10.17993/3ctecno.2021.specialissue7.97-113

x: X value on X axis

m: Slope of the line

b: Y intercept

For a log-log scale, the formula looks like; log(y) = m*log(x) + b

Now to find the slope(m), 2 points needs to be chosen from the sensitivity curve/graph.

The formula to calculate m is the following:

$$y = mx + b \quad (2)$$

where: value of x: X value on x-axis

value of m: Slope of line

b: Y interception Point on Graph (x1,y1) (x2,y2)

m = [log(y) - log(y0)] / [log(x) - log(x0)]

b = log(y) - m*log(x),

log(y) = m*log(x) + b,

This is how the two coefficients (m, b) are calculated using straight lines equations of sensitivity curve.

Another method to calculate coefficients (m, b) is using power regression based digitizing software tool, which converts the image file showing the sensor graph/curve into digital numbers. The digitizer tool recovers the data points from sensor graphs. The calculated data points are usually used as input to other software applications or programming the controllers to measure gas concentrations accurately from the sensors.

After finding the Coefficients, slope m and b using straight line equation method or power regression method from sensor gas sensitivity curve, finally calculating the gas concentration in ppm using the equation 3;

$$X \text{ in ppm} = 10^{\wedge} ((\log (Rs/Ro) - b) / m) \quad (3)$$

https://doi.org/10.17993/3ctecno.2021.specialissue7.97-113

2.2.3. MEASUREMENT OF ODOR CONCENTRATION & SAMPLING METHOD

From decades mainly research studies on odor concentration measurement were based laboratory testing, which means collection of Odor samples from different test fields and then measuring concentration of different odor gases at the laboratory.

In our research study we developed a customized electronic device (E-Nose) using Different odor sensors to determine the concentration of various odor gases at selected areas. Before the development of odor sensing device, firstly, we selected study areas and visited to investigate problems persisted in and around the study areas due to odor pollution. Conducted real-time survey by interacted with the residents staying around the selected study areas with various questionnaires related to health issues, lifestyle, frequency of occurrence, duration, etc., Secondly, we developed a customized electronic device (E-Nose) for measuring odor concentration at the field under test. Thirdly, we carried the Autonomous E-Nose odor sensing device for measuring odor concentration at various selected areas. Repeated the measurements were done for many days and then uploaded the measured odor concentrations to IoT cloud for further studies and performing risk assessment based on the measured levels.

2.2.4. DATA PROCESSING, STORAGE & REMOTE MONITORING

The data collection starts with the basic survey where the research study begins and continued till the real-time field measurement of odor concertation will be done, hence the data needs to be processed at various stages of the research development. The data processor reads odor levels from the odor sensors, then processes it by applying mathematical modelling algorithms to convert the output voltage levels into odor concentration in parts per million (ppm). After data processing, measured odor concentration data was uploaded to IoT cloud for storage and further studies. The data stored onto the IoT cloud helps us to further assess the data using user-friendly user interfaces like mobile/web applications or remote monitoring and decision-making purposes.

2.2.5. RISK ASSESSMENT & STANDARD GUIDELINES

As we know that constant exposure to odor pollution causes many health issues, therefore risk assessment must be done comparing the measured odor concentration levels at various

https://doi.org/10.17993/3ctecno.2021.specialissue7.97-113

areas against the standard Threshold Limit Levels (TLV) of various Odor gases published by agencies like Occupational Safety and Health Administration (OSHA), National Institute for Occupational Safety and Health (NIOSH), American Conference of Governmental Industrial Hygienists (ACGIH) (NIOSH, 2007; OSHA, 2011; ACGIH, 2021). Risk assessment was performed based on the measured odor concentration and permissible Threshold Limit Levels (TLV). After assessment, if the concentration of measured odor gas exceeds threshold limit values, then an alert indication with symptoms will be displayed on user application.

Table 1 shows the Standard Threshold Limit Levels (TLV), 8-hour Time-weighted Average (TWA), Short Term Exposure Limit Values (STEL) and Immediately Dangerous to Life & Health (IDLH),

Table 1. Threshold Limit values of various odor gases concentration in parts per million (ppm).

Odor Gas	TLV-TWA	TLV-STEL	IDLH
Ammonia (NH3)	25	35	300
Hydrogen Sulfide (H2S)	10	15	100
Sulphur Dioxide, SO2	2	5	100

Sources: TLV-TWA and TLV-STEL data extracted from the 2005 Threshold Limit Values & Biological Exposure Indices, copyright 2005 by the American Conference of Governmental Industrial Hygienists (ACGIH). IDLH values extracted from the NIOSH Pocket Guide to Chemical Hazards, 2004 published by the National Institute for Occupational Safety and Health (NIOSH).

3. RESULTS AND DISCUSSIONS

In this current research work, we followed new approach of measuring odor concentrations based on electronic devices rather than on human sensory olfaction methods. Figure 4 shows a self-powered portable electronic device (E-Nose) designed to measure the concertation of odour gases at selected areas.

In first phase we conducted real-time health survey of residents and peoples staying near the selected study areas like; waste dumping yard, Drainages, agriculture practices, livestock operations, industries and poultry forms. The survey involved the questionnaires in the form age, gender, type of health issue (disease), frequency of occurrence & duration. In this sampling survey around 80 peoples were interacted and collected the information mentioned in the questionnaire. The real-time survey data is shown in Table 2.

https://doi.org/10.17993/3ctecno.2021.specialissue7.97-113

Figure 4. Proposed Odor Measuring Portable Electronic Hardware Device.

Source: own elaboration.

Table 2 gives information about real-time survey at different areas, various symptoms or health issues reported by interacting with peoples staying at the areas and proximity areas. Most of the peoples reported the frequency of occurrence & duration of these symptoms is around 1 week to 1 month.

Table 2. Conducted Real-time Health survey data at different areas (Kuppam area).

Study Area	Health Symptoms	No. of Health issues reported
Waste Dumping Yard	Nausea, Coughing	35
	Headache, Loss of sleep	40
	Irritation (eyes, throat, nose) Respiratory problems	39
	Fatigue & Dizziness	37
Drainage at Residents	Nausea, Coughing	43
	Headache, Loss of sleep	40
	Irritation (eyes, throat, nose) Respiratory problems	38
	Fatigue & Dizziness	32
Agriculture practices Pesticides fertilizers	Nausea, Coughing	53
	Headache, Loss of sleep	49
	Irritation (eyes, throat, nose) Respiratory problems	29
	Fatigue & Dizziness	42
Livestock Operations Nausea, Coughing Headache, Loss of sleep	Nausea, Coughing	33
	Headache, Loss of sleep	30
	Irritation (eyes, throat, nose) Respiratory problems	28
	Fatigue & Dizziness	22

Source: own elaboration.

https://doi.org/10.17993/3ctecno.2021.specialissue7.97-113

In the second phase, we conducted real-time measurement of odour concentration at selected areas. The table III shows the measured odour concentrations of Ammonia (NH3), Hydrogen Sulphide (H2S) & Sulphur Dioxide (SO2) by considering temperature, humidity and wind speed & direction, measurement is conducted morning to evening at the every 1hr duration.

Table 3. Conducted Real-Time measurement of odour concentration at different sites.

Study Area	Ranges of Measured Odour Concentration in ppm		
Waste Dumping Yard	NH3	H2S	SO2
Drainage at Residents	15-105	0.5 - 12	0.25 – 1.5
Agriculture practices	10-85	1.5 - 11	0.5 – 2.0
Fertilizers, pesticides	45-115	2 - 15	1.5 – 4.5
Livestock Operations	5-95	0.85 - 8.5	0.2 – 1.25

Source: own elaboration.

Table 3 shows the measured odour concentration at different sites, at waste dumping site NH3 levels ranges from 15-105 ppm, H2S levels ranges from 0.5 - 12ppm, SO2 levels ranges from 0.25 – 1.5ppm. Drainage at Residents NH3 levels ranges from 10-85 ppm, H2S levels ranges from 1.5 - 11ppm, SO2 levels ranges from 0.5 – 2.0 ppm. Agriculture practices Fertilizers, pesticides NH3 levels ranges from 45-115 ppm, H2S levels ranges from 2 – 15 ppm, SO2 levels ranges from 1.5 – 4.5 ppm. Livestock Operations NH3 levels ranges from 5-95 ppm, H2S levels ranges from 0.85 - 8.5 ppm, SO2 levels ranges from 0.2 – 1.25 ppm. The rage of odour concentrations at different sites are clearly showing exceed in its levels i.e 8-hr Time Weighted Average (TWA) Threshold Limit Value (TLV) and Short Time Exposure Limit (STEL) Threshold Limit Value (TLV) as shown in Table 2. According to OSHA, NIOSH and ACGIC regulation the symptoms or health issues associated with the measured concentration ranges are (ACGIH, 2021; NIOSH, 2011) nausea, coughing, headache, loss of sleep, irritation (eyes, throat, nose), respiratory problems, fatigue & dizziness, etc.

Finally measured odour concertation levels are uploaded to IoT cloud and further studies. The data stored onto the IoT cloud helps us to further assess the health impacts associated with odour levels using user-friendly mobile/web applications. After risk assessment, if odour levels are exceeds the threshold limit values, then precautionary alert is generated as shown in Figure 5. IoT application displays Odour concentration levels in ppm at measures site on the map as well as in the dashboard.

https://doi.org/10.17993/3ctecno.2021.specialissue7.97-113

Figure 5. Design of IoT Mobile Application.

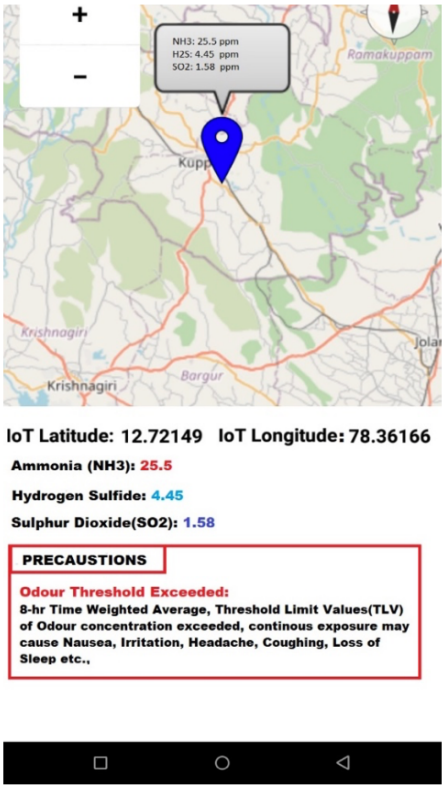

Source: Developed on MIT APP Inventor 2.

4. CONCLUSIONS

We successfully designed an OdorSense a solar-powered, portable handheld electronic device, and conducted the real-time measurement of odor gas concentrations at various study areas. The device has shown satisfactory results in measuring the odor levels. A real-time health survey has been conducted at selected study areas involving around 80 peoples in the sampling process based on questionnaires. After conducting the odor concentration measurement, a Risk assessment was performed to check the associated health issues based on the measured odor concentration and permissible Threshold Limit Values (TLV) i.e TLV-TWA and TLV-STEL. After the assessment, if the concentration of measured odor gas exceeds threshold limit values, then an alert indication with symptoms will be displayed on the user application. Hence a user-friendly system was developed to measure and assess the odor pollution at any application.

https://doi.org/10.17993/3ctecno.2021.specialissue7.97-113

5. ACKNOWLEDGEMENTS

The author of research paper would like to express gratitude to G. N. Kodanda Ramaiah, Professor & Director R&D, Kuppam Engineering College for supporting and guiding throughout the research work. Also grateful to the Dr. Rangaraju and Dr. Vijay Prakash, Doctoral Committee members or giving valuable suggestions or carrying out research work. Finally, I feel thankful to KEC management for the motivation and research facilities provided in the R&D Centre in the Institution.

REFERENCES

Association Advancing Occupational and Environmental Health. (2021, February 24). *Association Advancing Occupational and Environmental Health*. ACGIH. https://www.acgih.org

Bax, C., Sironi, S., & Capelli, L. (2020). How Can Odors Be Measured? An Overview of Methods and Their Applications. *Atmosphere, 11*(1), 92. https://doi.org/10.3390/atmos11010092

CDC - The National Institute for Occupational Safety and Health (NIOSH). (2007). https://www.cdc.gov/niosh/index.htm

Ceballos, D. M., & Burr, G. A. (2012). Evaluating a Persistent Nuisance Odor in an Office Building. *Journal of Occupational and Environmental Hygiene, 9*(1), D1–D6. https://doi.org/10.1080/15459624.2012.635131

Elwell, D. L., Keener, H. M., Wiles, M. C., Borger, D. C., & Willett, L. B. (2001). Odorous Emissions and Odor Control In Composting Swine Manure/Sawdust Mixes Using Continuous And Intermittent AERATION. *Transactions of the ASAE, 44*(5), 1307–1316. https://doi.org/10.13031/2013.6436

Deshmukh, S., Bandyopadhyay, R., Bhattacharyya, N., Pandey, R. A., & Jana, A. (2015). Application of electronic nose for industrial odors and gaseous emissions measurement and monitoring – An overview. *Talanta, 144,* 329–340. https://doi.org/10.1016/j.talanta.2015.06.050

https://doi.org/10.17993/3ctecno.2021.specialissue7.97-113

Di, Y., Liu, J., Liu, J., Liu, S., & Yan, L. (2013). Characteristic analysis for odor gas emitted from food waste anaerobic fermentation in the pretreatment workshop. *Journal of the Air & Waste Management Association, 63*(10), 1173–1181. https://doi.org/10.1080/10962247.2013.807318

Erisman, J. (2001). Instrument development and application in studies and monitoring of ambient ammonia. A*tmospheric Environment, 35*(11), 1913–1922. https://doi.org/10.1016/s1352-2310(00)00544-6

Gongora, A., Jaenal, A., Chaves, D., Monroy, J., & Gonzalez-Jimenez, J. (2019). Urban Monitoring of Unpleasant Odors with a Handheld Electronic Nose. In *2019 IEEE International Symposium on Olfaction and Electronic Nose (ISOEN),* 1–3. https://doi.org/10.1109/isoen.2019.8823219

Hayes, E. T., Curran, T. P., & Dodd, V. A. (2006). A dispersion modelling approach to determine the odour impact of intensive poultry production units in Ireland. *Bioresource Technology, 97*(15), 1773–1779. https://doi.org/10.1016/j.biortech.2005.09.019

Occupational Safety and Health Administration. (2011). https://www.osha.gov

Ministry of Environment & Forests, Government of India. (2007). *Guidelines On Odour Pollution & Its Control.* Central Pollution Control Board (CPCB).

Misselbrook, T. H., Clarkson, C. R., & Pain, B. F. (1993). Relationship Between Concentration and Intensity of Odours for Pig Slurry and Broiler Houses. *Journal of Agricultural Engineering Research, 55*(2), 163–169. https://doi.org/10.1006/jaer.1993.1040

Nicolas, J., Craffe, F., & Romain, A. C. (2006). Estimation of odor emission rate from landfill areas using the sniffing team method. *Waste Management, 26*(11), 1259–1269. https://doi.org/10.1016/j.wasman.2005.10.013

Pagans, E., Barrena, R., Font, X., & Sánchez, A. (2006). Ammonia emissions from the composting of different organic wastes. Dependency on process temperature. *Chemosphere, 62*(9), 1534–1542. https://doi.org/10.1016/j.chemosphere.2005.06.044

https://doi.org/10.17993/3ctecno.2021.specialissue7.97-113

Sarkar, U., & Hobbs, S. E. (2002). Odour from municipal solid waste (MSW) landfills. *Environment International, 27*(8), 655–662. https://doi.org/10.1016/s0160-4120(01)00125-8

Shinde, R. B., & Sagar, M. G. (2017). Odour Reducing Technique in Field at Kurkumbh. *International Journal of Engineering Research, 6*(6), 341. https://doi.org/10.5958/2319-6890.2017.00033.2

Szulczyński, B., & Gębicki, J. (2019). Electronic nose – an instrument for odour nuisances monitoring. *E3S Web of Conferences, 100,* 00079. https://doi.org/10.1051/e3sconf/201910000079

Takano, T. (2014). The measurement of the offensive odor and application of the measurement technology to the smell in living. *Journal of Japan Association on Odor Environment, 45*(1), 2–8. https://doi.org/10.2171/jao.45.2

United States Environmental Protection Agency. (2021, January 21). *Reference guide to odor thresholds for hazardous air pollutants listed in the clean air*. https://www.epa.gov/laws-regulations

Weather Spark. (2020). *Average Weather in Kuppam, India, Year Round.* https://weatherspark.com/y/109403/Average-Weather-in-Kuppam-India-Year-Round

Wenjing, L., Zhenhan, D., Dong, L., Jimenez, L. M. C., Yanjun, L., Hanwen, G., & Hongtao, W. (2015). Characterization of odor emission on the working face of landfill and establishing of odorous compounds index. *Waste Management, 42*, 74–81. https://doi.org/10.1016/j.wasman.2015.04.030

Zhu, Y., Zheng, G., Gao, D., Chen, T., Wu, F., Niu, M., & Zou, K. (2016). Odor composition analysis and odor indicator selection during sewage sludge composting. *Journal of the Air & Waste Management Association, 66*(9), 930–940. https://doi.org/10.1080/10962247.2016.1188865

https://doi.org/10.17993/3ctecno.2021.specialissue7.97-113

/07/

https://doi.org/10.17993/3ctecno.2021.specialissue7

SPHERICAL FUZZY SWARA-MARCOS APPROACH FOR GREEN SUPPLIER SELECTION

Mehmet Ali Taş
Department of Industrial Engineering, Turkish-German University.
Istanbul, (Turkey).
E-mail: mehmetali.tas@tau.edu.tr
ORCID: https://orcid.org/0000-0003-3333-7972

Esra Çakır
Department of Industrial Engineering, Galatasaray University
Istanbul, (Turkey).
E-mail: ecakir@gsu.edu.tr
ORCID: https://orcid.org/0000-0003-4134-7679

Ziya Ulukan
Department of Industrial Engineering, Galatasaray University
Istanbul, (Turkey).
E-mail: zulukan@gsu.edu.tr
ORCID: https://orcid.org/ 0000-0003-4805-2726

Recepción: 01/12/2020 **Aceptación:** 22/02/2021 **Publicación:** 07/05/2021

Citación sugerida:
Taş, M. A., Çakır, E., y Ulukan, Z. (2021). Spherical fuzzy SWARA-MARCOS approach for green supplier selection. *3C Tecnología. Glosas de innovación aplicadas a la pyme, Edición Especial*, (mayo 2021), 115-133. https://doi.org/10.17993/3ctecno.2021.specialissue7.115-133

ABSTRACT

In a supply chain management, supplier selection is an important step to determine the structure of the model. Multi-criteria decision making methods are appropriate tools for dealing with the selection of suitable suppliers. In addition, fuzzy multi-criteria decision making approaches are helpful to include different and uncertain views of decision makers. In this study, a new combined fuzzy methodology is proposed to handle green supplier selection problem. The proposed model consists of a spherical fuzzy-SWARA method, which is used to calculate the criteria weights, and MARCOS method, which is applied to rank the alternatives. In the case study, green supplier selection problem of a textile company located in Turkey is discussed. Six alternative suppliers are evaluated against twelve green criteria, and alternatives are ranked. Finally, a sensitivity analysis is performed to compare the results of different scenarios.

KEYWORDS

Green supplier selection, MARCOS, MCDM, Spherical fuzzy sets, Supply chain, Spherical fuzzy - SWARA.

https://doi.org/10.17993/3ctecno.2021.specialissue7.115-133

1. INTRODUCTION

Supply chains are of great importance for businesses to maintain their main activities (Stevens, 1989). For the establishment and proper functioning of supply chains, the appropriate supplier must be selected. The criteria (attributes) to be considered when choosing a supplier often conflict with each other and cause difficulty in decision making (Akcan & Taş, 2019). Multi-criteria decision-making methods (MCDM) can be used to overcome these difficulties. These methods help to evaluate alternatives using criteria with different characteristics (De Boer *et al.*, 2001). In addition, it is appropriate to use fuzzy sets for imprecise statements of decision makers. These methods are frequently used in supplier selection practices (Yazdani *et al.*, 2017). In recent years, thanks to the increase in environmental awareness, sustainable supply chain has gained importance. Therefore, the concept of green supply chain that cares about the environment has emerged (Bali *et al.*, 2013). Sustainable criteria should be taken into account and determined as environmental performance evaluations. Using the MCDM methods, the suitable supplier in the green supply chain can be determined according to the sustainable criteria. Various MCDM have been used for green supplier selection in the literature, including some methods such as AHP (Mavi, 2015), PROMETHEE (Govindan *et al.*, 2017), TOPSIS (Cao *et al.*, 2015), ANP (Chung *et al.*, 2016), DEA (Dobos & Vörösmarty, 2019), VIKOR (Akman, 2015), ELECTRE (Kumar et al, 2017), COPRAS (Liou, 2016), DEMATEL (Hsu, 2013), EDAS (He, 2019), TODIM (Sang & Liu, 2016), WASPAS (Ghorabaee, 2016), MULTIMOORA (Sen *et al.*, 2017), and more. In this study, SWARA and MARCOS are combined with spherical fuzzy sets (SFS) for fuzzy MCDM problems.

SWARA method was introduced to the literature by Keršuliene *et al.* (2010). The method was applied to evaluate the criteria for the selection of agile supplier of an automobile manufacturer in Iran (Alimardan *et al.*, 2013), the evaluation of investments in high technology sectors (Hashemkhani & Bahrami, 2014), the design of bottle package (Stanujkic *et al.*, 2015), the selection of renewable energy technology (Ijadi Maghsoodi *et al.*, 2018), the appraisal of sustainable properties for renewable energy systems (Ghenai *et al.*, 2020).

After Zadeh (1965) introduce the ordinary fuzzy sets, numerous extensions have been proposed such as type-2 fuzzy sets (Zadeh, 1975), intuitionistic fuzzy sets (Atanassov,

https://doi.org/10.17993/3ctecno.2021.specialissue7.115-133

1986), hesitant fuzzy sets (Torra, 2010), Pythagorean fuzzy sets (Yager, 2013), neutrosophic fuzzy sets (Smarandache, 1998), and so on. In the literature, many research combined SWARA and fuzzy sets. Some of these are those: ordinary fuzzy-SWARA (Perçin, 2019), hesitant fuzzy-SWARA (Kaya & Erginel, 2020), symmetric interval type-2 fuzzy-SWARA (Keshavarz-Ghorabaee, 2018), neutrosophic fuzzy-SWARA (Rani & Mishra, 2020). In 2018, as an extension of fuzzy sets, spherical fuzzy numbers are introduced (Gündoğdu & Kahraman, 2019a). These fuzzy sets differ from others in that they are three-dimensional. "In spherical fuzzy numbers, while the squared sum of membership, non-membership and hesitancy parameters can be between 0 and 1, each of them can be defined between 0 and 1 independently to satisfy that their squared sum is at most equal to 1" (Gündoğdu & Kahraman, 2019b). Additionally, this study proposes a new spherical fuzzy-SWARA combination to the literature.

The Measurement of Alternatives and Ranking according to Compromise Solution (MARCOS) method is first introduced to the literature by Stević *et al.* (2020). Ilieva *et al.* (2020) used fuzzy MARCOS for ordering cloud storage service. Chattopadhyay *et al.* (2020) conducted a supplier selection study for the iron and steel industry using D-MARCOS. Stević and Brković (2020) used integrated FUCOM-MARCOS methodology to evaluate the human resources of the transportation company and to select the employee of the month. Stanković *et al.* (2020) studied on the risks of the main road with the fuzzy MARCOS. Badi and Pamucar (2020) used MARCOS with gray numbers in the supplier selection of Libyan Iron and Steel Company. Vesković *et al.* (2020) assessed possible solutions to problems of railway transportation in Republic of Srpska. F-MARCOS was chosen as one of the MCDM methods to compare the results. Mijajlović *et al.* (2020) employed FUCOM and fuzzy MARCOS to examine the competition of spa centers. Ulutaş *et al.* (2020) researched on the manual stacker selection for small warehouses, using CCSD, ITARA, and MARCOS. They used the MARCOS to evaluate the alternatives. Puška *et al.* (2020) performed MARCOS in selection of project management software.

In this study examines the green supplier selection problem of a textile firm. To examine environmental performance, twelve green criteria are determined. Seven decision makers (DM) working within the company evaluate the criteria and alternatives with the spherical fuzzy numbers. The weights of the criteria are calculated by the spherical fuzzy-SWARA

https://doi.org/10.17993/3ctecno.2021.specialissue7.115-133

method. Applying the steps of the MARCOS, the alternatives are ranked. In the lights of the literature review, the original contribution of this study is that the proposed methodology is the pioneering work that combines spherical fuzzy-SWARA and MARCOS method. In addition, the proposed methodology is adapted to a real-life problem by investigating a green supplier selection case.

The rest of the paper is organized as follows. The preliminaries and definitions of the spherical fuzzy sets are given in Section 2. The proposed methodology involving the original combination of the spherical fuzzy-SWARA and MARCOS methods are also introduced in Section 2. Section 3 applies the proposed methodology on a green supplier selection case and a sensitivity analysis is applied for different weighting criteria scenarios. Finally, conclusion and future perspectives are discussed in Section 4.

2. METHODOLOGY

2.1. PRELIMINARIES

This section gives the preliminaries and definitions of the proposed method with spherical fuzzy information (Gündoğdu & Kahraman, 2019a; Gündoğdu & Kahraman, 2019b):

Definition 1: A spherical fuzzy set $\tilde{A}$ of the universe of discourse X is given by:

$$\tilde{A} = \{(x, \mu_A(x), \eta_A(x), v_A(x)) | x \in X\} \quad (1)$$

The $\mu_{\tilde{A}}$ (x), $\eta_{\tilde{A}}$ (x) and $v_{\tilde{A}}$ (x) represent membership degree, non-membership degree and hesitancy of x to $\tilde{A}$, respectively and they satisfy the condition $\mu_{\tilde{A}}(x), \eta_{\tilde{A}}(x), v_{\tilde{A}}(x) \in [0,1]$ ve $0 \leq \mu_{\tilde{A}}(x)^2 + \eta_{\tilde{A}}(x)^2 + v_{\tilde{A}}(x)^2 \leq 1$. The hesitancy parameter of $\tilde{A}$ is expressed as $\pi_{\tilde{A}}(x) = \sqrt{1 - \mu_{\tilde{A}}(x)^2 - \eta_{\tilde{A}}(x)^2 - v_{\tilde{A}}(x)^2}$. The expression ($\mu_{\tilde{A}}$ (x), $\eta_{\tilde{A}}$ (x), $v_{\tilde{A}}$ (x)) is simply called the spherical fuzzy number (SFN), which can be represented as $\alpha = (\mu, \eta, v)$. In Figure 1, the spherical fuzzy set is illustrated.

https://doi.org/10.17993/3ctecno.2021.specialissue7.115-133

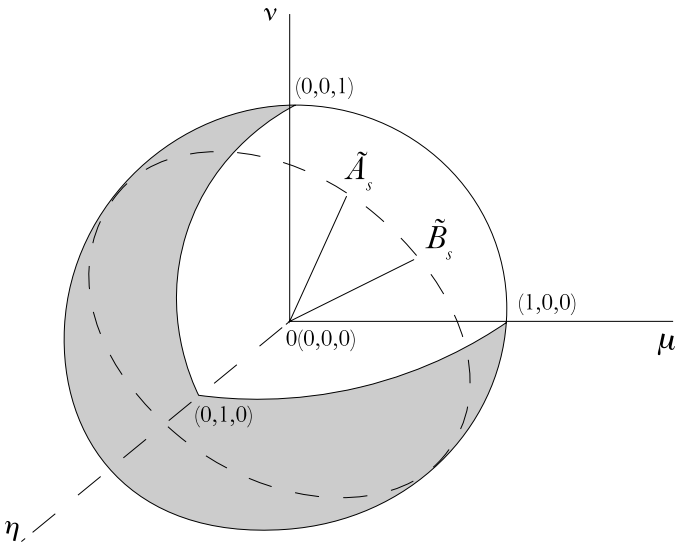

Figure 1. Geometric representation of SFS.
Source: (Gündoğdu & Kahraman, 2019b).

Definition 2: Let $a_1 = (\mu_1, \eta_1, v_1)$ and $a_2 = (\mu_2, \eta_2, v_2)$ be two SFN and let λ be a positive real number, then:

$$\alpha_1 \oplus \alpha_2 = \{\sqrt{{\mu_1}^2 + {\mu_2}^2 - {\mu_1}^2{\mu_2}^2}, \eta_1\eta_2 \sqrt{(1-{\mu_2}^2){v_1}^2 + (1-{\mu_1}^2){v_2}^2 - {v_1}^2{v_2}^2}\} \quad (2)$$

$$\alpha_1 \otimes \alpha_2 = \{\mu_1\mu_1, \sqrt{{\eta_1}^2 + {\eta_2}^2 - {\eta_1}^2{\eta_2}^2}, \sqrt{(1-{\eta_2}^2){v_1}^2 + (1-{\eta_1}^2){v_2}^2 - {v_1}^2{v_2}^2}\} \quad (3)$$

$$\lambda\alpha_1 = \{\sqrt{1-(1-{\mu_1}^2)^\lambda}, {\eta_1}^\lambda, \sqrt{(1-{\mu_1}^2)^\lambda + (1-{\mu_1}^2 - {v_1}^2)^\lambda}\} \quad (4)$$

$${\alpha_1}^\lambda = \{{\mu_1}^\lambda, \sqrt{1-(1-{\eta_1}^2)^\lambda}, \sqrt{(1-{\eta_1}^2)^\lambda + (1-{\eta_1}^2 - {v_1}^2)^\lambda}\} \quad (5)$$

The complement of the spherical fuzzy number α = (μ, η, v) is defined as follows:

$$a^C = (v, \eta, \mu) \quad (6)$$

2.2. PROPOSED METHODOLOGY

In this section, the steps of combined the spherical fuzzy-SWARA and MARCOS methods are introduced. Firstly, the spherical fuzzy-SWARA method is given to calculate the weights of the criteria and then, MARCOS (Stević *et al.*, 2020) method is applied to rank of the alternatives. This study implements the spherical fuzzy sets to SWARA (Stanujkic *et al.*, 2015) steps as follows:

Step 1. Set the problem and select the experts/decision makers according to the problem.

https://doi.org/10.17993/3ctecno.2021.specialissue7.115-133

Step 2. Ranking the criteria by the spherical fuzzy-SWARA. Criteria are ranked based on DM evaluations. The ranking is from highest importance to lowest.

Step 2.1. Determine $\tilde{s}_j$ value: $\tilde{s}_j$ is named "comparative importance of average value" by linguistic measures in Table 1.

Table 1. Linguistic measures of importance used for comparison.

Linguistic measures	(μ, η, ν)
Equally Importance (EI)	(0.5, 0.4, 0.4)
Slightly Low Importance (SLI)	(0.4, 0.6, 0.3)
Low Importance (LI)	(0.3, 0.7, 0.2)
Very Low Importance (VLI)	(0.2, 0.8, 0.1)
Absolutely Low Importance (ALI)	(0.1, 0.9, 0.0)

Source: (Gündoğdu & Kahraman, 2019b).

Step 2.2. Determine $\tilde{k}_j$ coefficient: $\tilde{k}_j$ coefficient is calculated using Eq. (7):

$$\begin{cases} (0.5, 0.4, 0.4) & j = 1 \\ \tilde{s}_j + (0.5, 0.4, 0.4) & j > 1 \end{cases} \tag{7}$$

Step 2.3. Calculate the scores of $\tilde{k}_j$ coefficient: the scores of the $\tilde{k}_j$ is calculated with Eq. (8):

$$SI(\tilde{k}_j) = \sqrt{|100 * [(\mu_{\tilde{k}_j} - \nu_{\tilde{k}_j})^2 - (\eta_{\tilde{k}_j} - \nu_{\tilde{k}_j})^2]|} \text{ for } \mu_{\tilde{k}_j} \geq \nu_{\tilde{k}_j} \tag{8}$$

Step 2.4. Determine q_j value: The importance vector value q_j is calculated with Eq. (9):

$$\begin{cases} 1 & j = 1 \\ \frac{x_{j-1}}{k_j} & j > 1 \end{cases} \tag{9}$$

Step 2.5. Determine w_j value: w_j values are the weights of the criteria, which is calculated using Eq. (10):

$$w_j = \frac{q_j}{\sum_{k=1}^{n} q_k} \tag{10}$$

Step 3. Ranking the criteria by MARCOS (Stević *et al.*, 2020). Creating an initial decision matrix.

Step 3.1. Extend the initial decision matrix. Ideal (AI) and Anti-ideal (AAI) solutions are included to the matrix. Ideal (AI) solution is the best alternative. The below is the expression of ideal (AI) solution (Eq. 11):

https://doi.org/10.17993/3ctecno.2021.specialissue7.115-133

$$AI = {}^{max}_{i} x_{ij} \;\; if\; j \in B \;\; and \;\; {}^{min}_{i} x_{ij} \;\; if\; j \in C \tag{11}$$

Anti-ideal (AAI) solution is the worst alternative. The expression of anti-ideal (AAI) solution (Eq. 12) is as follows:

$$AAI = {}^{min}_{i} x_{ij} \;\; if\; j \in B \; and \; {}^{max}_{i} x_{ij} \;\; if\; j \in C \tag{12}$$

Here, C symbolizes cost criteria to be minimized, whereas B symbolizes benefit criteria to be maximized. The extended decision matrix (X) is shown below:

$$X = \begin{matrix} AAI \\ A_1 \\ \cdots \\ A_m \\ AI \end{matrix} \begin{bmatrix} x_{aa1} & \cdots & x_{aan} \\ x_{11} & \cdots & x_{1n} \\ \cdots & \cdots & \cdots \\ x_{m1} & \cdots & x_{mn} \\ x_{ai1} & \cdots & x_{ain} \end{bmatrix}$$

Step 3.2. Normalize of matrix "X" with Eq. (13) and (14) for benefit criteria and cost criteria, respectively. x_{ij} and x_{ai} belong to matrix "X".

$$n_{ij} = \frac{x_{ij}}{x_{ai}} \;\; if\; J \in B \tag{13}$$

$$n_{ij} = \frac{x_{ai}}{x_{ij}} \;\; if\; J \in C \tag{14}$$

Step 3.3. Creating the weighted matrix "V" using Eq. (15). w_j values represent criteria weights which are calculated or determined.

$$v_{ij} = n_{ij} \times w_j \tag{15}$$

Step 3.4. Calculate the S_i and K_i. S_i stands for the sum of v_{ij} and K_i stands for the utility degree of alternatives. The values are calculated using Eq. (16), (17) and (18) below.

$$S_i = \sum_{i=1}^{n} v_{ij} \tag{16}$$

$$K_i^{+} = \frac{S_i}{S_{ai}} \tag{17}$$

$$K_i^{-} = \frac{S_i}{S_{aai}} \tag{18}$$

https://doi.org/10.17993/3ctecno.2021.specialissue7.115-133

Step 3.5. Formulate the utility function. $f(K_i^+)$ and $f(K_i^-)$ are used for the utility function with respect to the ideal and anti-ideal solution, respectively. These values are calculated using Eq. (19), (20) and (21) below.

$$f(K_i^+) = \frac{K_i^-}{K_i^+ + K_i^-} \tag{19}$$

$$f(K_i^-) = \frac{K_i^+}{K_i^+ + K_i^-} \tag{20}$$

$$f(K_i) = \frac{K_i^+ + K_i^-}{1 + \frac{1-f(K_i^+)}{f(K_i^+)} + \frac{1-f(K_i^-)}{f(K_i^-)}} \tag{21}$$

Step 3.6. Create the ranking of alternatives.

Step 4. Determining the best alternative which is the one with the highest score.

3. CASE STUDY

A textile manufacturer located in Marmara region in Turkey is selected as a case study of proposed model. The firm operates in the international market. Twelve sustainable criteria have been determined for the evaluation of six alternative suppliers, which supply raw materials. These green criteria are given in Table 2.

Table 2. The green criteria for textile manufacturer supplier selection.

Code	Criterion	Code	Criterion
C_1	Environmental management system	C_7	Resource/energy consumption
C_2	Green packaging	C_8	Green design
C_3	Green transportation	C_9	Green technology
C_4	Green image	C_{10}	Green purchasing
C_5	Staff environmental management	C_{11}	Pollution production
C_6	Green warehousing	C_{12}	Waste water

Source: own elaboration.

The criteria C_7, C_{11} and C_{12} are cost type, the others are benefit type. The spherical fuzzy-SWARA steps are implemented based on the assessment of each of the seven DM from the company. The importance order of the criteria is given in Table 3. The results are combined by taking the arithmetic mean of the results for seven decision makers and the final criteria weights are calculated as in Table 4.

https://doi.org/10.17993/3ctecno.2021.specialissue7.115-133

Table 3. The orders of importance.

Order	DM_1	DM_2	DM_3	DM_4	DM_5	DM_6	DM_7
1	C_4	C_3	C_1	C_7	C_7	C_{10}	C_1
2	C_8	C_6	C_4	C_4	C_3	C_2	C_9
3	C_1	C_2	C_5	C_3	C_4	C_3	C_4
4	C_6	C_1	C_7	C_1	C_9	C_4	C_3
5	C_2	C_4	C_8	C_2	C_2	C_1	C_{11}
6	C_9	C_{10}	C_{10}	C_8	C_1	C_7	C_8
7	C_3	C_7	C_{11}	C_{10}	C_{11}	C_9	C_2
8	C_5	C_{11}	C_2	C_{11}	C_5	C_8	C_6
9	C_{10}	C_{12}	C_9	C_{12}	C_{12}	C_{12}	C_7
10	C_{11}	C_5	C_3	C_9	C_8	C_6	C_5
11	C_7	C_8	C_6	C_6	C_{10}	C_{11}	C_{10}
12	C_{12}	C_9	C_{12}	C_5	C_6	C_5	C_{12}

Source: own elaboration.

Table 4. The spherical fuzzy-SWARA results.

C_n	DM_1	DM_2	DM_3	DM_4	DM_5	DM_6	DM_7	Avg.	Ranking Results
C_1	0,1072	0,1029	0,1575	0,0959	0,0853	0,0946	0,1572	0,1144	2
C_2	0,0851	0,1132	0,0636	0,0872	0,0896	0,1095	0,0746	0,0890	4
C_3	0,0736	0,1627	0,0551	0,1007	0,1087	0,1043	0,1081	0,1019	3
C_4	0,1356	0,0936	0,1432	0,1158	0,1035	0,0993	0,1243	0,1165	1
C_5	0,0701	0,0452	0,1061	0,0565	0,0739	0,0383	0,0398	0,0614	11
C_6	0,1021	0,1302	0,0501	0,0621	0,0580	0,0543	0,0622	0,0741	9
C_7	0,0528	0,0740	0,0964	0,1216	0,1141	0,0822	0,0518	0,0847	5
C_8	0,1232	0,0430	0,0877	0,0793	0,0640	0,0746	0,0783	0,0786	7
C_9	0,0810	0,0391	0,0578	0,0652	0,0941	0,0783	0,1429	0,0798	6
C_{10}	0,0610	0,0851	0,0701	0,0755	0,0609	0,1533	0,0362	0,0774	8
C_{11}	0,0581	0,0569	0,0668	0,0719	0,0776	0,0517	0,0901	0,0676	10
C_{12}	0,0503	0,0542	0,0455	0,0685	0,0704	0,0597	0,0345	0,0547	12
Tot.	1,0000	1,0000	1,0000	1,0000	1,0000	1,0000	1,0000	1,0000	

Source: own elaboration.

In Step 3, MARCOS method is performed to evaluate the suppliers (A_1, A_2, A_3, A_4, A_5, A_6) by using the criteria weights. The extended initial decision matrix "*X*" and normalized weighted matrix "*V*" are shown in Table 5 and Table 6.

Table 5. The extended initial decision matrix "X".

	C_1	C_2	C_3	C_4	C_5	C_6	C_7	C_8	C_9	C_{10}	C_{11}	C_{12}
Weights	0,1144	0,0890	0,1019	0,1165	0,0614	0,0741	0,0847	0,0786	0,0798	0,0774	0,0676	0,0547
Type	max	max	max	max	max	max	min	max	max	max	min	min

https://doi.org/10.17993/3ctecno.2021.specialissue7.115-133

AAI	3,7143	3,1429	2,1429	2,1429	4,5714	4,0000	7,2857	4,0000	3,8571	1,8571	8,1429	6,8571
A_1	3,8571	5,2857	3,0000	4,2857	7,5714	4,7143	3,2857	5,0000	3,8571	6,7143	6,7143	5,0000
A_2	5,0000	5,2857	5,1429	4,0000	6,8571	4,4286	3,0000	5,0000	5,1429	7,0000	3,8571	6,1429
A_3	5,4286	3,2857	5,0000	6,4286	5,0000	6,4286	7,2857	4,8571	8,4286	8,1429	8,1429	6,8571
A_4	6,7143	5,8571	2,1429	6,1429	4,5714	5,4286	4,7143	6,1429	4,1429	1,8571	5,1429	5,2857
A_5	3,7143	3,1429	5,0000	7,5714	7,7143	8,1429	7,0000	4,2857	5,0000	3,8571	3,5714	2,7143
A_6	4,4286	4,1429	3,4286	2,1429	6,5714	4,0000	4,5714	4,0000	4,7143	5,0000	1,5714	4,5714
AI	6,7143	5,8571	5,1429	7,5714	7,7143	8,1429	3,0000	6,1429	8,4286	8,1429	1,5714	2,7143

Source: own elaboration.

In the Step 3.4 with the help of the values from Table 4, S_i, K_i^+ and K_i^- values are calculated by Equations (16), (17), and (18). In Step 3.5, $f(K_i)$ values are found for utility functions and scores of alternatives are calculated by Equations (19), (20), and (21). The scores of the alternative suppliers (A_1, A_2, A_3, A_4, A_5, A_6) are shown in Figure 2. According to the results of MARCOS method, the best alternative of green supplier is A_2 with the highest score. Second one is A_3, and third is A_5.

Table 6. Normalized weighted matrix "V".

	C_1	C_2	C_3	C_4	C_5	C_6	C_7	C_8	C_9	C_{10}	C_{11}	C_{12}
AAI	0,0633	0,0477	0,0425	0,0330	0,0364	0,0364	0,0349	0,0512	0,0365	0,0177	0,0130	0,0217
A_1	0,0657	0,0803	0,0594	0,0659	0,0603	0,0429	0,0773	0,0640	0,0365	0,0639	0,0158	0,0297
A_2	0,0852	0,0803	0,1019	0,0615	0,0546	0,0403	0,0847	0,0640	0,0487	0,0666	0,0275	0,0242
A_3	0,0925	0,0499	0,0991	0,0989	0,0398	0,0585	0,0349	0,0621	0,0798	0,0774	0,0130	0,0217
A_4	0,1144	0,0890	0,0425	0,0945	0,0364	0,0494	0,0539	0,0786	0,0392	0,0177	0,0206	0,0281
A_5	0,0633	0,0477	0,0991	0,1165	0,0614	0,0741	0,0363	0,0548	0,0473	0,0367	0,0297	0,0547
A_6	0,0754	0,0629	0,0679	0,0330	0,0523	0,0364	0,0556	0,0512	0,0446	0,0476	0,0676	0,0325
AI	0,1144	0,0890	0,1019	0,1165	0,0614	0,0741	0,0847	0,0786	0,0798	0,0774	0,0676	0,0547

Source: own elaboration.

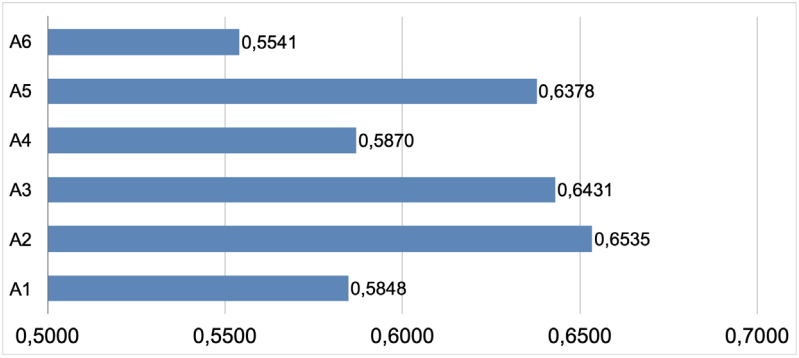

Figure 2. The ranking Scores of Alternatives.
Source: own elaboration.

https://doi.org/10.17993/3ctecno.2021.specialissue7.115-133

To perform a sensitivity analysis of the proposed methodology, thirteen different scenarios are created by changing the weights of the criteria and the results are compared. According to the results, A_2 is the first and A_6 is the last in the ranking in all thirteen scenarios. Although ranking results changes in four scenarios, it is generally the same as the results of combined the spherical fuzzy-SWARA-MARCOS method.

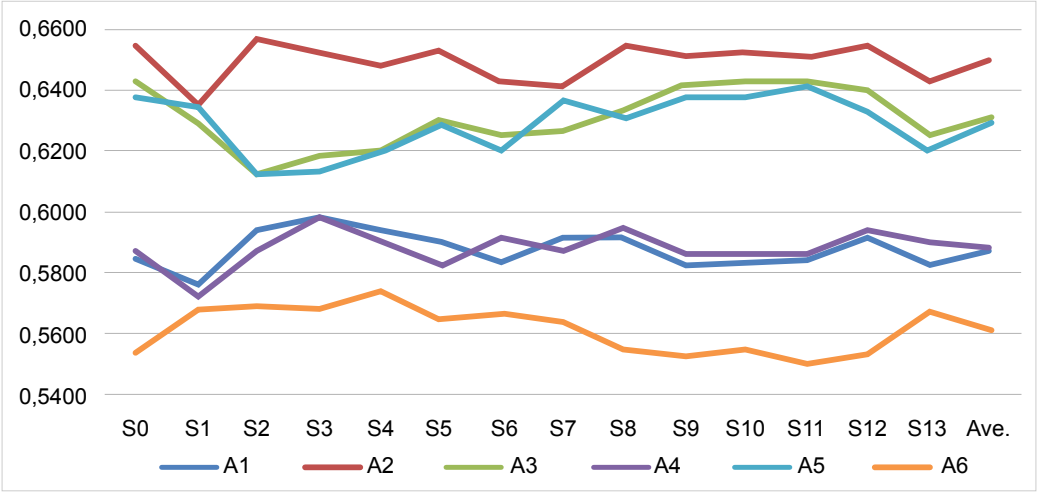

Figure 3. Comparison of different scenarios.
Source: own elaboration.

4. CONCLUSIONS

Nowadays, organizations are expected to be environmentally friendly in their supply chains. Therefore, selecting suitable green suppliers in sustainable supply chains is a very important task. In this study, the green supplier selection problem of a textile company is investigated. The spherical fuzzy-SWARA and MARCOS methods are handled in an integrated way. As a result of the combined spherical fuzzy-SWARA method, the highest weight criteria are green image, environmental management system and green transportation, respectively. According to the MARCOS method, the best green supplier is A_2 and the ranking of alternatives is $A_2>A_3>A_5>A_4>A_1>A_6$. Subsequently, for different scenarios, alternative suppliers are ranked, and the results are compared. Consequently, it is clear that the results of the proposed methodology is consistent. For future studies, the other fuzzy extentions of fuzzy sets can be considered in expressing the views of DMs, and new fuzzy MCDM methods should be implemented for sustainable supply chain problems.

https://doi.org/10.17993/3ctecno.2021.specialissue7.115-133

5. ACKNOWLEDGEMENTS

This work has been supported by the Scientific Research Projects Commission of Galatasaray University under grant number # FBA-2020-1036.

REFERENCES

Akcan, S., & Taş, M. A. (2019). Green supplier evaluation with SWARA-TOPSIS integrated method to reduce ecological risk factors. *Environmental Monitoring and Assessment, 191*(12), 736. https://doi.org/10.1007/s10661-019-7884-3

Akman, G. (2015). Evaluating suppliers to include green supplier development programs via fuzzy c-means and VIKOR methods. *Computers & industrial engineering, 86*, 69-82. https://doi.org/10.1016/j.cie.2014.10.013

Alimardani, M., Hashemkhani Zolfani, S., Aghdaie, M. H., & Tamošaitienė, J. (2013). A novel hybrid SWARA and VIKOR methodology for supplier selection in an agile environment. *Technological and economic development of economy, 19*(3), 533-548. https://doi.org/10.3846/20294913.2013.814606

Atanassov, K.T. (1986). Intuitionistic fuzzy sets. *Fuzzy Sets and Systems, 20*(1), 87-96. https://doi.org/10.1016/S0165-0114(86)80034-3

Badi, I., & Pamucar, D. (2020). Supplier selection for steelmaking company by using combined Grey-MARCOS methods. *Decision Making: Applications in Management and Engineering, 3*(2), 37-48. https://doi.org/10.31181/dmame2003037b

Bali, O., Kose, E., & Gumus, S. (2013). Green supplier selection based on IFS and GRA. *Grey Systems: Theory and Application, 3*(2), 158-176. https://www.emerald.com/insight/content/doi/10.1108/GS-04-2013-0007/full/html

Cao, Q., Wu, J., & Liang, C. (2015). An intuitionsitic fuzzy judgement matrix and TOPSIS integrated multi-criteria decision making method for green supplier selection. *Journal of Intelligent & Fuzzy Systems, 28*(1), 117-126. https://content.iospress.com/articles/journal-of-intelligent-and-fuzzy-systems/ifs1281

https://doi.org/10.17993/3ctecno.2021.specialissue7.115-133

Chakraborty, S., Chattopadhyay, R., & Chakraborty, S. (2020). An integrated D-MARCOS method for supplier selection in an iron and steel industry. *Decision Making: Applications in Management and Engineering, 3*(2), 49-69. https://doi.org/10.31181/dmame2003049c

Chung, C. C., Chao, L. C., & Lou, S. J. (2016). The establishment of a green supplier selection and guidance mechanism with the ANP and IPA. *Sustainability, 8*(3), 259. https://doi.org/10.3390/su8030259

De Boer, L., Labro, E., & Morlacchi, P. (2001). A review of methods supporting supplier selection. *European journal of purchasing & supply management, 7*(2), 75-89. https://research.utwente.nl/en/publications/a-review-of-methods-supporting-supplier-selection

Dobos, I., & Vörösmarty, G. (2019). Inventory-related costs in green supplier selection problems with Data Envelopment Analysis (DEA). *International Journal of Production Economics, 209,* 374-380. https://doi.org/10.1016/j.ijpe.2018.03.022

Ghenai, C., Albawab, M., & Bettayeb, M. (2020). Sustainability indicators for renewable energy systems using multi-criteria decision-making model and extended SWARA/ARAS hybrid method. *Renewable Energy, 146*, 580-597. https://doi.org/10.1016/j.renene.2019.06.157

Ghorabaee, M. K., Zavadskas, E. K., Amiri, M., & Esmaeili, A. (2016). Multi-criteria evaluation of green suppliers using an extended WASPAS method with interval type-2 fuzzy sets. *Journal of Cleaner Production, 137*, 213-229. https://doi.org/10.1016/j.jclepro.2016.07.031

Govindan, K., Kadziński, M., & Sivakumar, R. (2017). Application of a novel PROMETHEE-based method for construction of a group compromise ranking to prioritization of green suppliers in food supply chain. *Omega, 71,* 129-145. https://doi.org/10.1016/j.omega.2016.10.004

https://doi.org/10.17993/3ctecno.2021.specialissue7.115-133

Gündoğdu, F. K., & Kahraman, C. (2019a). Spherical fuzzy sets and spherical fuzzy TOPSIS method. *Journal of Intelligent & Fuzzy Systems, 36*(1), 337-352. https://content.iospress.com/articles/journal-of-intelligent-and-fuzzy-systems/ifs181401

Gündoğdu, F. K., & Kahraman, C. (2019b). Spherical fuzzy analytic hierarchy process (AHP) and its application to industrial robot selection. In *International Conference on Intelligent and Fuzzy Systems* (pp. 988-996). Springer, Cham.

Hashemkhani Zolfani, S., & Bahrami, M. (2014). Investment prioritizing in high tech industries based on SWARA-COPRAS approach. *Technological and Economic Development of Economy, 20*(3), 534-553. https://doi.org/10.3846/20294913.2014.881435

He, Y., Lei, F., Wei, G., Wang, R., Wu, J., & Wei, C. (2019). EDAS method for multiple attribute group decision making with probabilistic uncertain linguistic information and its application to green supplier selection. *International Journal of Computational Intelligence Systems, 12*(2), 1361-1370. https://www.atlantis-press.com/journals/ijcis/125921808

Hsu, C. W., Kuo, T. C., Chen, S. H., & Hu, A. H. (2013). Using DEMATEL to develop a carbon management model of supplier selection in green supply chain management. *Journal of cleaner production, 56,* 164-172. https://doi.org/10.1016/j.jclepro.2011.09.012

Kaya, S. K., & Erginel, N. (2020). Futuristic airport: A sustainable airport design by integrating hesitant fuzzy SWARA and hesitant fuzzy sustainable quality function deployment. *Journal of Cleaner Production, 275,* 123880. https://doi.org/10.1016/j.jclepro.2020.123880

Ijadi Maghsoodi, A., Ijadi Maghsoodi, A., Mosavi, A., Rabczuk, T., & Zavadskas, E. K. (2018). Renewable energy technology selection problem using integrated h-swara-multimoora approach. *Sustainability, 10*(12), 4481. https://www.mdpi.com/2071-1050/10/12/4481/htm

https://doi.org/10.17993/3ctecno.2021.specialissue7.115-133

Ilieva, G., Yankova, T., Hadjieva, V., Doneva, R., & Totkov, G. (2020). Cloud Service Selection as a Fuzzy Multi-criteria Problem. *TEM Journal, 9*(2), 484. https://www.temjournal.com/content/92/TEMJournalMay2020_484_495.pdf

Keršuliene, V., Zavadskas, E. K., & Turskis, Z. (2010). Selection of rational dispute resolution method by applying new step-wise weight assessment ratio analysis (SWARA). *Journal of business economics and management, 11*(2), 243-258. https://doi.org/10.3846/jbem.2010.12

Keshavarz-Ghorabaee, M., Amiri, M., Zavadskas, E. K., Turskis, Z., & Antucheviciene, J. (2018). An extended step-wise weight assessment ratio analysis with symmetric interval type-2 fuzzy sets for determining the subjective weights of criteria in multi-criteria decision-making problems. *Symmetry, 10*(4), 91. https://doi.org/10.3390/sym10040091

Kumar, P., Singh, R. K., & Vaish, A. (2017). Suppliers' green performance evaluation using fuzzy extended ELECTRE approach. *Clean Technologies and Environmental Policy, 19*(3), 809-821. https://doi.org/10.1007/s10098-016-1268-y

Liou, J. J., Tamošaitienė, J., Zavadskas, E. K., & Tzeng, G. H. (2016). New hybrid COPRAS-G MADM Model for improving and selecting suppliers in green supply chain management. *International Journal of Production Research, 54*(1), 114-134. https://doi.org/10.1080/00207543.2015.1010747

Mavi, R. K. (2015). Green supplier selection: a fuzzy AHP and fuzzy ARAS approach. International *Journal of Services and Operations Management, 22*(2), 165-188. https://econpapers.repec.org/article/idsijsoma/v_3a22_3ay_3a2015_3ai_3a2_3ap_3a165-188.htm

Mijajlović, M., Puška, A., Stević, Ž., Marinković, D., Doljanica, D., Jovanović, S. V., Stojanović, I., & Beširović, J. (2020). Determining the Competitiveness of Spa-Centers in Order to Achieve Sustainability Using a Fuzzy Multi-Criteria Decision-Making Model. *Sustainability, 12*(20), 8584. https://doi.org/10.3390/su12208584

https://doi.org/10.17993/3ctecno.2021.specialissue7.115-133

Perçin, S. (2019). An integrated fuzzy SWARA and fuzzy AD approach for outsourcing provider selection. *Journal of Manufacturing Technology Management, 30*(2), 531-552. https://www.emerald.com/insight/content/doi/10.1108/JMTM-08-2018-0247/full/html

Puška, A., Stojanović, I., Maksimović, A., & Osmanović, N. (2020). Project management software evaluation by using the Measurement of Alternatives and Ranking According to Compromise Solution (MARCOS) method. *Operational Research in Engineering Sciences: Theory and Applications, 3*(1), 89-102. https://www.researchgate.net/profile/Adis-Puska/publication/340491985_Project_meanagment_software_evaluation_by_using_the_measurement_of_alternatives_and_ranking_according_to_compromise_solution_MARCOS_method/links/5e8ccd5c92851c2f52885bcd/Project-meanagment-software-evaluation-by-using-the-measurement-of-alternatives-and-ranking-according-to-compromise-solution-MARCOS-method.pdf

Rani, P., & Mishra, A. R. (2020). Single-valued neutrosophic SWARA-VIKOR framework for performance assessment of eco-industrial thermal power plants. *ICSES Transactions on Neural and Fuzzy Computing, 3*(11), 1-9.

Smarandache, F. (1998). *Neutrosophy: neutrosophic probability, set, and logic: analytic synthesis & synthetic analysis.* American Research Press, Rehoboth.

Sang, X., & Liu, X. (2016). An interval type-2 fuzzy sets-based TODIM method and its application to green supplier selection. *Journal of the Operational Research Society, 67*(5), 722-734. https://doi.org/10.1057/jors.2015.86

Sen, D. K., Datta, S., Patel, S. K., & Mahapatra, S. S. (2017). Green supplier selection in fuzzy context: a decision-making scenario on application of fuzzy-MULTIMOORA. *International Journal of Services and Operations Management, 28*(1), 98-140. https://www.inderscience.com/info/inarticle.php?artid=85907

Stanković, M., Stević, Ž., Das, D. K., Subotić, M., & Pamučar, D. (2020). A new fuzzy MARCOS method for road traffic risk analysis. *Mathematics, 8(*3), 457. https://doi.org/10.3390/math8030457

https://doi.org/10.17993/3ctecno.2021.specialissue7.115-133

Stanujkic, D., Karabasevic, D., & Zavadskas, E. K. (2015). A framework for the selection of a packaging design based on the SWARA method. *Engineering Economics, 26*(2), 181-187. https://www.researchgate.net/publication/281832408_A_Framework_for_the_Selection_of_a_Packaging_Design_Based_on_the_SWARA_Method

Stevens, G. C. (1989). Integrating the supply chain. *International Journal of physical distribution & Materials Management, 19*(8), 3-8. https://www.emerald.com/insight/content/doi/10.1108/EUM0000000000329/full/html

Stević, Ž., & Brković, N. (2020). A Novel Integrated FUCOM-MARCOS Model for Evaluation of Human Resources in a Transport Company. Logistics, 4(1), 4. https://doi.org/10.3390/logistics4010004

Stević, Ž., Pamučar, D., Puška, A., & Chatterjee, P. (2020). Sustainable supplier selection in healthcare industries using a new MCDM method: Measurement of alternatives and ranking according to COmpromise solution (MARCOS). *Computers & Industrial Engineering, 140,* 106231. https://doi.org/10.1016/j.cie.2019.106231

Torra, V. (2010). Hesitant fuzzy sets. *International Journal of Intelligent Systems, 25*(6), 529-539. https://doi.org/10.1002/int.20418

Ulutaş, A., Karabasevic, D., Popovic, G., Stanujkic, D., Nguyen, P. T., & Karaköy, Ç. (2020). Development of a Novel Integrated CCSD-ITARA-MARCOS Decision-Making Approach for Stackers Selection in a Logistics System. *Mathematics, 8*(10), 1672. https://doi.org/10.3390/math8101672

Vesković, S., Stević, Ž., Karabašević, D., Rajilić, S., Milinković, S., & Stojić, G. (2020). A New Integrated Fuzzy Approach to Selecting the Best Solution for Business Balance of Passenger Rail Operator: Fuzzy PIPRECIA-Fuzzy EDAS Model. *Symmetry, 12*(5), 743. https://www.researchgate.net/publication/341160799_A_New_Integrated_Fuzzy_Approach_to_Selecting_the_Best_Solution_for_Business_Balance_of_Passenger_Rail_Operator_Fuzzy_PIPRECIA-Fuzzy_EDAS_Model

https://doi.org/10.17993/3ctecno.2021.specialissue7.115-133

Yager, R. R. (2013). Pythagorean fuzzy subsets. In *2013 joint IFSA world congress and NAFIPS annual meeting (IFSA/NAFIPS)* (pp. 57-61). IEEE. https://www.semanticscholar.org/paper/Pythagorean-fuzzy-subsets-Yager/7d615595bed34e5499ef0b5f017548eadd16dfd7

Yazdani, M., Chatterjee, P., Zavadskas, E. K., & Zolfani, S. H. (2017). Integrated QFD-MCDM framework for green supplier selection. *Journal of Cleaner Production, 142,* 3728-3740. https://doi.org/10.1016/j.jclepro.2016.10.095

Zadeh, L. A. (1965). Fuzzy Sets. *Information Control, 8*(3), 338-353. https://doi.org/10.1016/S0019-9958(65)90241-X

Zadeh, L. A. (1975). The concept of a linguistic variable and its application to approximate reasoning—I. *Information sciences, 8*(3), 199-249. https://doi.org/10.1016/0020-0255(75)90036-5

https://doi.org/10.17993/3ctecno.2021.specialissue7.115-133

/08/

https://doi.org/10.17993/3ctecno.2021.specialissue7

URBAN GREEN AREAS TO IMPROVE THE QUALITY OF LIFE IN THE SAN JUAN DE MIRAFLORES DISTRICT

Karina Hinojosa Pedraza
Federico Villarreal National University, Lima, (Peru).
E-mail: khinojosa@unfv.edu.pe
ORCID: https://orcid.org/0000-0003-1237-9110

Doris Esenarro
Federico Villarreal National University, Lima, (Peru).
E-mail: desenarro@unfv.edu.pe
ORCID: https://orcid.org/0000-0002-7186-9614

Lucy Brigite Mio Morales
Federico Villarreal National University, Lima, (Peru).
E-mail: 2016019827@unfv.edu.pe
ORCID: https://orcid.org/0000-0003-4975-1334

Wilson Vasquez Cerdan
Universidad Privada del Norte, Lima, (Peru).
E-mail: wilson.cerdan@upn.edu.pe
ORCID: https://orcid.org/0000-0001-7064-028X

Recepción: 01/12/2020 **Aceptación:** 25/02/2021 **Publicación:** 07/05/2021

Citación sugerida:
Hinojosa, K., Esenarro, D., Mio, L. B., y Vasquez, W. (2021). Urban green areas to improve the quality of life in the San Juan de Miraflores district. *3C Tecnología. Glosas de innovación aplicadas a la pyme, Edición Especial,* (mayo 2021), 135-147. https://doi.org/10.17993/3ctecno.2021.specialissue7.135-147

ABSTRACT

This research seeks to propose a design of ecological green areas in the district of San Juan de Miraflores, Panamericana Sur sector. The lack of green spaces increases environmental pollution and affects the health of the residents of the neighborhood, the proposal to incorporate green areas in public spaces aims to improve the quality of life, in the methodology used to determine the location, a topographic survey of the district identifying the existing green areas, as well as evaluating the climatology, soil science, flora and fauna of the place and the urban environment for the design in such a way that it generates microclimates. It also had the support of a virtual survey directed to the residents of the area. As a final result, the design of a proposal for ecological spaces that integrate with the urban environment without losing their identity and minimizing their relationship with nature is proposed for users' interaction and comfort using clean technologies.

KEYWORDS

Green Areas, Quality of life, Urban environment, Sustainability.

https://doi.org/10.17993/3ctecno.2021.specialissue7.135-147

1. INTRODUCTION

The Health Municipality Organization (WHO) recommends 9 to 12 m2 of green areas per inhabitant; this comes to make an indicator that highlights the level of quality of life in a district or city (Gómez & Velázquez, 2018). Lima, the capital, the fifth most populous city in the ranking of Latin America and the Caribbean, has a deficit of 56 million m2 of green areas, equivalent to more than five thousand soccer fields (Ramos *et al.*, 2020). In this regard, the District of San Juan de Miraflores, which is home to approximately 355,299 inhabitants (Amaya *et al.*, 2020), only has around 1.69 m2 of green areas per inhabitant, which is insufficient, ranking among the 15 districts with the least green spaces in all of Metropolitan Lima (INEI, 2017), that is, below that recommended by the World Health Organization, this increases the need to establish various mechanisms to achieve the recommended figure. This decrease in green areas causes citizens' quality of life to be negatively affected by not having the environmental benefits provided by green places or similar public spaces and not meeting recommended international standards (SINIA, 2016).

The influence of urban green areas on the quality of life of the population is an issue that has only recently been incorporated into the political and scientific agenda. There is not yet a strong current of public opinion interested in claiming the social importance of these natural areas (Berrocal, 2020), is what is evidenced in the District of San Juan de Miraflores, there is an excellent disinterest of the authorities added to the accelerated urban expansion, the sale of illegal land, which led to the transfer of spaces destined to green areas, and in many cases, free zones have been turned into informal waste dumps (Esenarro *et al.*, 2020). The little importance given to the planning of urban green areas means that the San Juan de Miraflores district does not have adequate green spaces, a fundamental element for improving the population's well-being, especially in large cities. Indeed, in the great cities of the world today, we speak not only of urban forests, ecological parks, networks, and green belts but also of urban green areas' naturalization (Reyes and Figueroa, 2010). Thus, it is a question of recognizing, amid urbanization or urban expansion, nature, its presence, its importance, and, therefore, the need for its conservation (Moyano & Priego, 2009). Additionally, urban green areas can be incorporated as an element for the application of the concept of sustainability (Vega *et al.*, 2020).

https://doi.org/10.17993/3ctecno.2021.specialissue7.135-147

1.1. QUALITY OF LIFE

The expression "quality of life" has been significantly used in everyday language and in different disciplines that deal with studying the complex economic, social, environmental, territorial, and relationship problems that characterize society. The concept of quality of life has become a pivotal perspective to understand and measure, on different scales, the conditions in which the population lives. In cities, the importance of equipment and services to improve the inhabitants' quality of life has been pointed out (Morales *et al.*, 2018).

2. METHODS AND MATERIALS

2.1. STUDY AREA

The district of San Juan de Miraflores, in figure 1, located in the department of Lima, in Peru. It limits the north with La Molina's community, to the east with Villa María del Triunfo's district, to the south with Villa El Salvador and San Pedro de los Chorrillos, and the west with the community of Santiago de Surco. San Juan de Miraflores' district was founded on January 12, 1965, by Law 15382, and is divided into 6 zones (Municipalidad distrital de San Juan de Miraflores, 2012).

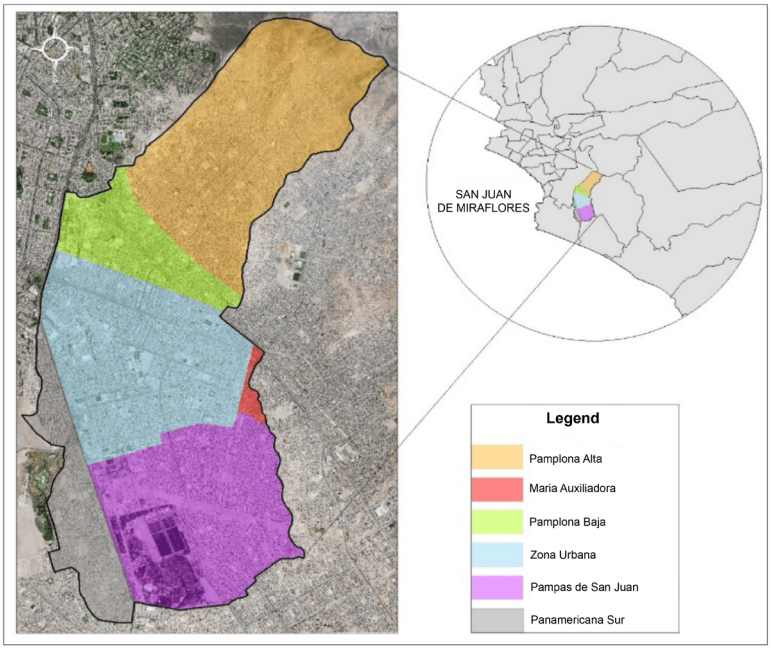

Figure 1. Map of sectors of the San Juan de Miraflores district.
Source: own elaboration.

https://doi.org/10.17993/3ctecno.2021.specialissue7.135-147

Figure 1 shows the delimitation of the study area and the geographical location.

2.2. CHARACTERISTICS OF THE STUDY AREA

The District of San Juan de Miraflores mentions the following physical and ecological characteristics (Miyasako, 2009).

Table 1. Characteristics of the San Juan de Miraflores District.

Characteristic	Description
Climate and Ecology	The district corresponds to the tropical climatic region; However, arid and semi-arid desert environments occur due to the cold Humboldt current and the Andes Mountains.
Temperature	The annual average temperature is 18.5 ° C, with moderate monthly variations. During El Niño phenomena, the yearly average temperature can reach 22.84 ° C, raising the monthly averages to 18 and 27.01 ° C depending on the month.
Maximum Relative Humidity	The maximum relative humidity remains between 70% and 87% and is higher in the winter months. This parameter acquires a higher register in the areas closest to the Rímac, Lurín rivers, and other water currents of natural or artificial origin.
Cloudiness	The annual average cloud cover is 6/8, which can be considered high since it covers 75% of the sky. The occurrence of cloudiness is closely linked to the thermal inversion that contributes to saturate the atmosphere with humidity in winter. The annual total evaporation is 1,028.6 mm, which is closely related to temperature since the intensity reflects the greater or lesser heat radiation of the soil, which is manifested through the gasification of retained moisture
Winds	In the study area, the West's prevailing winds are registered, reaching an average annual speed of approximately 6.4 km / H, which is classified as "Weak Breeze" according to the Beaufort scale. These winds are more from October to March.
Green Areas	The extension of green areas is 38.4 hectares. This coverage defines an average of 1.1 m2 per inhabitant, far from the minimum value indicated by the OMS, which is 8 m2 per inhabitant.
Ground	Type II soil, granular on alluvial or colluvial gravel strata, type III high danger soil, with fine dirt and thick sands, very high danger type IV soil, aeolian sands, marine deposits, and swampy soils, and type V soil specific areas of Heterogeneous waste deposits, with uncertain dynamic behavior.

Source: own elaboration.

The Table 1 shows the climatic characteristics and the vegetation cover of the study site.

2.3. WORK AREA

San Juan de Miraflores "Panamericana Sur" sector is located in the western part of the district. It runs along the right strip that runs parallel to the Panamericana Sur highway for an approximate extension of 6km. (Amauta bridge to kilometer 18 of the Panamericana). It limits the districts of Surco and Chorrillos. It has 36 human settlements, 8 Housing

https://doi.org/10.17993/3ctecno.2021.specialissue7.135-147

Associations, 5 Housing Cooperatives, and one Urbanization. It has 50 towns and a population of 45,000 inhabitants (9,000 families) (Segovia *et al.*, 2020).

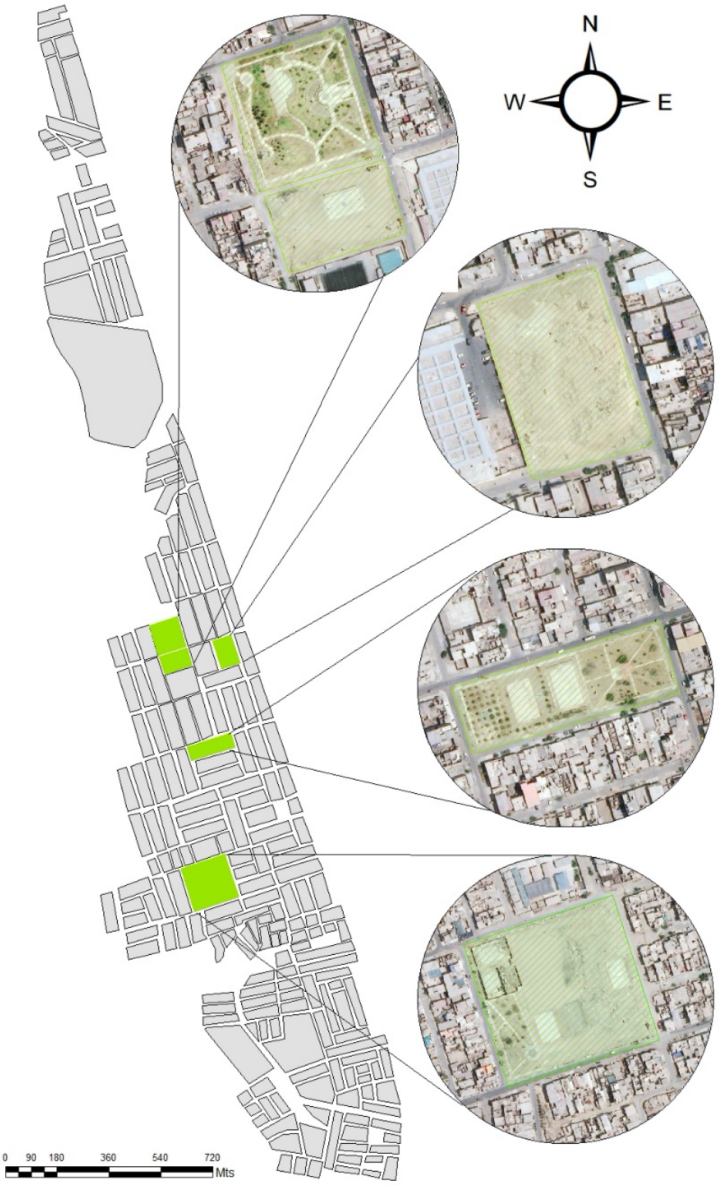

Figure 2. Map of the location of work areas.
Source: own elaboration.

Figure 2 shows the location map of the different location points of the research development, as well as the orientation of the green infrastructure.

https://doi.org/10.17993/3ctecno.2021.specialissue7.135-147

2.4. PROCESS FOR THE DESIGN OF GREEN AREAS

Figure 3. Processes for the design of green areas.
Source: own elaboration.

Figure 3 shows the methodological process of the green infrastructure research.

3. RESULTS

An online survey was conducted in October and November for a population sample of 81 people. The results obtained show the respondents' profile, mostly female (67%) and male (33%). In general, a level of education corresponding to university (42%) and complete secondary school (26%) predominates.

There is a concordance with previous studies where the contributions of green areas to improve the quality of life include two aspects, the first contributes to the well-being of people and is considered; the promotion of sports, leisure, recreation, and aesthetic elements (Flores & Gonzáles, 2010), similar to the result obtained in this study that shows a (75%) think that green areas play a role of recreation and (62%) believe that Green areas help to improve emotional well-being, however, environmental factors that affect the levels of well-being of any society that determine people's quality of life should also be considered (Falcon, 2007).

Those that have been considered in this study obtained results that show that (66%) consider green areas vital because they help fight pollution, which indicates an environmental awareness on the part of the respondents as well as (53%) He would like to see a large number of trees in his green areas, which is consistent with other research where trees help filter pollutant particles from the air. Research indicates that public green regions or free access (Salvador, 2003) present different types, depending on metropolitan areas. These typologies allow the differentiation of spaces according to their surface, architectural design, function (recreational, ecological, social, others), and social goals (target population). These studies are consistent with the results of the research for the design of the green area, which

https://doi.org/10.17993/3ctecno.2021.specialissue7.135-147

takes into consideration, and an aspect such as the inclusion of a small urban garden is added (Méndez *et al.*, 2020).

Figure 4. Design proposal for eco-friendly spaces. View towards the main pool with a predominance of abundant trees (a). Schinus terebinthifolius or coastal molles are easily adaptable to the capital's desert climate due to their minimal water consumption (b). Location in some areas of tree pits or bowls to store irrigation or rainwater (c). Solid Meet & Work system combinations of benches, tables, and planters offer an innovative alternative (d).
Source: own elaboration.

Figure 5. Innovative urban furniture responds to and adapts to the design in the study area (a) and (c). Concrete Tree Planters located in the park sectors (b).
Source: own elaboration.

https://doi.org/10.17993/3ctecno.2021.specialissue7.135-147

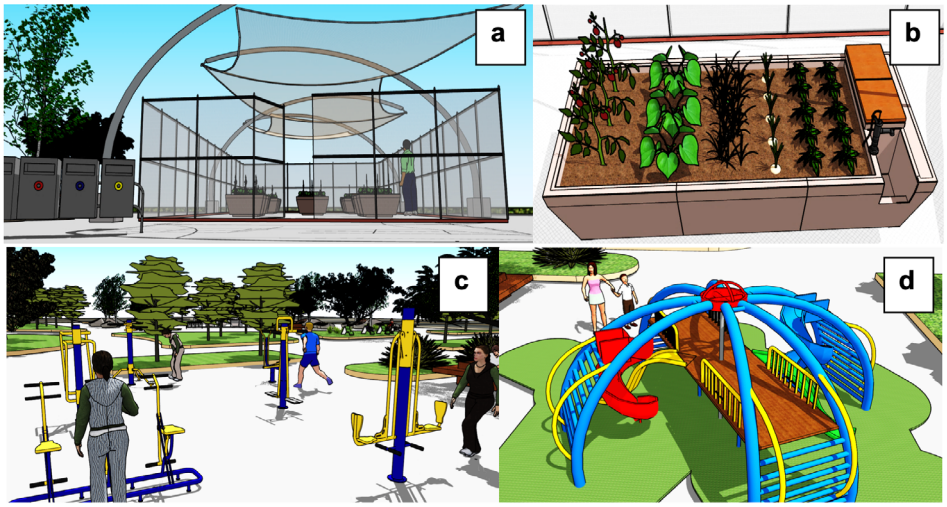

Figure 6. Design proposal for children's recreational spaces. Front view of the urban garden (a). Cultivation of vegetables, vegetables, fruits, legumes, aromatic plants, or medicinal herbs, among other varieties, on a domestic scale (b). Sports area dedicated to benefits for the practice of regular, stable, and moderate physical activity (c). Playground for children (d).
Source: own elaboration.

For the choice of trees in Table 2, the type of soil presented by the Panamericana Sur Sector in San Juan de Miraflores was taken into account. It is a superficial layer of granular soils formed by coarse particles such as sand or gravel, fine and clayey.

Based on the virtual tree guide of Metropolitan Lima, in Figures 4, 5, and 6, some trees for the type of soil that corresponds to our study area require little water consumption, fast growth, and excellent resistance to soils.

Tabla 2. Trees and features.

Scientific name	Common name	Characteristics
Schinus terebinthifolius	Molles costeños	Tree 7 to 10 m tall, with evergreen leaves with widespread ramifications, with red fruits, adapts very well to all soil types. It requires little maintenance.
Schinus molle	Molles Serranos	A medium-sized tree can measure between 15 meters in height and 30 cm in diameter, adapts very well to all types of soils, high resistance to water scarcity, and low maintenance.
Tecoma stans	Huaranhuay	8-meter tall tree, whose main characteristic is that during the summer, they fill with numerous yellow flowers, adding great beauty to the landscape. It prefers sandy soils with good drainage.
Koelreuteria paniculata	Papelillos	A medium tree that reaches between 10 and 15 m in height adapts very well to nutrient-poor and sandy soils. It resists prolonged droughts very well. Resists high contamination.

https://doi.org/10.17993/3ctecno.2021.specialissue7.135-147

Casuarina equisetifolia	Casuarinas	It is an evergreen tree; it can reach between 20 and 25 m in height. It lives naturally in arid and semi-arid climates of tropical and subtropical areas, sandy areas, and saline environments near the coast.
Jacaranda mimosifolia	Jacarandá	A tree that reaches 8 to 12 m in height. It prefers sandy-clay soils with good drainage. Resists urban pollution well.

Source: own elaboration.

Table 2 shows the characteristics of the vegetation that have been selected according to their nature and the adaptability of the trees.

3. CONCLUSIONS

The proposal for the design of green areas aims to improve the population's living conditions and respond to the urgent need to raise the environmental quality of the San Juan de Miraflores district, Panamericana Sur sector. In this sense, the proposal is considered viable, designed to meet those specific needs based on the area's diagnosis.

This work is a first approximation to the preferences of a public that, in general, seeks through green areas to improve their quality of life, since the availability of green spaces in the study area is below that recommended by The OMS.

This proposal for the design of green areas prioritizes spaces within the urban infrastructure that allow us to advance with a vision for the future and the central axis of the San Juan de Miraflores district's sustainability in the Panamericana Sur sector.

The limitations of this study provide the opportunity to carry out new mapping of unprofitable public properties belonging to the State, as well as to recover degraded areas converted into informal garbage dumps, to make way for green places in the different sectors of San Juan de Miraflores, which will allow significantly increase the size of public green space per inhabitant. It is necessary to find and give space to green places that help the sustainability of the district and therefore improve the quality of life.

REFERENCES

Berrocal, S. D. (2020). Resiliencia urbana, crecimiento demográfico y cambio climático: la estructura ecológica y las áreas verdes urbanas vinculadas al río Rímac de Lima. *South Sustainability, 6.*

https://doi.org/10.17993/3ctecno.2021.specialissue7.135-147

Esenarro, D., Escate, I., Anco, L., Tassara, C., & Rodriguez, C. (2020). Proposal for an Ecological Research Center for the Recovery and Revaluation of Biodiversity in the Town of Quichas-Lima, Peru. *International Journal of Environmental Science and Development, 11*(4), 212-216. http://www.ijesd.org/show-151-1743-1.html

Falcón, A. (2007). *Espacios verdes para una ciudad sostenible.* Editorial Gustavo Gilli, S.L. https://dialnet.unirioja.es/servlet/libro?codigo=301825

Flores-Xolocotzi, R., & González-Guillen, M. de J. (2010). Planificación de sistemas de áreas verdes y parques públicos. *Revista mexicana de ciencias forestales, 1*(1), 17-24. http://www.scielo.org.mx/scielo.php?pid=S2007-11322010000100003&script=sci_abstract&tlng=es

Gómez, N. J., & Velázquez, G. A. (2018). Asociación entre los espacios verdes públicos y la calidad de vida en el municipio de Santa Fe, Argentina. *Cuadernos de Geografía: Revista Colombiana de Geografía, 21*(1), 167-179. https://dialnet.unirioja.es/servlet/articulo?codigo=6301665

INEI. (2017). *Provincia de Lima Compendio Estadístico.* Lima.

Méndez, R., Esenarro, D., Amaya, P., & Rodriguez, C. (2020). Vulnerability of the soils of Metropolitan Lima and their relationship with urban sustainability. *3C Tecnología. Glosas de innovación aplicadas a la pyme. Edición Especial, Octubre 2020,* 161-177. https://ojs.3ciencias.com/index.php/3c-tecnologia/article/view/1101

Miyasako, E. C. (2009). *Las áreas verdes en el contexto urbano de la ciudad de México.* Universidad de Alicante (España). https://dialnet.unirioja.es/servlet/tesis?codigo=66881

Morales, V., Piedra, L., Romero, M., & Bermúdez, T. (2018). Indicadores ambientales de áreas verdes urbanas para la gestión en dos ciudades de Costa Rica. *Revista Biología Tropical, 66*(4), 1421-1435. https://medes.com/publication/138861

Moyano, E., & Priego, C. (2009). Marco teórico para analizar las relaciones entre paisaje natural, salud y calidad de vida. *Sociedad Hoy, 16,* 31-44. https://digital.csic.es/bitstream/10261/63540/1/Marco%20Te%C3%B3rico%20para%20analizar%20

https://doi.org/10.17993/3ctecno.2021.specialissue7.135-147

las%20relaciones%20entre%20paisaje%20natural%2C%20salud%20y%20calidad%20de%20vida.pdf

Municipalidad distrital de San Juan de Miraflores. (2012). *Plan de desarrollo concertado 2012-2021 distrito de San Juan de Miraflores.* Ordenanza Municipal Nº 241-2012. http://imp.gob.pe/wp-content/uploads/2020/09/san_juan_de_miraflores_plan_de_desarrollo_concertado_2012_2021.pdf

Amaya, P., Esenarro, D., Rodriguez, C., Vega, V., & López, J. (2020). Economic valuation of environmental attributes of the Yanachaga-Chemillén National Park via contingent valuation and choice experiment. *World Journal of Engineering*. https://doi.org/10.1108/WJE-09-2020-0407

Ramos, L., Esenarro, D., Rodriguez, C., & Lagos, J. (2020). Recovery of public spaces for the conservation of green areas in Tablada Lurin. In *IOP Conference Series: Materials Science and Engineering, 910,* 012020. https://doi.org/10.1088/1757-899X/910/1/012020

Reyes, S., & Figueroa, I. M. (2010). Distribución, superficie y accesibilidad de las áreas verdes en Santiago de Chile. *EURE, 36*(109), 89-110. http://dx.doi.org/10.4067/S0250-71612010000300004

Salvador, P. (2003). *La planificación verde en las ciudades.* Editorial Gustavo Gilli, S. L. https://dialnet.unirioja.es/servlet/libro?codigo=171424

Segovia, E. L., Esenarro, D., Ascama, L., Rodriguez, C., & Julca, M. S. Y. R. (2020). Design of Green Infrastructure for Sustainable Urban Transportation in Lomas Del Paraiso in Villa Maria Del Triunfo. *Journal of Green Engineering (JGE), 10*(11), 11180-11192. https://siis.unmsm.edu.pe/es/publications/design-of-green-infrastructure-for-sustainable-urban-transportati

SINIA. (2016). *Anuario de Estadísticas Ambientales 2016.* Lima. https://sinia.minam.gob.pe/documentos/anuario-estadisticas-ambientales-2016

Vega, V., Esenarro, D., Maldonado, C., Rodriguez, C., & Córdova, A. (2020). Green infrastructure design for connectivity in the villa wetlands wildlife refuge.

https://doi.org/10.17993/3ctecno.2021.specialissue7.135-147

Journal of Green Engineering (JGE), 10(12), 2753-12765. https://siis.unmsm.edu.pe/es/publications/green-infrastructure-design-for-connectivity-in-the-villa-wetland

https://doi.org/10.17993/3ctecno.2021.specialissue7.135-147

/09/

https://doi.org/10.17993/3ctecno.2021.specialissue7

CRM BUCK CONVERTER WITH HIGH INPUT POWER FACTOR

Abdul Hakeem Memon
Institute of Information and Communication Technologies (IICT),
Mehran UET, Jamshoro, Sindh, (Pakistan).
E-mail: hakeem.memon@faculty.muet.edu.pk
ORCID: https://orcid.org/0000-0001-8545-3823

Manzoor Ali
Institute of Information and Communication Technologies (IICT),
Mehran UET, Jamshoro, Sindh, (Pakistan).
E-mail: manzoorabro84@gmail.com
ORCID: https://orcid.org/0000-0002-6430-472X

Zubair Ahmed Memon
Institute of Information and Communication Technologies (IICT),
Mehran UET, Jamshoro, Sindh, (Pakistan).
E-mail: zubair.memon@faculty.muet.edu.pk
ORCID: https://orcid.org/0000-0001-5967-3152

Ashfaque Ahmed Hashmani
Institute of Information and Communication Technologies (IICT),
Mehran UET, Jamshoro, Sindh, (Pakistan).
E-mail: ashfaque.hashmani@faculty.muet.edu.pk
ORCID: https://orcid.org/0000-0001-6412-211X

Recepción: 15/12/2020 **Aceptación:** 10/03/2021 **Publicación:** 07/05/2021

Citación sugerida:
Memon, H. A., Ali, M., Memon, Z. A., y Hashmani, A. A. (2021). CRM Buck Converter with High Input Power Factor. *3C Tecnología. Glosas de innovación aplicadas a la pyme, Edición Especial,* (mayo 2021), 149-161. https://doi.org/10.17993/3ctecno.2021.specialissue7.149-161

ABSTRACT

The buck converter is generally utilized in many applications because of various advantages like maintaining high efficiency for the wide range of input voltage, cost reduction, low output voltage, protection against inrush current and lifetime improvement. However, when on-time of buck converter is kept constant, the input voltage and current remains out of phase that cause's low PF and high total harmonic distortion (THD). Therefore a power factor improvement technique is implemented in this paper that permits the average input current sinusoidal without need of extra converter to work in cascade with buck converter. The critical conduction mode (CRM) buck converter operating with constant on-time (COT) control scheme have low PF because of harmonic contained input current waveform. So in order to make the input current waveform as a sinusoidal by changing the on-time of buck switch, a variable-on-time (VOT) control scheme for CRM buck converter is proposed in this paper. The theoretical analysis is given, and the simulation results confirm the advantages of the proposed control scheme. The object of the research paper is to propose the control scheme to realize high PF for CRM buck converter by only modulating the on-time of buck switch and without need of extra converter to work with buck converter.

KEYWORDS

Buck Converter, Critical Conduction Mode (CRM), Power Factor (PF), DC/DC Converters, Constant On-Time (COT), Variable On-Time (COT).

https://doi.org/10.17993/3ctecno.2021.specialissue7.149-161

1. INTRODUCTION

Power electronic innovation is utilized in different types of present day equipment's which has made our life easier, lavish and simpler. However, this innovation depends on semiconductor devices, because of which the shape of average input current is distorted. The distorted current has different disadvantages, for example, increased power loss, noise and voltage distortion etc. So the industries have formed different standards like IEC61000-3-2 limit and IEEE 519. In order to meet relevant harmonic standard and reducing input current distortion, various researchers have proposed different types of power factor correction (PFC) converters (Memon *et al.*, 2020a, 2020b, 2020c). The DC/DC converters or choppers such as buck, boost and buck-boost etc. are normally employed for PFC application. Each converter has its own advantages and disadvantages. The buck converter now days have attracted the attention of the many researchers (Endo *et al.*, 1992; Memon *et al.*, 2019a, 2019b, 2019c 2019d, 2019e). Its advantages include less voltage stress on the switch, low component cast, low output voltage, low inrush current, protection against short circuit and high efficiency at universal input voltage. However, the input PF of buck converter in low because of dead zone in the average input current that is present until input voltage is more than output voltage. It causes the input current to contain large harmonic disturbances.

For modifying the performance of buck converter, various researchers have proposed various techniques and control schemes (Endo *et al.*, 2020; Memon *et al.*, 2019a, 2019b, 2019c 2019d, 2019e).

In Endo *et al.* (1992), buck converter is introduced for PF improvement. The application along with analysis and modeling operating in discontinuous current mode (DCM) is discussed in Lee *et al.* (1997). The work in Spiazzi *et al.* (2000) has put forward a converter to compensate the dead zone in buck converter. In Huber *et al.* (2009), the analysis and evaluation of DCM buck converter is given. The bridgeless buck converter is introduced to enhance the efficiency in Jang *et al.* (2010). The research in Wu *et al.* (2011) has discussed various aspects regarding the design of buck converter with constant on-time control scheme (COTC).

https://doi.org/10.17993/3ctecno.2021.specialissue7.149-161

In Lamar *et al.* (2012), the AC/DC driver working in boundary current mode for tapped inductor buck converter is introduced to replace incandescent lamp by high brightness light emitting diode. For the reduction of input current harmonic for high brightness light emitting diode, a control scheme is proposed in Wu *et al.* (2012). In Ki *et al.* (2012), a new technique is introduced to reduce losses due to transformer in buck converter. The interleaved critical current mode (CRM) buck converter is introduced in Choi *et al.* (2012) to increase efficiency.

In Fardoun *et al.* (2014), a bridgeless buck is proposed to increase the efficiency. For compensating dead zone, double integrated buck converter is introduced for power supplies (Sichirollo *et al.*, 2014). The integration of another converter with buck converter is discussed to enhance the PF in Liu *et al.* (2020). The works in Memon *et al.* (2016), Memon *et al.* (2018a, 2018b) and Memon *et al.* (2019a, 2019b, 2019c 2019d, 2019e) have introduced various control schemes and topologies for buck converter to attain high PF and efficiency.

In this paper, a PF improvement technique is implemented for CRM buck converter that permits the average input current to be sinusoidal. It can improve input PF without need of other converter to work with buck during dead zone time and also need only one feed forward circuit.

This paper is divided into six sections. In section 2, the operation states of CRM buck converter are analyzed with traditional constant on-time (COT) control scheme. The introduced VOT control scheme is discussed in section 3. Then the comparative analysis is discussed in section 4 in terms of PF. In section 5, the effectiveness of proposed topology is evaluated by simulation results. Finally, some conclusions are drawn in section 6.

2. RESEARCH METHODOLOGY

The research methodology is based on:

1. Mathematical analysis of the operating principle of the traditional control scheme for BCM IBBC with the help of MATHCAD software.

2. Analysis of input PF of BCM integrated BBC.

https://doi.org/10.17993/3ctecno.2021.specialissue7.149-161

3. Introducing the proposed control scheme to obtain high PF with low THD.

4. Comparative analysis of the converter for COT control scheme and VOT control scheme strategy in terms of input PF and THD.

5. Developing the simulation model of the converter with traditional and proposed control scheme with the help of MATLAB software.

6. Confirming the results.

3. CONVENTIONAL COTCONTROL SCHEME FOR BUCK CONVERTER

Figure 1 shows the main circuit of the buck converter.

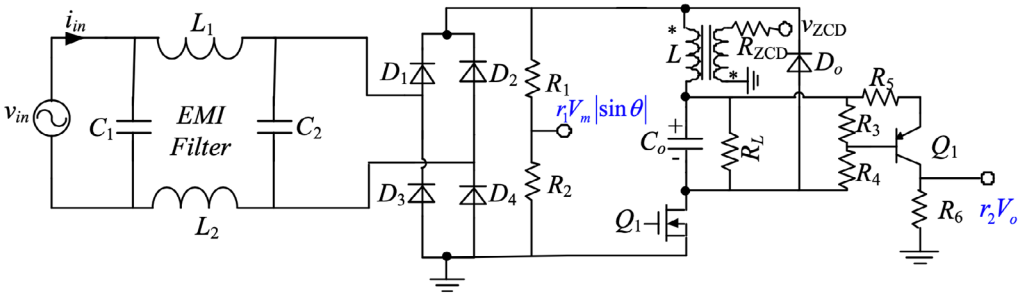

Figure 1. Schematic Diagram of Buck Converter.
Source: (Memon *et al.*, 2019a).

The input voltage and rectified input voltage is expressed as

$$v_{in}(\theta) = v_g = \sqrt{2}V_{rms}\sin\theta \tag{1}$$

Where V_{rms} is the rms value

When buck switch is on, the inductor voltage is expressed as

$$L\frac{di_L}{dt} = \sqrt{2}V_{rms}\left|\sin\theta\right| - V_o \tag{2}$$

where $\theta_0 = \arcsin\dfrac{V_{boundary}}{\sqrt{2}\,V_{rms}}$

So its peak value is

$$i_{L\_pk}(\theta) = \frac{\sqrt{2}V_{rms}\left|\sin\theta\right| - V_o}{L}t_{on} \tag{3}$$

https://doi.org/10.17993/3ctecno.2021.specialissue7.149-161

Where t_{on} is the on-time of the switch

While Q_{buck} is off, the inductor is discharged through load.

$$-L\frac{di_L}{dt}=V_o \tag{4}$$

For each switching cycle, the value of off-time is calculated from inductor's volt-second balance

$$t_{off}=\frac{L}{V_o}i_{L(pk1)}(\theta) \tag{5}$$

From (3) and (5), the following relation is obtained

$$t_{off}=\frac{\sqrt{2}V_{rms}\left|\sin\theta\right|-V_o}{V_o}t_{on} \tag{6}$$

In addition

$$t_s=t_{on}+t_{off} \tag{7}$$

Substituting (6) into (7)

$$t_s=\left(\frac{\sqrt{2}V_{rms}\left|\sin\theta\right|}{V_o}\right)t_{on} \tag{8}$$

The value of average input current for buck converter is got as

$$i_{buck(avg)}(\theta)=\frac{i_{L\_pk}(\theta)t_{on}}{2t_s} \tag{9}$$

Substituting (3) and (8) into (9)

$$i_{buck(avg)}(\theta)=i_{buck(COTCS)}(\theta)=\frac{t_{on}V_o}{2L}\left(\frac{\sqrt{2}V_{rms}\left|\sin\theta\right|-V_o}{\sqrt{2}V_{rms}\left|\sin\theta\right|}\right) \tag{10}$$

Based on (1) and (10), the input power of the buck converter is expressed as

$$P_{in(COTCS)}=\frac{V_o t_{on}}{2\pi L}\int_{\theta_0}^{\pi-\theta_0}\left(\sqrt{2}V_{rms}\left|\sin\theta\right|-V_o\right)d\theta \tag{11}$$

Now t_{on} can be calculated by assuming the efficiency of buck converter as 100%

$$t_{on}=\frac{2\pi P_o L}{\int_{\theta_0}^{\pi-\theta_0}V_o\left(\sqrt{2}V_{rms}\left|\sin\theta\right|-V_o\right)d\theta} \tag{12}$$

And input power factor can be calculated as

$$PF=\frac{P_{in}}{V_{rms}I_{rms}} \tag{13}$$

https://doi.org/10.17993/3ctecno.2021.specialissue7.149-161

Based on (11-13) and specification, the curve of the input PF can be drawn and is given in Figure 2 from which it can be concluded that the input PF is low for universal input voltage range.

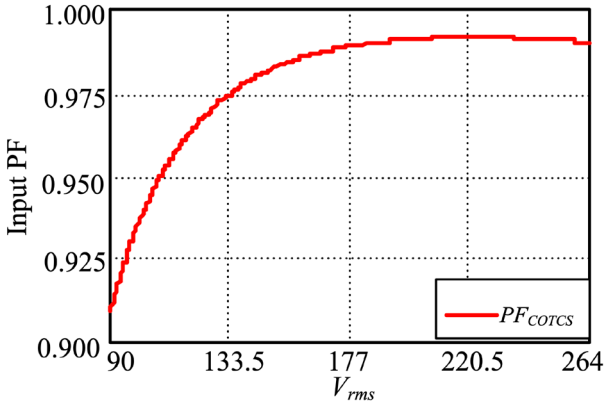

Figure 2. Input PF of COTCS [Mathcad eq:(10-14)].

3. PROPOSED VOT CONTROL SCHEME FOR CRM BUCK CONVERTER

For obtaining high PF for the buck converter, the on-time of Q_{buck} in (10) should vary as

$$t_{on(VOTC)} = k_{on1} \frac{\left(\sqrt{2}V_{rms}\left|\sin\theta\right|\right)^2}{V_o\left(\sqrt{2}V_{rms}\left|\sin\theta\right| - V_o\right)} \tag{14}$$

Where k_{on1} is a constant

Substituting (14) into (10), the average input current of the buck converter is

$$i_{buck(VOTC)}(\theta) = \frac{\sqrt{2}V_{rms}\left|\sin\theta\right|}{2L} k_{on1} \quad (\theta_0 \le \theta \le \pi - \theta_0) \tag{15}$$

From (15), it can be seen that if the on-time of the buck converter varies as (14), the input current waveform looks like pure sinusoidal and the PF is high

Because of the power balance of the input and output, the input current for the unity PF can be expressed as

$$i_{in}(\theta) = \frac{\sqrt{2}P_o\left|\sin\theta\right|}{V_{rms}} \tag{16}$$

Based on (15-16), the input current at θ_0 can be written as

https://doi.org/10.17993/3ctecno.2021.specialissue7.149-161

$$i_{in}(\theta_0) = \frac{k_{on1}\sqrt{2}V_{rms}|\sin\theta_0|}{2L} = \frac{\sqrt{2}P_o|\sin\theta_0|}{V_{rms}} \quad (17)$$

From (17), it can be concluded that

$$k_{on1} = \frac{2P_oL}{V_{rms}^2} \quad (18)$$

4. COMPARATIVE ANALYSIS

From (14), the input PF curve with proposed control scheme is shown in Figure 3 which also includes the PF values with traditional control scheme of Figure 2. It can be concluded that the PF of the converter with proposed control is higher as compared to COTC. It can conclude that improvement in PF is at all input voltage.

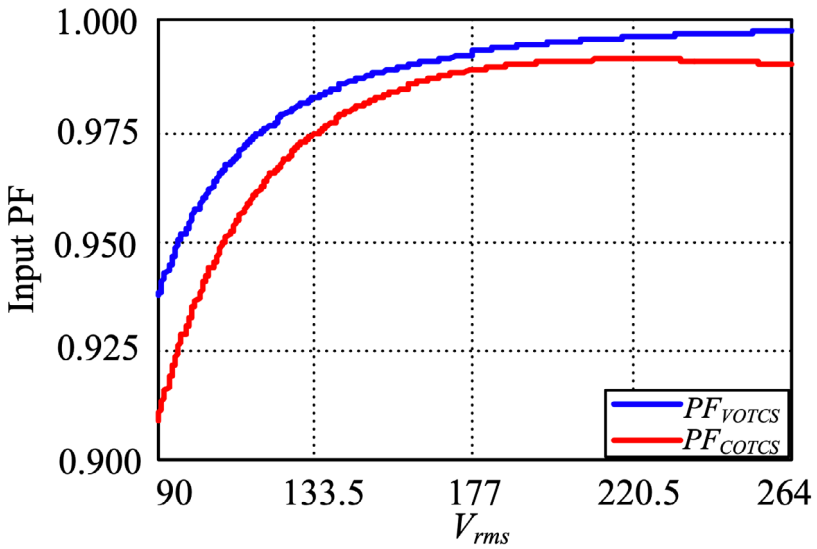

Figure 3. Input PF comparison between COT & VOT control scheme [Mathcad eq:(10-18)].

The THD comparison of the buck converter with COTCS and VOTCS is depicted in Figure 4. It indicates that THD is reduced in case of VOTCS as compared to COTCS.

https://doi.org/10.17993/3ctecno.2021.specialissue7.149-161

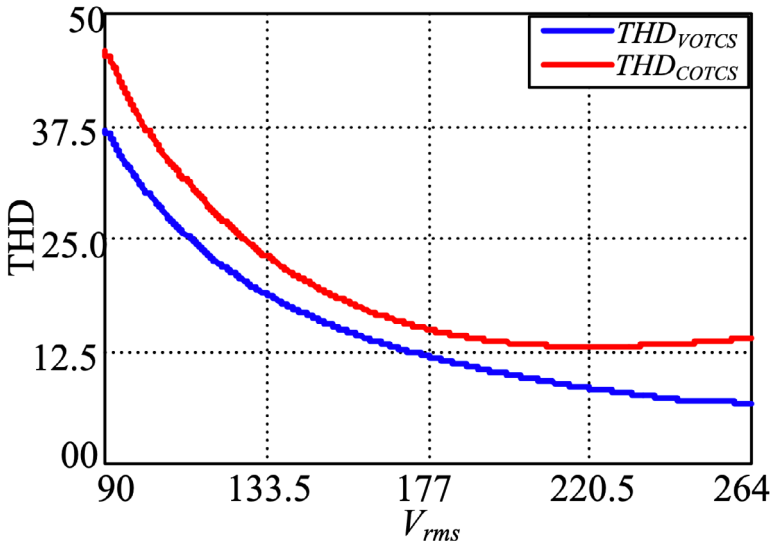

Figure 4. THD comparison between COT & VOT control scheme [Mathcad eq:(10-18) Relationship between PF and THD].

5. SIMULATION RESULTS

In order to verify the effectiveness of VOTCS, simulations results are given. The range of input voltage is 90-264 V_{rms}. The output voltage is selected as 80 V. The control IC 6561 will ensure the current to be in CRM. Ideal components are used in simulation

Figure 5 and Figure 6 show the simulation waveforms of v_{in}, & i_{in} of buck converter with COTCS and VOTCS at 220VAC inputs, respectively. It can be conducted that current is more sinusoidal in case of VOTCS as compared to COTCS. Thus VOTCS can attain high PF.

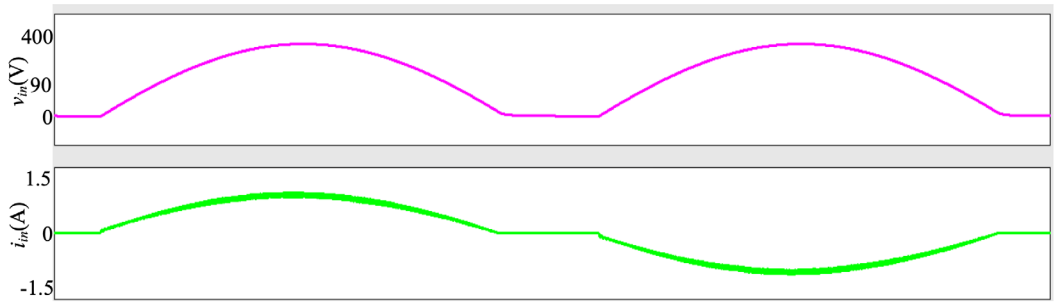

Figure 5. Input voltages and current of buck converter with COT control scheme [Saber Software].

https://doi.org/10.17993/3ctecno.2021.specialissue7.149-161

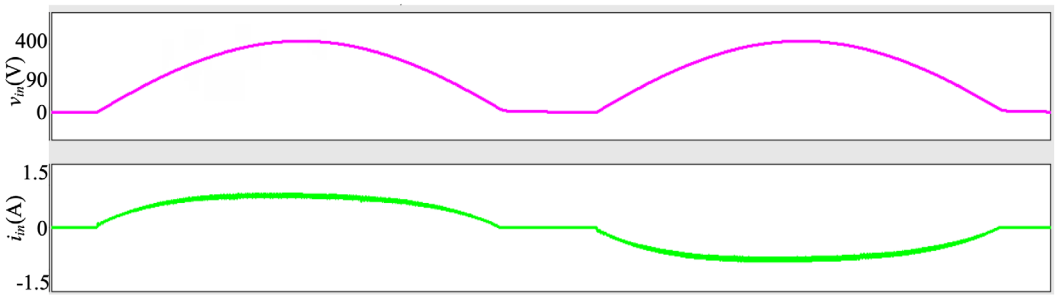

Figure 6. Input voltages and current of buck converter with VOT control scheme [Saber Software].

6. CONCLUSIONS

The buck converter is generally utilized in many applications because of various advantages. However, when on-time of buck converter is kept constant, the input voltage and current remains out of phase that cause's low PF and high total harmonic distortion (THD). Therefore, in this paper, a power factor improvement technique is implemented that permits the average input current sinusoidal without need of extra converter to work in cascade with buck converter. With COTCS, the input PF of the buck converter is low. In order to attain high input PF, VOT control scheme is proposed. Simulation results are presented for the verification of the analysis.

REFERENCES

Choi, H. (2012). Interleaved boundary conduction mode (BCM) buck power factor correction (PFC) converter. *IEEE Transactions on Power Electronics, 28*(6), 2629-2634. https://doi.org/10.1109/TPEL.2012.2222930

Endo, H., Yamashita, T., & Sugiura, T. (1992). A high-power-factor buck converter. In *PESC'92 Record. 23rd Annual IEEE Power Electronics Specialists Conference* (pp. 1071-1076). IEEE. https://doi.org/10.1109/PESC.1992.254766

Fardoun, A. A., Ismail, E. H., Khraim, N. M., Sabzali, A. J., & Al-Saffar, M. A. (2014). Bridgeless high-power-factor buck-converter operating in discontinuous capacitor voltage mode. *IEEE Transactions on Industry Applications, 50*(5), 3457-3467. https://doi.org/10.1109/TIA.2014.2305771

https://doi.org/10.17993/3ctecno.2021.specialissue7.149-161

Huber, L., Gang, L., & Jovanovic, M. M. (2009). Design-oriented analysis and performance evaluation of buck PFC front end. *IEEE Transactions on power electronics, 25*(1), 85-94. https://doi.org/10.1109/TPEL.2009.2024667

Jang, Y., & Jovanović, M. M. (2010). Bridgeless high-power-factor buck converter. *IEEE Transactions on Power Electronics, 26*(2), 602-611. https://doi.org/10.1109/TPEL.2010.2068060

Ki, S. K., & Lu, D. D. C. (2012). A high step-down transformerless single-stage single-switch AC/DC converter. *IEEE Transactions on Power Electronics, 28*(1), 36-45. https://doi.org/10.1109/TPEL.2012.2195505

Lamar, D. G., Fernandez, M., Arias, M., Hernando, M. M., & Sebastian, J. (2012). Tapped-inductor buck HB-LED AC–DC driver operating in boundary conduction mode for replacing incandescent bulb lamps. *IEEE Transactions on Power Electronics, 27*(10), 4329-4337. http://dx.doi.org/10.1109/TPEL.2012.2190756

Lee, Y. S., Wang, S. J., & Hui, S. Y. R. (1997). Modeling, analysis, and application of buck converters in discontinuous-input-voltage mode operation. *IEEE Transactions on Power Electronics, 12*(2), 350-360. https://doi.org/10.1109/63.558762

Liu, X., Wan, Y., He, M., Zhou, Q., & Meng, X. (2020). Buck-Type Single-Switch Integrated PFC Converter With Low Total Harmonic Distortion. *IEEE Transactions on Industrial Electronics*. https://doi.org/10.1109/TIE.2020.3007121

Memon, A. H., & Yao, K. (2018a). UPC strategy and implementation for buck–buck/boost PF correction converter. *IET Power Electronics, 11*(5), 884-894. https://doi.org/10.1049/iet-pel.2016.0919

Memon, A. H., Baloach, M. H., Sahito, A. A., Soomro, A. M., & Memon, Z. A. (2018b). Achieving High Input PF for CRM Buck-Buck/Boost PFC Converter. *IEEE Access, 6,* 79082-79093. https://doi.org/10.1109/ACCESS.2018.2879804

Memon, A. H., Memon, M. A., Memon, Z. A., & Hashmani, A. A. (2019a). Critical Conduction Mode Buck-Buck/Boost Converter with High Efficiency. *3C Tecnología.*

Glosas de innovación aplicadas a la pyme. Edición Especial, Noviembre 2019, 201-219. http://dx.doi.org/10.17993/3ctecno.2019.specialissue3.201-219

Memon, A. H., Memon, Z. A., Shaikh, N. N., Sahito, A. A., & Hashmani, A. A. (2019b). Boundary conduction mode modified buck converter with low input current total harmonic distortion. *Indian Journal of Science and Technology, 12,* 17. http://doi.org/10.17485/ijst/2019/v12i17/144613

Memon, A. H., Nizamani, M. O., Memon, A. A., Memon, Z. A., & Soomro, A. M. (2019c). Achieving High Input Power Factor for DCM Buck PFC Converter by Variable Duty-Cycle Control. *3C Tecnología. Glosas de innovación aplicadas a la pyme. Edición Especial, Noviembre 2019,* 185-199. http://dx.doi.org/10.17993/3ctecno.2019.specialissue3.185-199

Memon, A. H., Noonari, F. M., Memon, Z., Farooque, A., & Uqaili, M. A. (2020a). AC/DC critical conduction mode buck-boost converter with unity power factor. *3C Tecnología. Glosas de innovación aplicadas a la pyme. Edición Especial, Abril 2020,* 93-105. http://doi.org/10.17993/3ctecno.2020.specialissue5.93-105

Memon, A. H., Pathan, A. A., Kumar, M., & Sahito, A. A., & Memon, Z. A. (2019d). Integrated buck-flyback converter with simple structure and unity power factor. *Indian Journal of Science and Technology, 12*(17), 1-8. http://doi.org/10.17485/ijst/2019/v12i17/144612

Memon, A. H., Shaikh, N. N., Kumar, M., & Memon, Z. A. (2019e). Buck-buck/boost converter with high input power factor and non-floating output voltage. *International Journal of Computer Science and Network Security, 19*(4), 299-304.

Memon, A. H., Yao, K., Chen, Q., Guo, J., & Hu, W. (2016). Variable-on-time control to achieve high input power factor for a CRM-integrated buck–flyback PFC converter. *IEEE Transactions on Power Electronics, 32*(7), 5312-5322. https://www.semanticscholar.org/paper/Variable-On-Time-Controlled-Flyback-PFC-Converter-Yan-Xu/6fe0a89e8c674dc3a4c58402b7fc27e8d5ad8b77

Memon, A., Samejo, J. A., Memon, Z. A., & Hashmani, A. A. (2020b). Realization Of Unity Power Factor For Ac/Dc Boundary Conduction Mode Flyback Converter With Any Specific Turn's Ratio. *Journal of Mechanics Of Continua And Mathematical Sciences,* (spl6). https://doi.org/10.26782/jmcms.spl.6/2020.01.00014

Memon, A., Shaikh, S. A., Memon, Z. A., Memon, A. A., & Memon, A. A. (2020c). DCM Boost Converter with High Efficiency. *Journal Of Mechanics Of Continua And Mathematical Sciences,* (spl6). https://doi.org/10.26782/jmcms.spl.6/2020.01.00006

Sichirollo, F., Alonso, J. M., & Spiazzi, G. (2014). A novel double integrated buck offline power supply for solid-state lighting applications. *IEEE transactions on industry applications, 51*(2), 1268-1276. https://doi.org/10.1109/TIA.2014.2350071

Spiazzi, G., & Buso, S. (2000). Power factor preregulators based on combined buck-flyback topologies. *IEEE transactions on Power Electronics, 15*(2), 197-204. https://doi.org/10.1109/63.838091

Wu, X., Yang, J., Zhang, J., & Qian, Z. (2012). Variable on-time (VOT)-controlled critical conduction mode buck PFC converter for high-input AC/DC HB-LED lighting applications. *IEEE Transactions on power Electronics, 27*(11), 4530-4539. https://ieeexplore.ieee.org/document/6030954

Wu, X., Yang, J., Zhang, J., & Xu, M. (2011). Design considerations of soft-switched buck PFC converter with constant on-time (COT) control. *IEEE transactions on power electronics, 26*(11), 3144-3152. https://ieeexplore.ieee.org/document/5753946

https://doi.org/10.17993/3ctecno.2021.specialissue7.149-161

/10/

https://doi.org/10.17993/3ctecno.2021.specialissue7

DEFICIENCIES IN THE OLD BUILDINGS OF THE EDUCATIONAL INSTITUTIONS IN THE DISTRICT OF COMAS

Edgar Enrique Aroni Geldres
Federico Villarreal National University EUPG-UNFV, Lima, (Peru).
E-mail: 2020005075@unfv.edu.pe
ORCID: https://orcid.org/0000-0001-7928-3637

Doris Esenarro
Federico Villarreal National University EUPG-UNFV, Lima, (Peru).
E-mail: desenarro@unfv.edu.pe
ORCID: https://orcid.org/0000-0002-7186-9614

Karina Hinojosa
Federico Villarreal National University-UNFV, Lima, (Peru).
E-mail: khinojosa@unfv.edu.pe
ORCID: https://orcid.org/0000-0003-1237-9110

Nelly Mendez Gutierrez
Federico Villarreal National University-UNFV, Lima, (Peru).
E-mail: nmendez@unfv.edu.pe
ORCID: https://orcid.org/0000-0001-5524-6081

Recepción: 26/02/2021 **Aceptación:** 02/04/2021 **Publicación:** 07/05/2021

Citación sugerida:
Aroni, E. E., Esenarro, D., Hinojosa, K., y Mendez, N. (2021). Deficiencies in the old buildings of the educational institutions in the district of Comas. *3C Tecnología. Glosas de innovación aplicadas a la pyme, Edición Especial,* (mayo 2021), 163-175. https://doi.org/10.17993/3ctecno.2021.specialissue7.163-175

ABSTRACT

The present research aims to analyze the deficiencies in the old buildings of the educational institutions of the Comas district; the government has put its interest in reducing the gap in the educational infrastructure in a complementary way in which preventive and corrective maintenance actions are carried out, while school construction follows a cumbersome path. This delays the investment required in schools and universities. The methodology is based on the percentage variations of the schools by levels; for this, a sample of educational institutions was considered, based on critical components such as basic infrastructure, essential services, and advanced infrastructure, deficiencies in basic infrastructure were analyzed, verifying that this is a significant indicator that heralds quality and safety. Hence, it is crucial to work on the replacement of educational infrastructure. The results showed that, in the period 2017-2020, the percentage variation was 7.5% for initial education; meanwhile, for primary education, it was 3.61%, and for secondary education, the percentage variation was 7.14%.

KEYWORDS

Deficiencies, Old buildings, Basic infrastructure, Essential services, Advanced infrastructure.

https://doi.org/10.17993/3ctecno.2021.specialissue7.163-175

1. INTRODUCTION

A significant step forward in improving educational infrastructure in Peru was the approval of the National Educational Infrastructure Plan (PNIE) to 2025 (Minedu, 2017). As a result, a series of educational infrastructure works have been carried out nationwide, in line with the identification of the problem established by the National Educational Infrastructure Census (execution period: October 2013 - March 2014), i.e., the imperative need for reinforcement and rehabilitation of educational infrastructure (51.0%) and replacement of infrastructure (demolition) (25.0%), and, to a lesser extent, maintenance (non-structural) (15.0%). Only 9% of the educational institutions did not require intervention (Ministry of Education, 2014). The data are alarming and give an x-ray of the state in which educational institutions operate, contravening physical quality precepts as a basic aspect of the quality of education (Parasuraman, Zeithaml & Berry, 1985).

In this framework, the PNIE to 2025 has two critical columns on which public investment is destined; the first refers to the existing infrastructure gap and the second one to the additional investment needs (Minedu, 2019). Although the efforts to reduce the current educational infrastructure gap are laudable, in the geographic area of UGEL 04, especially in the district of Comas, there are deficiencies in the old constructions of educational institutions, which implies the need to improve the aesthetic quality and infrastructure conditions of academic environments.

Population growth in Metropolitan Lima has meant the emergence of new housing spaces in the city. In northern Lima, one of the districts that grew was Comas. Human settlements sprang up, and their inhabitants needed schools and colleges. This action implied the construction of educational infrastructure. However, this brought two further problems. The first one referred to the physical and legal clearing of the land occupied by the educational premises and the empirical criteria used in the construction of classrooms without adequate planning. A significant advance to this problem was the Guide for the Design of Educational Spaces (Ministry of Education, 2015).

Although the state has put its interest in reducing the educational infrastructure gap, they complementarily perform preventive and corrective maintenance actions. At the same

https://doi.org/10.17993/3ctecno.2021.specialissue7.163-175

time, the construction of schools follows a cumbersome path. This delays the investment required in schools and colleges.

The study's objective was to analyze the deficiencies in the old constructions of educational institutions in the district of Comas, based on the percentage variations in the period 2017-2020; likewise, for the specific objectives: basic infrastructure, essential services, and advanced infrastructure.

2. METHOD

A quantitative study was carried out using historical information, which implied going back in time by observing events that had taken place previously. Hence, it corresponds to a retrospective study (Alto, Lopez & Benavente, 2013) with a non-experimental design at a descriptive level (Hernandez, Fernandez & Baptista, 2014).

Likewise, the study population consisted of 97 public educational institutions built in the Comas district, corresponding to the Regular Basic Education levels. Of this population, 50.5% were at the pre-school level, 32.0% at the primary level, and 17.5% at the secondary level (Sanchez & Reyes, 2015).

Thus, the selected sample was non-probabilistic by convenience because it focused only on educational institutions with old buildings (25 years or more) in the district of Comas, using the criteria of the current state of walls, roofs, and floors, obtaining a sample of 79 educational institutions. Additionally, content analysis and documentary analysis were considered.

In order to evaluate the deficiencies in the old constructions of the educational institutions in the district of Comas, the defects were quantified by means of reports extrapolated from the office of educational infrastructure, based on a card in which three dimensions were considered: basic infrastructure, essential services and infrastructure described by 15 indicators. The card was subjected to KR 20 reliability, obtaining a coefficient of 0.720 higher than the established 0.700.

As for the procedure, a historical sequence was elaborated between the years 2017 and 2020 inclusive. The data were analyzed descriptively using the Excel tool.

https://doi.org/10.17993/3ctecno.2021.specialissue7.163-175

3. RESULTS

Below are the results obtained from the studied variable old constructions of educational institutions, described from its components: basic infrastructure, essential services, and advanced infrastructure:

As presented in Table 1, the percentage values refer to the proportion of colleges and schools that constitute old constructions, finding for the period 2017-2018, a percentage variation of 2.50%, corresponding to the initial education level; likewise, another variation of 2.41% was found at the primary level, finally, the finding of a variation of 2.38% that corresponded to the secondary level (Ministry of Education, 2020).

Concerning the 2018-2019 period, a percentage variation of 2.43% was found for the initial education level, while for the primary education level, it was -1.18%; on the other hand, in the secondary education level, the variation was 2.33%.

On the other hand, regarding the 2019-2020 period, a percentage variation of 2.38% was found for the initial education level. The percentage variation was 2.38%, and, at the secondary education level, it was 2.2%.

Finally, in the period 2017-2020, the percentage variation was 7.5% for initial education; while, for primary education, this was 3.61% and, for secondary education, the percentage variation was 7.14%.

Table 1. Percentage of deficiencies in old buildings, by levels of regular basic education.

EBR levels	Old buildings			
	2017	2018	2019	2020
Initial	80 %	82 %	84 %	86 %
Elementary	83 %	85 %	84 %	86 %
Secondary	84 %	86 %	88 %	90 %

Source: own elaboration.

Concerning the essential infrastructure component with its indicators for walls, roofs, and floors, the following results were obtained:

Table 2. Percentage of the basic infrastructure of old buildings by levels of regular primary education.

EBR levels	Old buildings			
	2017	2018	2019	2020
Initial	85 %	87 %	88 %	89 %

https://doi.org/10.17993/3ctecno.2021.specialissue7.163-175

Elementary	86 %	88 %	89 %	91 %
Secondary	87 %	88 %	90 %	92 %

Source: own elaboration.

In Table 2, the percentage values refer to the proportion of schools and schools, regarding walls, roofs, and floors, finding for the period 2017-2018, a percentage variation of 2.35%, corresponding to the initial education level; in the same way, another variation of 2.33% was found in the primary level, finally, the finding of a variation of 1.15% that corresponded to the secondary level (Campana *et al.*, 2014).

In the 2018-2019 period, the percentage variation obtained was 1.15% for initial education, while for the primary education level, it was 1.14%, and the percentage variation for the secondary education level was 2.27%.

In the 2019-2020 period, the percentage variation achieved was 1.14% at the initial education level. Meanwhile, the percentage variation was 2.25% for the primary education level and, for the secondary education level, the percentage variation was 2.22% for secondary education level.

Finally, to point out that the percentage variation for the period 2017-2020 was 4.71% for initial education, while for primary education, it was 5.81%. Finally, for the primary education level, the percentage value was 5.75%.

The following results were obtained for the essential building services component, composed of the indicators electricity, water, drainage, good toilets, and bad toilets:

Table 3. Percentage of essential services of old constructions, by levels of regular primary education.

EBR levels	Old buildings			
	2017	2018	2019	2020
Initial	82 %	86 %	89 %	90 %
Elementary	84 %	87 %	90 %	91 %
Secondary	86 %	88 %	92 %	93 %

Source: own elaboration.

In Table 3, the percentage values allude to the proportion of schools and colleges, regarding electricity, water, drainage, good toilets, and bad toilets, finding for the period 2017-2018, a percentage variation of 2.38%, corresponding to the initial education level; in the same

https://doi.org/10.17993/3ctecno.2021.specialissue7.163-175

way, another variation of 3.57% was found in the primary level, finally, the finding of a variation of 2.33% that corresponded to the secondary level (Palacio, 2018).

In the 2018-2019 period, the percentage variation obtained was 3.45% for initial education, while for the primary education level, it was 3.33%, and the percentage variation for the secondary education level was 4.55%.

In the 2019-2020 period, the percentage variation achieved was 1.12% at the initial education level. Meanwhile, the percentage variation was 1.11% for the primary education level and, for the secondary education level, the percentage variation was 1.09% for secondary education level.

Finally, to point out that the percentage variation for the period 2017-2020 was 9.56% for initial education, while for primary education, it was 8.33%. Finally, for the primary education level, the percentage value was 8.14%.

Concerning the advanced infrastructure component composed of its indicators library, laboratory, workshops, teachers, administrative, computer and internet, the following result was obtained:

Table 4. Percentage of the advanced infrastructure of old buildings by the level of regular primary education.

EBR levels	Old buildings			
	2017	2018	2019	2020
Initial	72 %	74 %	76 %	78 %
Elementary	78 %	80 %	82 %	84 %
Secondary	80 %	82 %	84 %	86 %

Source: own elaboration.

In Table 4, the percentage values allude to the proportion of colleges and schools, regarding library, laboratory, workshops, teachers, administrative, computer and internet, finding for the period 2017-2018, a percentage variation of 2.78%, corresponding to the initial education level; in the same way, another variation of 2.56% was found in the primary level, finally, the finding of a variation of 2.50% that corresponded to the secondary level.

In the 2018-2019 period, the percentage variation obtained was 2.70% for initial education, while for the primary education level, it was 2.50%, and the percentage variation for the secondary education level was 2.44%.

https://doi.org/10.17993/3ctecno.2021.specialissue7.163-175

In the 2019-2020 period, the percentage variation achieved was 2.63% at the initial education level. Meanwhile, the percentage variation was 2.44% for the primary education level and, for the secondary education level, the percentage variation was 2.38%.

Finally, to point out that the percentage variation for the period 2017-2020 was 8.33% for initial education, while for primary education, it was 7.50%. Finally, for the primary education level, the percentage value was 7.50%.

The objective of the study was to analyze the deficiencies in the old constructions of the educational institutions of the district of Comas, based on the percentage variations in the period 2017-2020; for this purpose, a sample of educational institutions was considered, based on critical components such as basic infrastructure, essential services, and advanced infrastructure.

4. DISCUSSION

These components have been considered by the Ministry of Education, based on the PNIE 2025, which has become a tool to implement the educational infrastructure policy; however, the infrastructure gap has been increasing year by year as a result of population growth and the lack of capacity to channel state resources and direct it to the investment of infrastructure projects, constituting a substantial problem faced by educational institutions in the jurisdiction of Comas. Although the efforts of the governing bodies are monumental, as, in the case of the allocation of 50 million soles for the construction of 5 schools, it is insufficient, it barely represents 6.32% of the 79 schools that require infrastructure replacement; this means that at an average rate of 5 schools per year in 10 years the horizon of 50 schools will be covered. This is a stark reality, considering the increase in the school population year by year. The results found are in line (Campana *et al.*, 2014) when they argue that what governments have done is to focus on strengthening flagship schools, but they have not concentrated on closing infrastructure gaps. They found a sustained increase in the levels of public investment in education, but without any positive impact; on the contrary, he notes the increase in the infrastructure gap.

The first specific objective, which focused on analyzing the deficiencies in old buildings' basic infrastructure, confirms that educational institutions have been gradually confirming

https://doi.org/10.17993/3ctecno.2021.specialissue7.163-175

year by year the deterioration of their basic infrastructure. So this finding is similar when he verified that an educational institution in Chorrillos was on the verge of collapse (Palacios, 2018). Gradually, the classrooms have been succumbing to the passage of time and putting schoolchildren's lives at risk. These results corroborate, on the other hand, the deterioration of the physical quality, that is, the perceptions that parents have about the educational institution where their children study, finding it to be adverse. This reality is located in the district of Comas, and that is why the improvement of the educational service is required, as Rodrigo (2019) argues when addressing the progress of the academic service through the design of the infrastructure, in this case, of primary and secondary education, emphasizing quality and safety.

The second specific objective focused on analyzing the essential services in the basic infrastructure of old buildings: electricity, water, drainage, full toilets, and excellent or bad toilets. The result reveals percentage variations that remain stationary over time but show severe limitations in essential services, especially water and drainage. This reality's harshness only further deteriorates the quality of life of schoolchildren, thus affecting their right to quality education. Education is an essential asset in people's lives because, in the long term, it guarantees quality professionals; therefore, attention must be paid to educational infrastructure because there is a significant relationship between educational infrastructure and student performance.

The third specific objective focused on advanced infrastructure, based on indicators such as a library, laboratory, workshops, teachers, administrative, computer, and internet. The result found for this component also confirms the percentage variations to the detriment of a better educational and human development of schoolchildren. Therefore, this line of denials ensures the existing weaknesses in educational infrastructure, which extends to the area of human development, the undermining of the right to education, and a growing deterioration of academic quality, which goes hand in hand with educational infrastructure. For this reason, the PNIE to 2025 will have a basis if the advanced infrastructure is improved, as a result of viable strategic actions that ensure the primary conditions of safety and functionality in the existing educational infrastructure.

https://doi.org/10.17993/3ctecno.2021.specialissue7.163-175

5. CONCLUSIONS

The deficiencies in the old constructions of the educational institutions of the district of Comas were analyzed, whose reflection is the percentage variations found between 2017-2020, reveal that maintenance does not mitigate or strengthen the educational infrastructure, but are palliatives that are worsening over time pressured by the academic coverage.

Deficiencies in basic infrastructure were analyzed, confirming that this is a significant indicator that foreshadows the quality and safety that both parents and students need to have a quality education, so it is essential to replace educational infrastructure.

Deficiencies in essential services were analyzed, confirming that this is a significant indicator that must be addressed if we seek to promote the right to quality education.

Deficiencies in advanced infrastructure were analyzed, confirming that this is a significant indicator that must be addressed if the right to quality education is promoted.

The limitations of the study may lie in the instrument designed to collect data from the structured reports in the area of Educational Infrastructure, so it is suggested that a robust mechanism be designed to measure in its actual dimension the level of educational infrastructure, carrying out a pilot study that includes several educational institutions in Metropolitan Lima, to validate it later and serve as a reference to collect data for fieldwork.

As a future perspective, it would be essential to focus on recently built schools to determine, through a longitudinal study with other educational institutions that only benefit from maintenance items, the effect of the perceptions produced by the design of an educational infrastructure academic performance of students.

REFERENCES

Ato, M., López, J., & Benavente, A. (2013). Un sistema de clasificación de los diseños de investigación en psicología. *Anales de psicología, 29*(3), 1038-1059. http://dx.doi.org/10.6018/analesps.29.3.178511

https://doi.org/10.17993/3ctecno.2021.specialissue7.163-175

Campana, Y., Velasco, D., Aguirre, J., & Guerrero, E. (2014). *Inversión e infraestructura educativa: una aproximación a la medición de sus impactos a partir de la experiencia de los colegios emblemáticos. Informe final.* Consorcio de Investigación Económica y Social.

Hernández, R., Fernández, C., & Baptista, P. (2014). *Metodología de la investigación* (6.ª ed.). McGraw Hill Educación.

Ministerio de Educación. (2014). *Censo Nacional de Infraestructura Educativa*. MINEDU/INEI.

Ministerio de Educación. (2015). *Guía de diseños de espacios educativos.* MINEDU. http://www.minedu.gob.pe/p/pdf/guia-ebr-jec-2015.pdf

Ministerio de Educación. (2020). *Estadística online 2020, UGEL 04.* Escale.

Palacios, J. B. (2018). *La inversión pública en educación y la brecha en infraestructura física en la educación básica regular durante el período 2000-2015* (Tesis de Maestría en gobierno y gestión pública). Universidad San Martin de Porres. https://repositorio.usmp.edu.pe/handle/20.500.12727/3273?show=full

Parasuraman, A., Zeithaml, V., & Berry, L. (1985). A Conceptual Model of Service Quality and its Implications for Future Research. *Journal of Marketing, 49*(4), 41-50. https://www.jstor.org/stable/1251430?origin=crossref&seq=1

Ramón, S. (2020). *Infraestructura educativa y el rendimiento académico de estudiantes de segundo grado de secundaria en el Perú en el año 2018* (Tesis de Pregrado). Pontificia Universidad Católica del Perú. http://tesis.pucp.edu.pe/repositorio/bitstream/handle/20.500.12404/16873/RAM%c3%93N_HUAM%c3%81N_SANDRA_MARIELLA_Infraestructura%20educativa.pdf?sequence=1&isAllowed=y

Resolución Ministerial Nº 153-2017- MINEDU. (2017, 6 de marzo). En *Normas legales, N° 13992. Diario Oficial "El Peruano"*. Ministerio de Educación.

Resolución Ministerial Nº 621-2019- MINEDU. (2019, 27 de diciembre). En *Normas legales, N° 15209. Diario Oficial "El Peruano"*. Ministerio de Educación.

https://doi.org/10.17993/3ctecno.2021.specialissue7.163-175

Rodrigo, S. (2019). *Mejoramiento del servicio educativo mediante el diseño de la infraestructura primaria N°10254 Santa Clara, Ferreñafe-2018* (Tesis de Pregrado). Universidad César Vallejo. http://repositorio.ucv.edu.pe/bitstream/handle/20.500.12692/46291/Rodrigo_VSYSD.pdf?sequence=1&isAllowed=y

Sánchez, H., & Reyes, C. (2015). *Metodología y diseños en la investigación científica* (5.ª ed.). Business Support Aneth.

https://doi.org/10.17993/3ctecno.2021.specialissue7.163-175

https://doi.org/10.17993/3ctecno.2021.specialissue7.163-175

https://doi.org/10.17993/3ctecno.2021.specialissue7